Alexandra Ciorîță

Vinca and *Catharanthus* plant extracts and their therapeutic potential applications

Presa Universitară Clujeană

Alexandra Ciorîță

Vinca and *Catharanthus* plant extracts and their therapeutic potential applications

PRESA UNIVERSITARĂ CLUJEANĂ

2022

Referenți științifici:

CS I dr. Maria-Loredana SORAN

Conf. dr. habil. Anca BUTIUC

ISBN 978-606-37-1705-5

Universitatea Babeş-Bolyai
Presa Universitară Clujeană
Director: Codruţa Săcelean
Str. Hasdeu nr. 51
400371 Cluj-Napoca, România
Tel./fax: (+40)-264-597.401
E-mail: editura@editura.ubbcluj.ro
http://www.editura.ubbcluj.ro/

There are not enough methods to express gratitude for the assistance received throughout the years spent creating this work, but I will do so here.

I would want to thank Prof. Dr. Parvu Marcel for their coordination and support.

I want to dedicate this Ph.D. thesis to my family, friends, and colleagues, without the help of whom none of these would have been possible.

SUMMARY

List of abbreviations

A – starch granule;
A375 – human melanoma cell line;
Ab – abaxial;
ABTS –2,2`-azino-bis(3-etilbenzotiazolin-6-sulfonic) acid;
Ad – adaxial;
ADN – desoxyribonucleic acid;
AGS – gastric cancer cell line;
ANOVA – Analysis of Variance;
ATCC – American Type Culture Collection;
Ca – adiacent cell;
CCD – charge-coupled device;
Ce – epidermal cell;
cl – chloroplast;
CMI – Minimal Inhibitory Concentration;
CmNPs – *C. majus* synthesized nanoparticles;
Crp – *Catharanthus roseus* cv. Pacifica;
Cs – stomatal cell;
CUPRAC – cupric reducing antioxidant capacity;
DMEM – Dulbecco Modified Eagle Media
DPPH – 2,2-difenil-1-picrilhidrazil;
DS – stomatal density;
DT – trichome density;
E – epidermal cells density;
EDX –energy-dispersive X-ray analysis;
Ei – inferior epidermis;
EMC – 'Constantin Crăciun' Electron Microscopy Centre;
Es – superior epidermis;
EUCAST – European Union Committee for Antimicrobial Susceptibility Testing;
F – velocity function;
FTIR – Fourier Transformed Infrared Spectroscopy;
GF – leaf thickness;
GTA – glutaraldehyde;
HaCaT – keratinocyte human cell line;
HCT116 – human colorectal cancer cell line;
HepG – hepatocarcinoma cell line;
HMDS – hexametyldisilazane;
HPLC – high performance liquid chromatography;
I – idioblast;
IAS – stomatal aperture index;
IC_{50} – 50% inhibition concentration;
INCDTIM – National Institute for Research and Development of Isotopic and Molecular Technologies;
IPNI – International Plant Name Index
IS – Stomatal index;
ISO – International Standardization Organization;
L – lipid;
LDH – lactate dehydrogenase;
LIME – Integrated Electron Microscopy Laboratory;
LS – stomatal aperture length;
LSF – level function;
MCF-7 – breast human adenocarcinoma cell line;
MH – Mueller-Hinton;
MNPs – nanoparticles obtained with mixture of plant extracts (*V. minor* and *C. majus*);
MTT – 3(4,5-dimetiltiazol-2-yl)-2,5-difeniltetrazolium bromide;
n – nucleolus;
N – nucleus;
N1-NAP – N-(-1-naptil)-ethylenediamine;

NAD – nicotinamide adenine dinucleotide;

NADH – nicotinamide adenine dinucleotide+hydrogen;

Nm – Midvein;

NO – nitric oxide;

NP – Nanoparticle/-s;

Ns – secondary vein;

O – aperture;

OCR – optical character recognition;

pb – protuberances;

PBS – phosphate buffered saline;

PCA – Principal Component Analysis;

PDE – Partial differential equation;

PFA – paraformaldehyde;

pg – plastoglobuli;

Pp – pallisadic parenchyma;

Ps – spongy parenchyma;

PTT – pallisadic parenchyma thickness;

REAC – rutin equivalent antioxidant capacity;

RS – spongy parenchyma tension report;

RTC – cellular tension report;

s – stomata;

scl – sclerenchyma;

SDBS – Spectral Database for Biochemical compounds;

SEM – scanning electron microscope;

STT – spongy parenchyma thickness;

T – trichome;

TAC – total alkaloid content;

TBzaC – total hydroxybenzoic acid content;

TCaC – total cinnamic acid content;

TEM – transmission electron microscope;

TFC – total flavonoid content;

TPC – total polyphenol content;

UBB – 'Babeș-Bolyai' University

UFC – colony forming units;

UV-Vis – ultraviolet and visible spectra;

v – vascular bundle;

Vh – *Vinca herbacea*;

VM – *Vinca major*;

Vm – *Vinca minor*;

VmNPs – *V. minor* synthesized nanoparticles;

VMv – *Vinca major* var. *variegata*;

Wt% – mass wight percentages;

XRD – X-Ray diffraction;

List of figures

List of tables

INTRODUCTION

This interdisciplinary doctoral thesis (***Vinca* and *Catharanthus* plant extracts and their therapeutic potential applications**) unites and develops subjects related to newly discovered information and well-known facts, regarding the pharmacological potential of hydroalcoholic leaf extracts. The plant species studied in this research work belong to *Vinca* L. genus (periwinkle), like *Vinca minor* L., *Vinca major* L., *Vinca herbacea* Waldst. & Kit., and the culture variety *Vinca major* L. var. *variegata* Louden; a *Catharanthus* genus hybrid (*Catharanthus roseus* (L.) G. Don cv. Pacifica); and *Chelidonium majus* L. species (celandine). In order to ascertain the key distinctions or similarities between these plant species, the morphological, anatomical, and ultrastructural characteristics of the leaves of *Vinca* and *Catharanthus roseus* were examined. The composition of the plant extracts, antioxidant properties, antibacterial potential, in vitro cytotoxicity against human cell lines, and green metal nanoparticle formation were also determined.

Four main chapters bring up the structure of the PhD thesis. The thesis' first chapter (Literature data) includes in-depth information on: the historical significance of plant use in medicine (Subchapter 1.1); Some biological traits of plants (Subchapter 1.2): their appearance and chemical content, the state of study on the significance of the examined plants economically; and the implications of nanotechnology and metal nanoparticles for contemporary medicine (Subchapter 1.3).

To examine the morphology and ultrastructure of *Vinca* leaf and *C. roseus*, to determine the phytochemical composition of *Vinca* and *C. roseus* extracts, and to determine the antioxidant, antibacterial, and cytotoxic activities are all covered in the second chapter (Personal contribution), "Research Materials and Methods" (Subchapter. 2.1). Light microscopy, scanning electron microscopy, and transmission electron microscopy are thus used to describe leaf-level characteristics. Using high-performance liquid chromatography and colorimetric techniques, the extracts were chemically evaluated. In addition, the cytotoxicity of the plant extracts on normal human cell lines (keratinocytes) and tumor cells (human melanoma) was assessed, as well as their antioxidant potential and antibacterial activity on *Escherichia coli* and *Staphylococcus aureus*.

Additionally, the extract that produced the best results was combined with an extract from the well-known medicinal herb *C. majus* to create metallic Ag-MnO_2 nanoparticles (Subchapter 2.2). By using techniques like X-ray diffraction, Fourier transform infrared spectroscopy, antibacterial potential (against *E. coli*, *S. aureus*, and *Candida albicans*), and anticancer impact, the produced nanoparticles were morphologically and physiologically evaluated. The statistical analyses completed for the purpose of interpreting the results are presented in Chapter 2's conclusion (Subchapter 2.3).

The original contribution is presented in chapter three (Chapter 3 – Results and discussion) which is divided into five subchapters. The study's key conclusions are presented in chapter four (Chapter 4 - Conclusions).

The scopes and objectives of the research

The foundation of phytomedicine is the therapeutic application of substances derived from medicinal plants (Scarlat, 2019). Consequently, the goal of the finalized doctoral thesis (***Vinca* and *Catharanthus* plant extracts and their therapeutic potential applications**) was to compare the foliar plant extracts and therapeutic applications of *Vinca* and *Catharanthus*.

The goals of the research conducted for the doctorate were focused on plant extracts obtained of *Vinca minor* L. (**lesser periwinkle**), *Vinca major* L. (**bigleaf periwinkle**), *Vinca major* L. var. *variegata* Loudon, *Vinca herbacea* Waldst. & Kit. (**herbaceous periwinkle**) and *Catharanthus roseus* (L.) G. Don (**Madagascar periwinkle**). Alkaloids, polyphenols, and flavonoids were all quantitatively determined using a phytochemical examination of these extracts. To test various experimental effects, the therapeutic potential of these extracts was assessed using *in vitro* tests for antioxidant activity, antibacterial activity, cytotoxic activity, and green nanoparticle formation.

The research activities detailed in the doctoral thesis were conducted in the following laboratories: „Constantin Crăciun" Electron Microscopy Center – UBB Cluj-Napoca (EMC); Natural Extracts Laboratory of Biology and Geology Faculty, UBB Cluj-Napoca (3bCenter); Chemistry Department – Faculty of Chemistry and Chemical Engineering Babeș-Bolyai University, Cluj-Napoca (UBBChem); Integrated Electron Microscopy Laboratory (LIME), Research Center of Advanced Technologies and Alternative Energies (CETATEA), Integrated Cell Cultures and Microbiology Laboratory, Molecular and Biomolecular Physics Department and Nanostructured Systems' Physics Department, of National Institute for Research and Development of Isotopic and Molecular Technologies, Cluj-Napoca (INCTDIM).

We have improved our understanding of the chemical composition and therapeutic potential of *Vinca* and *Catharanthus* plants through a variety of research techniques. The study's findings offer crucial information that may be applied practically and in a variety of phytomedicine partnerships.

1 Literature research: from medicinal plants to 'green' nanotechnology

1.1 Medicinal plants: *Vinca* genus and *Catharanthus roseus* species

1.1.1 Brief background

The foundation of modern medicine is formed of fresh plants, whether they are in the form of powders, teas, gemoderivatives, or tinctures. Phytopharmacology has a wide range of applications in the prevention and treatment of veterinary and human diseases. Depending on the plant parts employed as well as the technique of production, aqueous or alcoholic plant extracts have varied effects.

The discovery of antibiotics over 70 years ago represented a significant step in the advancement of medicine and agriculture. This major health benefit also doubles as a disadvantage because more and more antibiotics with broad spectrums of action are losing their effectiveness, necessitating the use of stronger drugs with focused action. Lack of population awareness and administrative education are other contributing factors to this outcome. As a result, the persistence of disease is a significant issue that is difficult to overcome (Bhagwat *et al.*, 2014; Jhanji *et al.*, 2019; Newman, 2008).

It was previously thought that microbes acquire their resistance mechanism through a succession of mutations and pass it down from generation to generation, but a fascinating finding has brought up new concerns. D'Costa et al. (2011) reconstructed the protein sequence of a protein that is also present in modern bacteria that develop antibiotic resistance through mutations using a DNA sequence from a 30,000-year-old sediment. As a result, it has been demonstrated that resistance is a common natural phenomenon in nature that first emerged long before the discovery of antibiotics. (D'Costa *et al.*, 2011).

This doctoral dissertation compares the chemistry and pharmacological potential of hydroalcoholic leaf extracts from: *V. minor* L., *V. major* L., *V. herbacea* Waldst. & Kit.; culture variety *V. major* L. var. *variegata* Louden; and *C. roseus* (L.) G. Don cv. Pacifica cultivar. *Vinca* species have long been used in alternative medicine to treat hypertension since they contain indole alkaloids, which also have a hypotensive action (vincamine, vincanine, vincadine, vinerine, vineridine, etc.) (Foddai *et al.*, 2017; Redda *et al.*, 2014; Tulyaganov, 2000).

1.2 Biological characterization of *Vinca* and *Catharanthus roseus* plant species

1.2.1 Systematic classification and speciation

The **Apocynaceae** family is known for its alkaloid-rich plants, which are primarily found in the Mediterranean region of Europe, Southwest Asia, North Africa, and North America. (Boga *et al.*, 2011; Cepkova *et al.*, 2016; Cheng *et al.*, 2016; Cheng *et al.*, 2014; Csiky *et al.*, 2013; Khanavi *et al.*, 2010; Sukhdev *et al.*, 2017; Yin *et al.*, 2011). Some authors group the Apocynaceae family's genera and species into subfamilies, bringing the total to around 411 genera and more than 4000 species (El-Fiki *et al.*, 2019; Gurău, 2007). Other researchers attribute 315 genera and 2900 species to the Asclepiadaceae family, which they believe to be separate

from the Apocynaceae family (El-Fiki *et al.*, 2019). Both versions place the genus *Vinca* inside the Apocynaceae family.

There are roughly 50 cultivars of *Vinca* species (I.P.N.I.). As a result, some writers categorize the species of the genus *Vinca* differently, including species like *V. difformis* in the group of synonyms of the species *V. major* or considering *V. erecta* a synonym of *V. herbacea*, as shown by confirmed and attested online databases (Table 1) (Bianco *et al.*, 2005; Boga *et al.*, 2011; Carriquí *et al.*, 2015; Koyuncu, 2012). Furthermore, *V. difformis* has as synonyms *Vinca acutiflora* Bertol. and *Vinca media* Hoffmanns. & Link, while *V. herbacea* has as synonyms *V. mixta* Valen. and *V. pumila* Clarke. The *Vinca* species studied herein (*Vinca minor* L., *Vinca major* L. and *Vinca herbacea* Waldst. & Kit.) are all part of the same genus.

Table 1. Systematic classification of *Vinca* species according to accepted databases

No.	Clasificassion	U.S. Department of Agriculture (PLANTS)	The Plants List (T.P.L.)*	Plants of the World Online (P.O.W):	European Environment Agency (E.E.A.)
1	Kingdom	Plantae	Plantae	Plantae	Plantae
2	Sub-kingdom	Tracheobionta	-	-	-
3	Super-division	Spermatophyta	-	-	-
4	Division	Magnoliophyta	Tracheophyta	Tracheophyta	Tracheophyta
5	Class	Magnoliopsida	Magnoliopsida	Magnoliopsida	Magnoliopsida
6	Sub-class	Asteridae	-	-	-
7	Order	Gentianales	Gentianales	Gentianales	Gentianales
8	Family	Apocynaceae	Apocynaceae	Apocynaceae	Apocynaceae
9	Genus	*Vinca* L.	*Vinca* L.	*Vinca* L.	*Vinca* L.
10	Species	*Vinca minor* L.	*Vinca difformis* Pourr.	*Vinca difformis* Pourr.	*Vinca balcanica* Pénzes
11		*Vinca major* L.	*Vinca erecta* Regel. & Schmalh.	*Vinca erecta* Regel. & Schmalh.	*Vinca difformis* Pourr.
12		*Vinca herbacea* Waldst. & Kit.	*Vinca herbacea* Waldst. & Kit.	*Vinca herbacea* Waldst. & Kit.	*Vinca herbacea* Waldst. & Kit.
13			*Vinca major* L.	*Vinca ispartensis* Koyuncu & Eksi	*Vinca major* L.
14			*Vinca minor* L.	*Vinca major* L.	*Vinca minor* L.
15				*Vinca minor* L.	
16				*Vinca soneri* Koyuncu	
19	Varieties	*Vinca major* var. *variegata* Louden			
20	Sub-species				*Vinca difformis* subsp. *difformis*
21					*Vinca difformis* subsp. *sardoa*

*This database comprises 36 scientific names for plants in the *Vinca* genus, out of which 5 are accepted as species.

Catharanthus roseus (L.) G. Don (Madagascar periwinkle) also known as *Vinca rosea* (Naaz *et al.*, 2019) is considered the only species of the *Catharanthus* genus in some databases (Table 2).

Table 2. Systematic clasificassion of *Catharanthus* plants according to accepted databases

No.	Clasificassion	U.S. Department of Agriculture (PLANTS)	The Plants List (T.P.L.)	Plants of the World Online (P.O.W):
1	Kingdom	Plantae	Plantae	Plantae
2	Sub-kingdom	Tracheobionta	Tracheobionta	-
3	Super-division	Spermatophyta	Spermatophyta	-
4	Division	Magnoliophyta	Magnoliophyta	Tracheophyta
5	Class	Magnoliopsida	Magnoliopsida	Magnoliopsida
6	Sub-class	Asteridae	Asteridae	-
7	Order	Gentianales	Gentianales	Gentianales
8	Family	Apocynaceae	Apocynaceae	Apocynaceae
9	Genus	*Catharanthus* (L.) G. Don	*Catharanthus* (L.) G. Don	*Catharanthus* (L.) G. Don
10	Species	*Catharanthus roseus* (L.) G. Don	*Catharanthus roseus* (L.) G. Don	*Catharanthus roseus* (L.) G. Don.
11			*C. pusillus* (Murray) G. Don	*C. pusillus* (Murray) G. Don
12			*C. coriaceus* Markgr.	*C. coriaceus* Markgr.
13			*C. ovalis* Markgr.	*C. ovalis* Markgr.
14			*C. longifolius* (Pichon) Pichon	*C. longifolius* (Pichon) Pichon
15			*C. scitulus* (Pichon) Pichon	*C. scitulus* (Pichon) Pichon
16			*C. trichophyllus* (Baker) Pichon	*C. trichophyllus* (Baker) Pichon
17			*C. lanceus* (Bojer ex A.DC.) Pichon	*C. lanceus* (Bojer ex A.DC.) Pichon
18				*C. makayensis* L. Allorge, Phillipson & Razakamal.

1.2.2 Morphology

1.2.2.1 Vinca minor

Vinca minor also known as lesser periwinkle or common periwinkle, is a perennial, evergreen plant with creeping and aerial stems. More than 40 years ago, the species' botanical characteristics were documented (Ochirova *et al.*, 2018; Păun *et al.*, 1988). The aerial stems can grow up to 40 cm tall, and the root is adventitious to the creeping stems. When they hit the ground, they begin to root at the nodes to create marcots. The opposite, ovate-elliptic, glossy, dark green, non-ciliate, and short-petiolate leaves are succulent. The plant produces solitary, axillary, long-pedunculated, androgenic, pentamerous blooms that range in color from light blue to violet-blue, with the amount of flowering depending on the light and the location of the plant. It blooms from March through June and sporadically throughout the other seasons. The fruits have 2-3 seeds within and are acuminate with two divergent follicles (Fleming, 2000; Ochirova *et al.*, 2018). It is an allogamous plant that only produces seeds when cross-fertilization occurs. It exhibits generative multiplication, which is quite uncommon, as well as clonal vegetative proliferation by stolons, dragons, or cuttings (Moeller *et al.*, 2015; Muntean *et al.*, 2007; Tiță, 2008). Currently, *V. minor* plants are genetically altered to increase the amount of alkaloid content; this practice has the potential to alter the plant's phenotype over time (Abouzeid *et al.*, 2019a). According to popular belief, the lesser periwinkle, which has green leaves even in winter, is a sign of eternal life and is frequently planted on graves and cemeteries (Muntean *et al.*, 2007).

1.2.2.2 Vinca major and *Vinca major* var. *variegata*

Vinca major (big-leaf periwinkle) is a perennial plant, with leaves that are 2-3 cm wide, 5–7 cm long, and have ciliate margins in contrast to *Vinca minor*. The leaves of the cultivar *V. major* L. var. *variegata* are glossier and have edges that are very pale green, bordering on white (Crăciun *et al.*, 1977; Tiță, 2008). The flowering time varies depending on the location of the plant, which reproduces vegetatively by stolons (e.g. in India it blooms in January-March, and in Mediterranean Europe, in April-May) (Sukhdev *et al.*, 2017).

1.2.2.3 Vinca herbacea

The perennial herbaceous plant known as vinca herbacea *Vinca herbacea* (herbaceous periwinkle), it thrives in rocky coastal areas as well as sunny meadows and thickets. In contrast to *V. minor*, the fruit has many seeds and the leaves are deciduous, fragile, dull, and hardly ciliated, almost sessile (Tiță, 2008).

1.2.2.4 Catharanthus roseus

C. roseus, often known as Madagascar periwinkle, is a tropical perennial plant that grows up to 1 m tall (Jaleel *et al.*, 2009; Mukunthan *et al.*, 2011). The entire leaf is opposite, matte, obovate-elliptic, shortly pedunculate, and ranges in length from 2.5 to 9 cm and limb width from 1 to 3.5 cm. Depending on the cultivar, flowers can range from purple to white in hue (Barrales-Cureño *et al.*, 2019; Hua Shu, 1995).

1.2.3 The chemical composition

The primary active ingredient in plants in the Apocynaceae family is an alkaloid, of which more than 2000 have been isolated and described. Alkaloids are organic nitrogenous bases that occur naturally in plants and are classified by Stenesh (1989) as having potent medicinal effects. The majority of alkaloids are heterocyclic compounds with elaborate structures. Tropanes, pyrrolidines, piperidines, pyrrolizidines, quinolizidines, isoquinolines, terpenes, and indoles (O'Connor, 2008) are the primary groups into which they are classified as well as the precursors from which alkaloids are biosynthesized (Fig. 1).

V. minor's chemical composition was not of interest until recently, but after vincamine was found to be present, researchers started doing more and more tests to isolate and characterize this species' alkaloids (Cepkova *et al.*, 2016; Scheindlin *et al.*, 1955). Only after the second half of the 19th century was the alkaloid content of the *V. major* species brought to light (Muntean *et al.*, 2007).

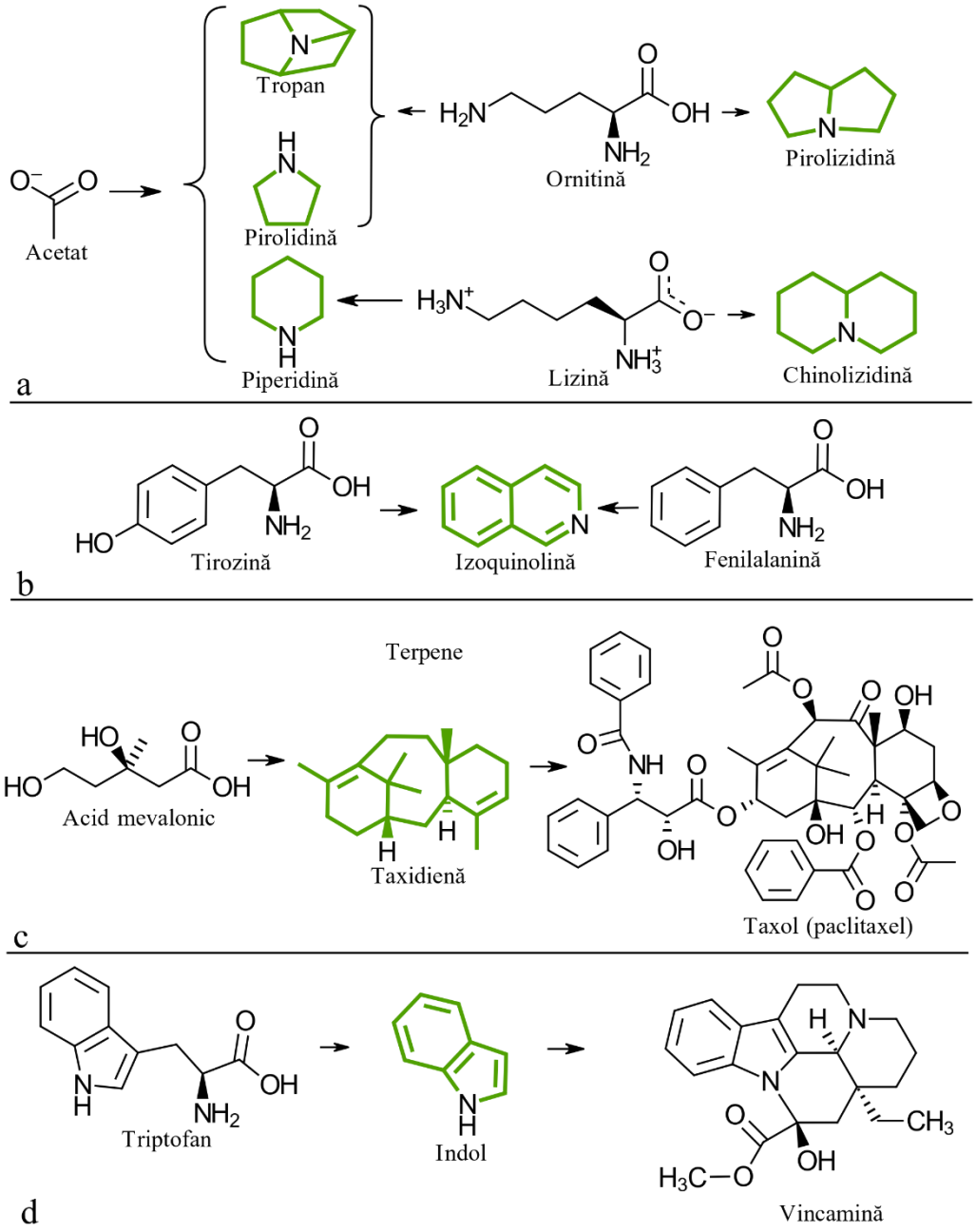

Figure 1. Main groups in which alkaloids (molecules marked in green) and their precursors are classified: acetate, ornithine or lysine are precursors for tropane, pyrrolidine, piperidine, pyrrolizidine, and quinolizidine alkaloids **(a)**; tyrosine or phenylalanine are precursors for isoquinoline alkaloids **(b)**; mevalonic acid is a precursor for terpene alkaloids, taxidiene being a diterpene precursor for taxol (paclitaxel) **(c)**; tryptophan is a precursor for indole alkaloids, including vincamine **(d)**.

Plants also include micro- and macro-elements, phenolic acids, carotenoids, free amino acids, iridoids, flavones, caffeic acid, and other substances in addition to alkaloids (Cheng *et al.*, 2016; Söhretoglu *et al.*, 2013).

1.2.3.1 Vinca minor

This plant has long been used for therapeutic purposes in addition to its decorative value. It can be utilized in modern medicine to obtain medications that affect the nervous system, notably those that aid in blood flow fluidization and brain homeostasis, the prevention of attention issues and neural senescence (Cepkova *et al.*, 2016; Ghédira *et al.*, 2017; Khanavi *et al.*, 2010; Moeller *et al.*, 2015; Tulyaganov, 2000; Yin *et al.*, 2011).

The most significant alkaloid in this plant's chemical composition is vincamine, which is only produced by *V. minor* in nature (Chen *et al.*, 2017; Liu *et al.*, 2015; Verma *et al.*, 2014; Verma *et al.*, 2012). Vincamine can also be produced chemically, the resulting drug being vinpocetine, and has beneficial properties (antioxidant and antitumor activities, treatment of cognitive, cerebrovascular, and hypertension disorders, relief of stroke symptoms, etc.), but qualitatively, pure vincamine from the plant is much more effective (Liu *et al.*, 2015; Scheindlin *et al.*, 1955; Yin *et al.*, 2011).

It is continually being researched how to create quick processes for isolating and purifying vincamine from plants in the most effective and inexpensive way feasible. By using endophytic fungal species that can produce the same bioactive compounds as the host plant on which they are located, Yin et al. (2011) were able to acquire vincamine in significant amounts (Yin *et al.*, 2011).

Vincaburine, vincaminorine, vincaminoreine, vincadine, vinerine, vineridine, vallesiachotamine, perivincine, minovine, minovincine, isovallesiachotamine, tryptamine, serpentine, and tabersonine are only a few of the up to 50 distinct alkaloids that *V. minor* can produce in addition to vincamine (Bahadori *et al.*, 2012; Boyadzhiev *et al.*, 2004; Farahanikia *et al.*, 2011; Mokry *et al.*, 1962; Scheindlin *et al.*, 1955; Tulyaganov, 2000). Polyphenols, flavonoids, tannins, etc. are also found in the aerial organs of *V. minor* plants (Grujić *et al.*, 2015; Grujić *et al.*, 2014).

1.2.3.2 Vinca major and *Vinca major* var. *variegata*

Vinca major and *V. major* var. *variegata* are similar to *V. minor* when it comes to their chemical composition. According to Van de Venter et al. (2008), when they utilized liver cell lines they saw that the alkaloids present in the *V. major* leaf extract were toxic (van de Venter *et al.*, 2008). However, Rajput et al. (2011) showed that *V. major* extract was effective in treating rats with diarrhea brought on by castor oil (Rajput *et al.*, 2011). We list vinmajina (an alkaloid with many conformations, from A to I), vincamajorein, majoridine, venoterpine, and vincapyridine among the more than 30 alkaloids identified in *V. major* (Chatterjee *et al.*, 1975; Cheng *et al.*, 2014; Wei *et al.*, 2017). In addition to alkaloids, *V. major* also includes additional polyphenolic and flavonoid compounds, including iridoids, delphinidins, chlorogenic acids, sterols, and carbohydrates (Bahadori *et al.*, 2012; Cheng *et al.*, 2016; Ishikura *et al.*, 1978; Rajput *et al.*, 2011; Wei *et al.*, 2017).

V. major var. *variegata* is frequently used as an ornamental plant; nevertheless, little research has been done on the chemical composition of the plant. However, the presence of alkaloids and polyphenolic compounds has previously been noted (Liao *et al.*, 2013).

1.2.3.3 Vinca herbacea

Since the 1960s, novel alkaloids have been reported and isolated from the *V. herbacea* species, which is the least well-known species in this genus, at a very consistent rate until 2011 (Boga *et al.*, 2011; Gülçin *et al.*, 2012; Vachnadze *et al.*, 2010). In his paper, Ognyanov (1965) described a tenth alkaloid in addition to mentioning the presence of nine alkaloids in the chemical composition of *V. herbacea* (Ognyanov, 1965). Pyuskyulev et al. (1967) isolated and described six other alkaloids (Pyuskyulev *et al.*, 1967), and herbavine was isolated and described in 1968 (Zabolotnaya *et al.*, 1968). Vincoline, the plant's primary alkaloid, is also present along with majdine, isomajdine, reserpinine, kopsinine, tabersonine, etc. (Boga *et al.*, 2011; Vachnadze *et al.*, 2010). Additionally, polyphenols and flavonoids in *V. herbacea* have potent antioxidant properties (Gülçin *et al.*, 2012).

1.2.3.4 Catharanthus roseus

More than 130 alkaloids have been identified and isolated from the medicinal plant *C. roseus*, which has been the subject of intense research (Abouzeid *et al.*, 2019b; Rischer *et al.*, 2006). Vinblastine and vincristine, two of the alkaloids present, are used in conjunction with cytostatic medications to treat cancer patients, particularly leukemia patients (Mahmoudi *et al.*, 2016). In 1960, vinblastine was first isolated (Chagas *et al.*, 2019; Johnson *et al.*, 1963). In order to synthesize the vinblastine alkaloid in large amounts, several studies are now being conducted to determine the synthesis pathway. The major goal of these studies is to induce these processes in other plants (Abouzeid *et al.*, 2019b; Goklany *et al.*, 2009; McCoy *et al.*, 2008; O'Connor, 2008; O'Connor *et al.*, 2006). Serpentine, catharanthine, ajmalicine, and tabersonine are only a few of the significant alkaloids identified in *C. roseus* (Bhadra *et al.*, 1977; Binder *et al.*, 2009). The plant also has volatile substances, polyphenols, tannins, saponins, and other substances in addition to alkaloids (Ferreres *et al.*, 2008; Pandey-Rai *et al.*, 2006; Samiyarsih *et al.*, 2019).

1.2.4 Pharmacological potential

1.2.4.1 Antioxidant activity

When an organic substance may prevent or slow down the autoxidation of another compound after they are mixed, that compound exhibits antioxidant action (Stenesh, 1989). Thus, the natural components found in the chemical composition are primarily responsible for the antioxidant activity of *Vinca* and *C. roseus* extracts. (Ainsworth *et al.*, 2007).

Numerous *C. roseus* extract preparations have been shown to have antioxidant action (Barrales-Cureño *et al.*, 2019; Ferreres *et al.*, 2008; Jaleel *et al.*, 2008; Kabesh *et al.*, 2015; Mardani-Nejad, 2017; Moon *et al.*, 2018; Tiong *et al.*, 2013), as the plant has been investigated since the 19th century (Bahadori *et al.*, 2012).

According to other studies (Grujić *et al.*, 2015), certain complete extracts are more potent antioxidants than separated fractions. *V. minor* and *V. major* were synthesized as three different types of extracts (methanolic, alkaloidal, and non-alkaloidal), and their comparative antioxidant effects were investigated by Bahadori et al. (2012). Alkaloidal extracts demonstrated higher antioxidant activity than non-alkaloidal and methanolic extracts for both species. (Bahadori *et al.*, 2012).

Methanolic, alkaloidal, and non-alkaloidal extracts of *V. herbacea*'s leaves, stems, and flowers were contrasted by Boga et al. (2011). And in this instance, the alkaloidal extract outperformed the methanolic one and shown stronger antioxidant activity than the non-alkaloidal extract (Boga *et al.*, 2011). The antioxidant activity of the non-alkaloid substances that Cheng et al. (2016) isolated from *V. major* was examined independently. Of the seven polyphenolic substances studied, five showed promising antioxidant potential (Cheng *et al.*, 2016). In order to compare the antioxidant activity of *V. sardoa*'s flowers, leaves, and roots, Foddai et al. (2017) synthesized methanolic extracts of each. Since the leaf extract's chemical makeup was more complex than that of the extracts from the flowers and roots, it had a substantially stronger antioxidant impact (Foddai *et al.*, 2017).

According to (Grujić *et al.*, 2015), the aqueous extract of *V. minor* leaves showed a greater antioxidant impact than the extracts made from acetone and ethyl acetate, and the isolated antioxidants majdine and isomajdine from *V. herbacea* exhibit dose-dependent antioxidant activity (Gülçin *et al.*, 2012).

1.2.4.2 Antimicrobial and antiviral activities

Previous studies have shown that fractions and extracts from *Vinca* species have an antibacterial effect (Table 3). The antibacterial capacity is replicated by the diffusimetric approach, also known as the Kirby-Bauer method, through the zone of inhibition (internationally stated in mm) created around the examined culture, in a time specific to each unique microbial strain. (Leclercq *et al.*, 2013; Turker *et al.*, 2009). The microdilution method is used to determine the minimal solution concentration necessary to prevent the pathogen from growing (minimum inhibitory concentration - MIC) (Matuschek *et al.*, 2014).

The therapeutic potential of this plant was highlighted by some of the findings from other investigations on some *C. roseus* extracts and fractions (alkaloids, polyphenols, or flavonoids) that were chemically synthesized or extracted (Table 4).

Table 3. Antibacterial, antifungal, and antiviral effects of several *Vinca* extracts and/or isolated or chemically synthesized natural compounds

Microbial/viral species	*Vinca* extract	Natural compound	Aqueous extract	Alcoholic extract	Positive control	Reference
Bacteria						
Aeromonas hydrophila	*V. minor*			9.25 mm		(Turker *et al.*, 2009)
Bacillus cereus		Quercetin				(Arima *et al.*, 2002)
		350 µg/mL				
		Quercitrin				
		6-7 mm				
Bacillus pumilus	*V. minor*		625 µg/mL	19.53 µg/mL	0.11 µg/mL	(Grujić *et al.*, 2015)
				19.53 µg/mL	0.11 µg/mL	(Grujić *et al.*, 2014)
Bacillus subtilis	*V. minor*			78.13 µg/mL	0.11 µg/mL	
		Vincamine				
		2 µg/mL				(Özçelik *et al.*, 2011)
		Rutin				
		7 mm			8 mm	(Dubey *et al.*, 2013)
Staphylococcus aureus	*V. minor*		1250 µg/mL	1250 µg/mL	0.45 µg/mL	(Grujić *et al.*, 2015)
				11.3 mm	25.3 mm	(Yildirim *et al.*, 2012)
				8.2 mm*	42.7 mm	
	V. major			6 mm*	12.5 mm	(Redda *et al.*, 2014)
		Vincamine				
		2 µg/mL				(Özçelik *et al.*, 2011)
		Rutin				
		128 µg/mL			128 µg/mL	(Araruna *et al.*, 2012)
		15 mm			21 mm	(Dubey *et al.*, 2013)
Enterococcus faecalis	*V. minor*		1250 µg/mL	>2500 µg/mL	7.81 µg/mL	(Grujić *et al.*, 2015)
				9.25 mm	17.75 mm	(Turker *et al.*, 2009)

		Vincamine				
		2 µg/mL				(Özçelik *et al.*, 2011)
Pseudomonas aeruginosa	*V. minor*		>2500 µg/mL	>2500 µg/mL	250 µg/mL	(Grujić *et al.*, 2015)
		Vincamine				
		4 µg/mL				(Özçelik *et al.*, 2011)
		Rutin				
		12 mm			9 mm	(Dubey *et al.*, 2013)
Escherichia coli	*V. minor*		>2500 µg/mL	>2500 µg/mL	7.81 µg/mL	(Grujić *et al.*, 2015)
				9.3 mm	10.3 mm	(Yildirim *et al.*, 2012)
	V. major			6 mm*	7.2 mm	(Redda *et al.*, 2014)
		Vincamine				
		8 µg/mL				(Özçelik *et al.*, 2011)
		Rutin				
		128 µg/mL			128 µg/mL	(Araruna *et al.*, 2012)
		9 mm			9 mm	(Dubey *et al.*, 2013)
Proteus mirabilis	*V. minor*		>2500 µg/mL	>2500 µg/mL	250 µg/mL	(Grujić *et al.*, 2014)
		Vincamine				
		8 µg/mL				(Özçelik *et al.*, 2011)
Salmonella typhimurium	*V. minor*		>2500 µg/mL	>2500 µg/mL	15.6 µg/mL	(Grujić *et al.*, 2015)
	V. major			6.4 mm*	23.3 mm	(Redda *et al.*, 2014)
Salmonella enterica	*V. minor*		>2500 µg/mL	>2500 µg/mL	15.6 µg/mL	(Grujić *et al.*, 2015)
Fungi						
Penicillium italicum	*V. minor*		2500 µg/mL	2500 µg/mL	1000 µg/mL	(Grujić *et al.*, 2015)
Aspergillus niger			>2500 µg/mL	>2500 µg/mL	62.5 µg/mL	
A. flavus	*V. minor*		>2500 µg/mL	>2500 µg/mL	62.5 µg/mL	(Grujić *et al.*, 2015)
Botrytis cinerea	*V. minor*		>2500 µg/mL	>2500 µg/mL	31.25 µg/mL	(Grujić *et al.*, 2015)

Trichoderma viride			625 µg/mL	2500 µg/mL		
Fusarium oxysporum			~1%			(Rongai *et al.*, 2012)
Yeasts						
Candida albicans	*V. minor*		>2500 µg/mL	>2500 µg/mL	62.5 µg/mL	(Grujić *et al.*, 2015)
		Vincamine				
		4 µg/mL				(Özçelik *et al.*, 2011)
		Rutin				
		32 µg/mL			32 µg/mL	(Araruna *et al.*, 2012)
Rhodotorula spp.	*V. minor*		2500 µg/mL	625 µg/mL	62.5 µg/mL	(Grujić *et al.*, 2015)
Saccharomyces boulardii			>2500 µg/mL	>2500 µg/mL	31.25 µg/mL	
Viruses						
Herpes simplex tip 1 (HCV-1)		Vincamine				
		1.6 µg/mL				(Özçelik *et al.*, 2011)
Parainfluenza tip 3 (PI-3)		1.6 µg/mL				

Testing methods: diffuzimetric (inhibition diameter mm); microdilution (minimum inhibitory concentration - MIC).

Table 4. Antibacterial, antifungal, and antiviral effects of several *Catharanthus roseus* extracts and/or isolated or chemically synthesized natural compounds

Microbial/viral species	Plants species	Fraction	Aqueous extract	Alcoholic extract	Positive control	Reference
Bacteria						
Bacillus subtilis	*C. roseus*			5.39-10.9 mm	22.9 mm	(Goyal *et al.*, 2008)
			2-6 mm	3-8 mm**	10-14 mm	(Kabesh *et al.*, 2015)
	*C. roseus**			8.5-25 mm**		(Hanafy *et al.*, 2016)
Staphylococcus aureus	*C. roseus*			15-21.8 mm	30.4 mm	(Goyal *et al.*, 2008)
			3-4 mm	3-4 mm**	9-11 mm	(Kabesh *et al.*, 2015)
	*C. roseus**			8.9-24 mm**		(Hanafy *et al.*, 2016)
Pseudomonas aeruginosa	*C. roseus*			2 mm**		(Patil *et al.*, 2010)

			2-6 mm	3-8 mm**	6-7 mm	(Kabesh *et al.*, 2015)
	*C. roseus**			9.5-21.3 mm**		(Hanafy *et al.*, 2016)
Escherichia coli	*C. roseus*			5.2-13.6 mm	35.6 mm	(Goyal *et al.*, 2008)
				4-7 mm**	2-9 mm	(Kabesh *et al.*, 2015)
	*C. roseus**		2-8 mm	9.2-20.1 mm**		(Hanafy *et al.*, 2016)
Fungi						
Aspergillus niger	*C. roseus**			8.7-21.3 mm**		(Hanafy *et al.*, 2016)
A. flavus				9.5-20.5 mm**		
Yeast						
Candida albicans	*C. roseus*		2 mg/mL	4 mg/mL**		(Wankhede *et al.*, 2013)
				1 mg/mL**		
	*C. roseus**			8.7-21.6 mm**		(Hanafy *et al.*, 2016)
Viruses						
Poliovirus III		Vindoline				(Farnsworth *et al.*, 1968)
		15-20 mm				
Vaccinia virus		Vincaleucoblastine				
		24-33 mm				

Testing methods: diffuzimetric (inhibition diameter mm); microdilution (minimum inhibitory concentration - MIC).

*transgenic species and not wild type.

**methanol was used for extract preparation.

1.2.4.3 Antiparasitic activity

With the development of parasite resistance to anthelmintics, which was brought on by the careless use of these types of medications, researchers started looking into the antiparasitic properties of medicinal plant extracts (Carvalho *et al.*, 2012). *Allium* (Hezarjaribi *et al.*, 2015), *Berberis vulgaris* (Mahmoudvand *et al.*, 2014; Rouhani *et al.*, 2013), *Eleucine indica* (Ettebong *et al.*, 2012), *Nicotiana tabacum* (Nouri *et al.*, 2016) and other types of plant extracts (Hezarjaribi *et al.*, 2015; Hurtada *et al.*, 2012) were proven efficient against *Plasmodium falciparum*, *Giardia lamblia*, *Leishmania* spp., *Marshallagia marshalli*, or *Echinococcus granulosus.*

The antiparasitic effects of *Vinca* and *C. roseus* extracts have not been investigated, however isolated fractions (rutin, quercetin, vinblastine, and vincristine) have been demonstrated to be effective against parasites like: *Plasmodium falciparum* (Ganesh *et al.*, 2012) or *Trypanosoma cruzi* (Almagro *et al.*, 2015; Barrales-Cureño *et al.*, 2019; Grellier *et al.*, 1999).

1.2.4.4 Antitumor and cytotoxic effects

Medical plant extracts' in vivo anticancer and in vitro cytotoxic properties are still being thoroughly researched (Alam *et al.*, 2015; Alam *et al.*, 2013; Almosnid *et al.*, 2018; Eswaraiah *et al.*, 2020; Garcia-Lazaro *et al.*, 2020; Güneş *et al.*, 2019; Sharma *et al.*, 2015; Solowey *et al.*, 2014). Among the plants taken into account in this study, *C. roseus* has two natural alkaloids (vinblastine and vincristine) that are employed in the treatment of cancer patients. From these two alkaloids, several semi-synthetic ones (vinflunine, vinorelbine, and vindesine) with the same function were produced (Ceresoli *et al.*, 2015; Douillard *et al.*, 2007; Fumoleau *et al.*, 2012; Magge *et al.*, 2015; Martino *et al.*, 2018; Schutz *et al.*, 2011).

Vinca alkaloids specifically influence microtubules and the division spindle in the cytoskeleton (Gascoigne *et al.*, 2009; Lobert *et al.*, 1996; Martino *et al.*, 2018). Natural substances that inhibit tumor cell division by stabilizing microtubules include paclitaxel (Cao *et al.*, 2018) and colchicine (Amos, 2011); at the other end of the spectrum are *Vinca* alkaloids, which inhibit cell division by destabilizing microtubules (Jordan *et al.*, 1991; Risinger *et al.*, 2009). *Vinca* alkaloids interact with β-tubulin primarily in the 'vinca domain' which is located near the GTP end of microtubules (Jordan *et al.*, 2007).

Vinca alkaloids work in a dose-dependent manner (Checchi *et al.*, 2003). Thus, premature microtubule depolymerization occurs in large concentrations, suppressing microtubule dynamics, and chromosomes stay unsegregated and in a condensed condition (Fig. 2) *Vinca* alkaloids have the ability to alter the shape of β -tubulin at low doses, causing it to self-associate. They can also connect to the GTP end of microtubules, preventing polymerization and forcing depolymerization (Fig. 2).

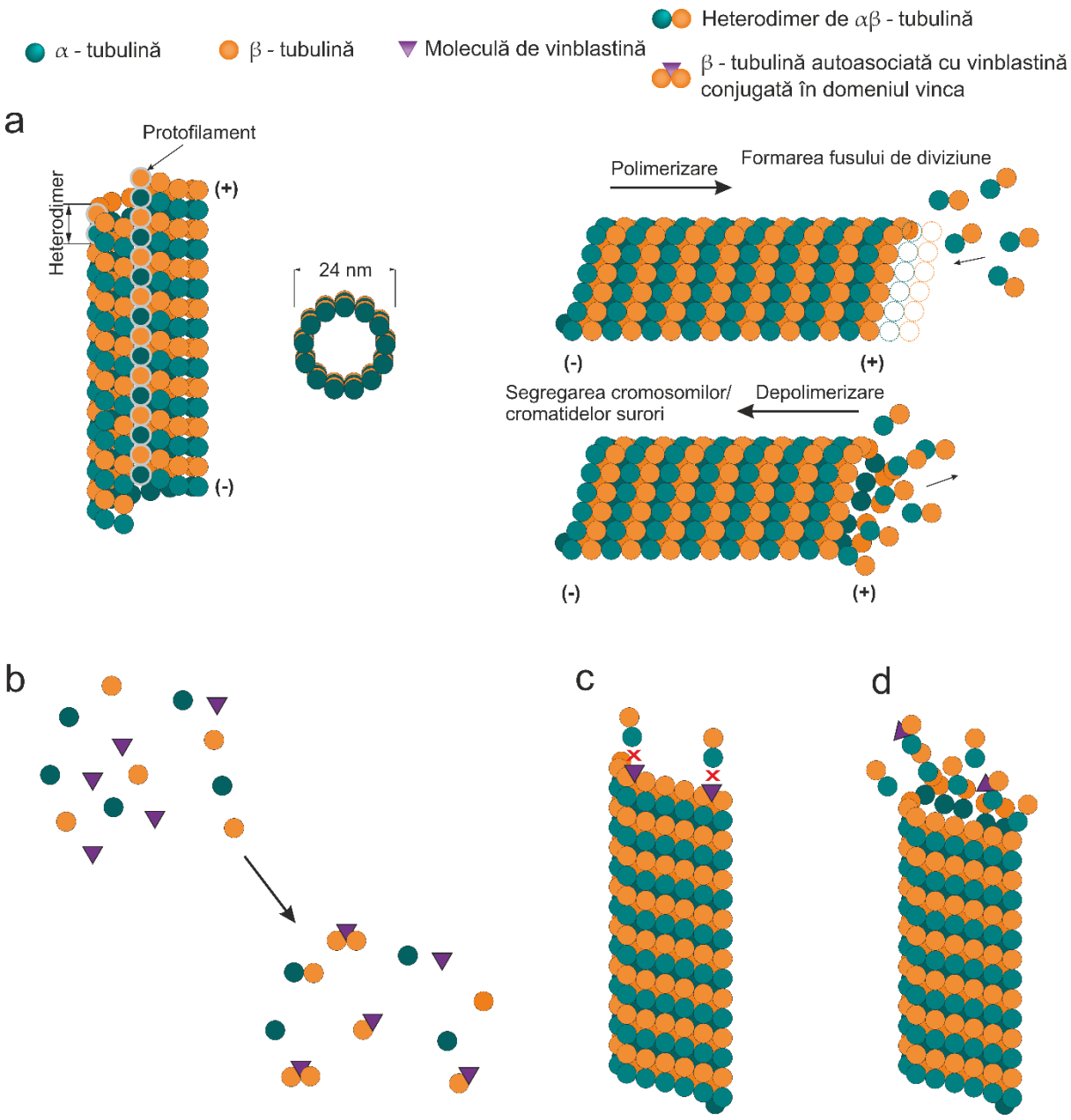

Figure 2. Graphic representation of the mode of interaction between α-tubulin, β-tubulin, microtubules and *Vinca* alkaloids (*i.e.*, vinblastine). **(a)** α-tubulin and β-tubulin associate and form heterodimers which, under conditions dictated by the cytosol, begin to form microtubules, a process called polymerization. A string of heterodimers, which have α-tubulin at the (-)end and β-tubulin at the (+)end, are known as protofilaments. A microtubule consists of 13 protofilaments, which acquire the conformation of a non-uniform cylinder with a diameter of 24 nm. The process of dissociating heterodimers is called depolymerization. **(b)** In cancer cells, inhibition of polymerization by vinblastine occurs at the level of microtubules involved in the coordination of mitosis/meiosis and in low concentrations, it associates with free β-tubulin in the cytosol, promoting self-association or **(c)** it binds to β-tubulin at the GTP end and prevents polymerization. **(d)** In high concentrations, vinblastine promotes premature depolymerization of microtubules.

Studies have demonstrated that, in addition to vinblastine, several other alkaloids and medications can also interact with the identified vinca domain (Jordan *et al.*, 2007; Zhou *et al.*, 2005), although it is unknown as of yet whether vincamine also does so. Vincamine is a supplement used in the treatment plans of stroke patients (Du *et al.*, 2019; Liu *et al.*, 2015). Although numerous other studies (Fandy *et al.*, 2016; Hasa *et al.*, 2013a; Hasa *et al.*, 2013b; Wang *et al.*, 2020; Wu *et al.*, 2018) have revealed the positive effect of this alkaloid, prior investigations have frequently indicated the cytotoxicity of *Vinca* extracts (Table 5).

Table 5. The cytotoxic effects of *Vinca* extract and/or other natural compounds of *Vinca* species

Vinca extracts	Chemical composition	*In vitro* assays on normal cells		*In vitro* assays on cancerous cells		Reference
		Cell type	IC_{50}	Cell type	IC_{50}	
V. minor	Total alkaloids	NIH/3T3	3.32 µg/mL	HT29	3.63 µg/mL	(Khanavi *et al.*, 2010)
				Caco2	0.62 µg/mL	
				T47D	1.34 µg/mL	
V. major	3 identified alkaloids*			HL60	>40 µM	(Zhang *et al.*, 2015)
				SMMC7721	>40 µM	
				A549	>40 µM	
				MCF7	>40 µM	
				SW480	>40 µM	
	Vincamajorine C			A549	19.8 µM	(Zhang *et al.*, 2016)
				MCF7	>40 µM	
				SW480	>40 µM	
				SMMC7721	>40 µM	
				HL60	>40 µM	
	Vincamajorine D			A549	>40 µM	
				MCF7	>40 µM	
				SW480	>40 µM	
				SMMC7721	>40 µM	
				HL60	>40 µM	
	Vincamajorine E			A549	34.8 µM	
				MCF7	>40 µM	
				SW480	>40 µM	
				SMMC7721	>40 µM	
				HL60	>40 µM	

*19-hidroxil-10-metoxi-19,20-dihidrovinorine; 19-O-acetil-10-metoxi-19,20-dihidrovinorine and 19,21α-dihidroxil-10-metioxi-19,20-dihidrovinorine.

IC_{50} = the concentration at which 50% of the cells are affected.

Numerous other researchers (Table 6) have also discovered these detrimental effects on some human cell lines because extracts of *C. roseus* have been used for their adverse effects on cancer since the beginning (Wang *et al.*, 2017). Vinblastine and vincristine are therefore used in conjunction with cytostatic medications, however some of the negative effects that have been noticed over time may also be caused by these alkaloids (Jordan *et al.*, 2007).

Table 6. Cytotoxicity of natural compounds found in *C. roseus*

Chemical composition	*In vitro* assays on normal cells		*In vitro* assays on cancerous cells		Reference
	Cell type	**IC_{50}**	**Cell type**	**IC_{50}**	
Total alkaloids	BL1395	720 ng/mL	JURKAT E.6	211 ng/mL	(Fernández-Pérez *et al.*, 2010)
			THP1	210 ng/mL	
Catharoseumine			HL60	6.28 M	(Wang *et al.*, 2012)
			CA9-KB	0.043 µg/mL	(Aslam *et al.*, 2010)
			ED50	0.043 µg/mL	
Vinflunine			U2OS	18 nM	(Okouneva *et al.*, 2003)
			CAL27	34.1 nM	(Simoens *et al.*, 2006)
			MCF7	47.2 nM	
			H292	56.3 nM	
			ECV304	93.6 nM	
	Fi360	474.1 nM			
Vinorelbine			U2OS	5 nM	(Okouneva *et al.*, 2003)
			A549	1 µM	(Chiu *et al.*, 2012)
	Murine cells*	80 µg/mL			(Rabbani-Chadegani *et al.*, 2015)
Vinblastine			U2OS	5 nM	(Okouneva *et al.*, 2003)
Vincristine			A549	14.9 nmol/L	(Chiu *et al.*, 2017)
			CL1	4.2 nmol/L	

*mice non-adherent cell types.

IC_{50} = the concentration at which 50% of the cells are affected.

1.3 Nanotechnology: metal nanoparticles synthesis methods and their importance in medicine

Technology in recent years has increasingly focused on the characteristics of materials at the micro- and nanometric scales, as well as cutting-edge synthesis techniques and transdisciplinary applications (Egorova *et al.*, 2016). This feature of nanotechnology has recently transformed the scientific community by enabling us to comprehend and control matter at the atomic and molecular level. Nanoparticles are nanometric objects with dimensions below 100 nm (Alavi *et al.*, 2018; Ganguly *et al.*, 2019) with unique optical, electrical, and magnetic capabilities (Khan *et al.*, 2016).

Numerous industries, including biomedicine, where nanomaterials are utilized as contrast agents in magnetic resonance imaging, have expanded due to the incredibly small size of nanoparticles (Gubin, 2008). A top of ceramic nanoparticles (50%), carbon nanotubes (20%), nanoporous materials (20%), metal nanoparticles, graphene, nanocapsules, and quantum dots was achieved by firms that produce nanomaterials in 2009 ("National Research Council of the National Academies," 2012).

The National Initiative for Nanotechnology in the United States of America has set aside more than 27 billion dollars over the past ten years, while the operational initiatives HORIZON 2020 of the European Commission have set aside 1.1 billion euros for this subject through the end of 2020 (European Commission; National Nanotechnology Initiative). The People's Republic of China and Japan are competing in Asia for nanotechnology, and since 2003, expenditures in both countries have increased exponentially by 20% yearly (European Commission Decision C, 2019; Grewal, 2019). This Global effort has resulted in the publication of 6193 articles between 2003- 2018 and over 2800 articles for the year 2019, only on green chemical synthesis of nanoparticles (Du *et al.*, 2018; Web of Science).

The most crucial step in the processes of creating nanomaterials is their synthesis, which determines the function, shape, application, and sustainability of the nanoparticles. The method does have some drawbacks, though, including a few understudied features and qualities and the manifestation and behavior of nanomaterials, which can have negative impacts on humans both in vitro and in vivo (Egorova *et al.*, 2016; Kharissova *et al.*, 2013). The primary obstacles to systemic medicine today include toxicity and other side effects, the necessity to provide a high dose to achieve the ideal concentration at the target level, the wide dispersion of the relevant substance, and the lack of specificity in a given disorder (Kadzinski *et al.*, 2016; Nakawaga *et al.*, 2016).

Researchers are therefore concentrating on the use of targeted therapy using nanoparticles to address these deficiencies. If the treatment can be localized, it becomes possible to monitor the medication at the level of the problem (Kadzinski *et al.*, 2016; Suciu *et al.*, 2020).

It is possible to synthesize nanoparticles (Fig. 3) both physically and chemically (Braakhuis *et al.*, 2015). This study focused on the green synthesis branch of chemical synthesis, which uses plant extracts.

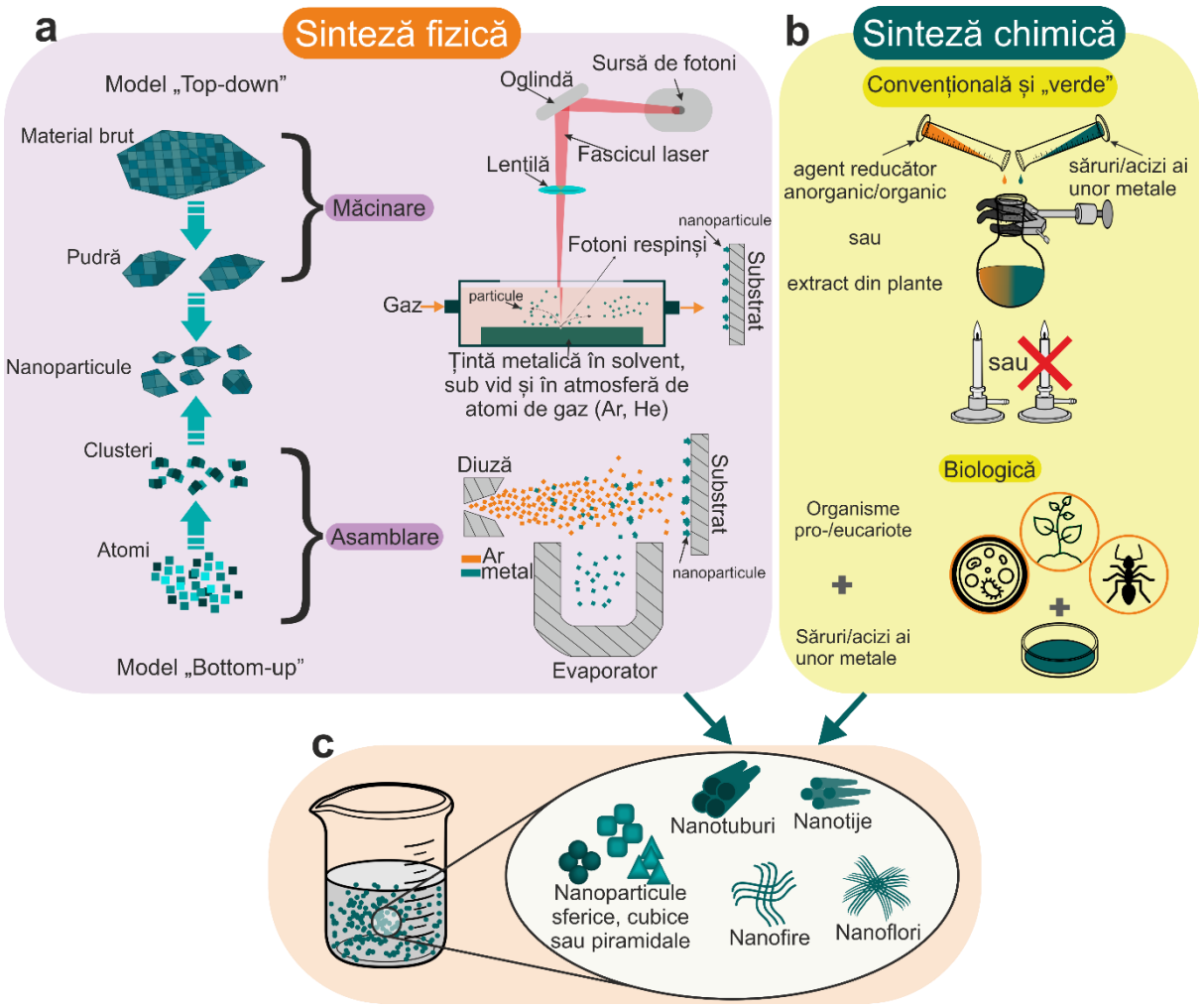

Figure 3. Representative scheme for models of physical or chemical synthesis of metal nanoparticles. **(a)** by the physical method, nanoparticles can be synthesized through the top-down model which involves grinding the raw material down to the level of nanoparticles, and under controlled conditions the dimensions of the nanoparticles can also be established (ablation of the raw material with the help of a beam laser, strong); or by the bottom-up model, which involves the assembly of atoms of some metals (in a vacuum and atmosphere of argon or any type of heavy gas); **(b)** through green or conventional chemical synthesis, nanoparticles can be synthesized from salts or acids of some metals, which are reduced in the presence of plant extracts or an-/organic solvents; another type of chemical synthesis is also the biological synthesis of nanoparticles by means of pro-/eukaryotic living organisms; **(c)** following any of the mentioned syntheses, nanomaterials of several types can result, such as polygonal nanoparticles (spherical, cubic, pyramidal, hexagonal, etc.), nano-rods, nano-tubes, nano-wires, nano-flowers, and many others.

1.3.1 Physical synthesis

The most popular methods are mechanical (grinding the raw material into micro- then nanoparticle size), thermal, or a mix of the two. The metal or semiconductor material is put in a vacuum at a pressure of 10^{-4}-10^{-8} atm in order to manage the size distribution. A saturated vapor made up of the constituent parts of the target material is created by direct heating. The atoms of the target material collide with the argon gas in an argon environment, which

causes the particles to develop quickly (nucleation phase). All atomic particles created afterwards will adhere to the nuclei that already exist (growth phase). Since cooling happens quickly when a substrate is present and growth happens quickly, the resulting nanoparticles become metastable (Braakhuis *et al.*, 2015).

1.3.2 Chemical synthesis

Aqueous or non-aqueous inorganic molecular solutions, such as hydrazine, hypophosphites, and sodium borohydride, or organic molecular solutions, such as glucose, formaldehyde, ascorbic acid, and citrates, can be used for chemical synthesis (Egorova *et al.*, 2016; Khan *et al.*, 2012; Kunkalekar *et al.*, 2012). Along with solution temperature, pH, type of reactant, and reactant concentration, reducing agents play a significant effect on the shape and size of nanoparticles (Wu *et al.*, 2009).

The method is based on the reduction of a metal's salt or acid with a reducing agent, and when the metal atoms are created in solution, the steps of nanoparticle nucleation and growth are carried out (Braakhuis *et al.*, 2015).

1.3.2.1 Green synthesis of nanoparticles using plant extracts

A technique for creating nanoparticles known as 'green chemistry' is valued for its high yield and low cost. It uses less harmful and renewable materials while consuming little energy (Kadzinski *et al.*, 2016).

Plant extracts can be utilized to create *de novo* nanoparticles as well as to functionalize those created by other physical or chemical processes outside green chemistry. Over time, different plant extracts of all kinds have been used to create metallic nanoparticles (Hanan *et al.*, 2018) of varied shapes and sizes, among which we highlight: *Nigella sativa* (Amooaghaie *et al.*, 2015), *Allium cepa* (Cvjetko *et al.*, 2017; Gomaa, 2017), *Aloe barbadensis* (Gunalan *et al.*, 2012), *Berberis vulgaris* (Anzabi, 2018; Behravan *et al.*, 2019; Nasrollahzadeh *et al.*, 2015), *Trichosanthes tricuspidata* (Yuvarajan *et al.*, 2015), *Chelidonium majus* (Alishah *et al.*, 2016; Dobrucka *et al.*, 2017), *Coleus sforskohlii* (Naraginti *et al.*, 2016; Naraginti *et al.*, 2014), *Coptis chinensis* (Ahmad *et al.*, 2017), etc.

Despite being a significant medicinal plant, *Vinca* extracts have not showed much interest in the nanoparticles' synthesis. There was only one study found: Maincent *et al.* (1984) tested the absorption and dispersion of nanoparticles in vivo in rabbits using vincamine (Maincent *et al.*, 1984). On the other hand, *Catharanthus roseus* extract was successful in synthesizing silver nanoparticles (Sharma *et al.*, 2014).

1.3.2.2 Biological synthesis

Often pro- and eukaryotic microorganisms, but also complex plant organisms, are used in this sort of synthesis. Through their metabolic processes, these organisms take metal salts, which they then convert into nanoparticles (Dar *et al.*, 2013; Fayaz *et al.*, 2010). However, there is still misunderstanding among scientists because the phrase 'green synthesis' is sometimes used to refer to chemical synthesis involving extracts (Nasrollahzadeh *et al.*, 2018; Ogunyemi *et al.*, 2019;

Sathyavathi *et al.*, 2010; Singhal *et al.*, 2011; Veerasamy *et al.*, 2011) also for in vivo synthesis (Cauerhff *et al.*, 2013). As we regard in vivo synthesis to be biosynthesis in this paper, we shall employ green synthesis for synthesis using plant extracts.

Ascomycete fungi are a popular and affordable alternative for biosynthesis, although this approach has a number of drawbacks (Barabadi *et al.*, 2014). By generating mycotoxins, which can later cause allergies, skin conditions, or lung problems, mushrooms employed in biosynthesis pose a serious threat to staff contamination (Barabadi *et al.*, 2014).

Biosynthesis can be carried out extracellularly or intracellularly. The size and distribution of the resulting nanoparticles can be regulated through extracellular biosynthesis, and they are extracted from the environment by centrifugation in a manner akin to chemical synthesis. This approach allowed for the production of metallic nanoparticles using fungi such: *Aspergillus flavus* (Vigneshwaran *et al.*, 2007), *A. fumigatus* (Bhainsa *et al.*, 2006), *Fusarium acuminatum* (Ingle *et al.*, 2008), *F. semitectum* (Basavaraja *et al.*, 2008), *F. oxysporum* (Ahmad *et al.*, 2003; Durán *et al.*, 2005), *Penicillium crustosum* (Barabadi *et al.*, 2014), *P. chrysogenum*, *P. expansum* (Mohammadi *et al.*, 2015), *P. phellutanum* (Kathiresan *et al.*, 2009), or *Phoma glomerata* (Birla *et al.*, 2008).

Also bacteria such as *Aeromonas hydrophylla* (Jayaseelan *et al.*, 2012), *Bacillus subtilis* (Saifuddin *et al.*, 2009), or *Actinobacter* spp. (Bharde *et al.*, 2008) can be used for metal nanoparticle biosynthesis.

1.3.3 Silver and Mn nanoparticles: pro's and con's

Salts or oxides of some noble metals with exceptional qualities, such as gold, silver, platinum, or palladium, as well as more readily available metals like zinc, copper, manganese, or iron, are utilized in the chemical production of nanoparticles. The results are impressive in antibacterial, antifungal, or anticancer activity, and some researchers consider that the capabilities of nanomaterials can be enhanced by creating nanocomposites (combinations of 2 or more metal salts) (Ethiraj *et al.*, 2016; Naraginti *et al.*, 2016).

Silver (Ag) is a noble metal extensively studied for both its environmental impact and its therapeutic potential (Du *et al.*, 2018; Noghabi *et al.*, 2017). Recent studies bring to the fore the antitumor potential of silver nanoparticles on some types of cancer such as: MCF-7, breast cancer (Salaheldin *et al.*, 2019), A549, pulmonary cancer (Anandan *et al.*, 2019), HCT116, colon cancer (Naraginti *et al.*, 2017), HepG, hepatocellular carcinoma (Gopinath *et al.*, 2017) or AGS, gastric cancer (Mousavi *et al.*, 2018). Since manganese (Mn) is a crucial micronutrient, Mn nanoparticles have a lot of potential uses in biology (Soejima *et al.*, 2018). However, when produced chemically, Mn nanoparticles can have negative effects (Negahdary *et al.*, 2019), therefore employing plant extracts as a synthetic agent is a less hazardous option (Asaikkutti *et al.*, 2016; Moon *et al.*, 2014; Nair Sreekala *et al.*, 2019).

Additionally, some investigations have shown that Ag ions might have damaging effects on non-cancerous human cell types as well (Butler *et al.*, 2015). Silver and manganese have therefore been combined for research purposes (Bai *et al.*, 2016; Guan *et al.*, 2018), and it has been demonstrated from a biological perspective that silver ions can stabilize in the presence of MnO_2 (Kunkalekar *et al.*, 2012), lowering cellular cytotoxicity.

2 Personal contribution

2.1 Materials and methods

2.1.1 Equipment and software

2.1.1.1 Light microscope

Olympus BX51 microscope coupled with CCD camera, from the 'Constantin Crăciun' Electron Microscopy Center (EMC) from the Biology and Geology Faculty, BBU, Cluj-Napoca.

2.1.1.2 Electron microscopes

Electron microscopes use a vacuum electron beam, and the magnetic or electrostatic lens system that replaces the optical lenses in photon microscopy. There are two main types of electron microscopes, classified by the information they provide. By combining the two types of microscopes, other models can be obtained that also combine the type of information provided, and by coupling with various other attachments (photon beams of different wavelengths – fluorescence, X-rays, etc.), one can complete information about the studied specimen.

- Scanning Electron Microscope

Scanning electron microscope (SEM) Hitachi SU8230 coupled with EDX detector and AZtec software (Oxford Instruments), from Integrated Electron Microscopy Laboratory (LIME) of National Institute for Research and Development of Isotopic and Molecular Technologies (INCDTIM), Cluj-Napoca.

- Transmission Electron Microscope

Transmission electron microscope (TEM) Hitachi HD2700 operated at 200 kV, coupled with double EDX detector and AZtec software (Oxford Instruments) from LIME-INCDTIM and TEM Jeol JEM 1010 operated at 80 kV with MegaView III camera, from EMC-BBU, Cluj-Napoca.

The samples were prepared using Leica UC6 and Leica UC7 ultramicrotomes, DiATOME diamond knife and Quorum Q150T ES coating sputter, from EMC-UBB and LIME-INCDTIM.

2.1.1.3 High Performance Liquid Chromatography

Agilent 1200 HPLC system, from Chemistry Faculty of BBU, Cluj-Napoca.

2.1.1.4 Spectrophotometers and diffractometers

Bio-Tek EPOCH spectrometer and Gen5 software from INCDTIM, Cluj-Napoca; Tecan SPARK 10M spectrometer from Chemistry Faculty of BBU, Cluj-Napoca; JASCO 6100 Fourier Transformed InfraRed (FTIR) spectrometer and X-ray SmartLab diffractometer, operated at 9 kW SmartLab Guidance software, from INCDTIM, Cluj-Napoca.

2.1.1.5 Other software used

Python 3.8.6 available online; MATLAB R2019b, Image J Java 8 available online; CorelDRAW X8, free trial; Adobe Photoshop CS6, Adobe Ilustrator CS6 and MS Ofice365, from BBU available through POCU/360/6/13/123886 program; OriginPro Lab 2016 b9.3.226, free trial.

2.1.2 Plant material

The samples were collected from 'Alexandru Borza' (UBB) Botanical Garden, in Cluj-Napoca, Romania, during the flowering seasons (April, May, and September) of 2017-2019. The plants were authenticated by Prof. Dr. Marcel Pârvu, each with a voucher registered in the Botanical Garden Herbarium:

- Voucher CL 665977 for *V. minor* L. (Fig. 4);
- Voucher CL 668019 for *V. major* L. (Fig. 5);
- Voucher CL 668018 for *Vinca major* L. var. *variegata* 'Loudon' (Fig. 6);
- Voucher CL 668021 for *Vinca herbacea* Waldst. and Kit. (Fig. 7);
- Voucher CL 668782 for *Catharanthus roseus* (L.) G. Don cv. Pacifica (Fig. 8);
- Voucher CL 663692 for *Chelidonium majus* (Fig. 9).

Figure 4. *Vinca minor*: aerial parts; April 2018, ('A. Borza' Botanical Garden, Cluj-Napoca, Romania).

Figure 5. *V. major*: aerial parts, May 2018; ('A. Borza' Botanical Garden, Cluj-Napoca, Romania).

Figure 6. *V. major* var. *variegata*: aerial parts, March 2018; ('A. Borza' Botanical Garden, Cluj-Napoca, Romania; image taken by dr. M. Parvu and published with his approval).

Figure 7. *V. herbacea*: aerial parts, April 2018; ('A. Borza' Botanical Garden, Cluj-Napoca, Romania).

Figure 8. *C. roseus* cv. Pacifica: aerial parts, September 2019 (A), September 2020 (B); Cluj-Napoca ('A. Borza' Botanical Garden, Cluj-Napoca, Romania; images taken by dr. M. Parvu and published with his approval).

Figure 9. *Chelidonium majus*: aerial parts, April 2018; ('A. Borza' Botanical Garden, Cluj-Napoca, Romania).

2.1.3 The morphological and ultrastructural analysis of the leaf

The leaf is frequently the principal organ employed in the production of herbal extracts (Andrade *et al.*, 2017). As a result, we valued the morphological and ultrastructural examination of a sample of plant leaves that would subsequently be used to produce the extracts. Harvested leaves were examined on both sides, in the region of the midvein or a secondary vein, using light, scanning, and transmission electron microscopes. To identify the key distinctions and similarities between the leaves of the plants employed, morphometric analyses were initiated.

2.1.3.1 Leaf harvesting

Thea leaves were collected from each mature plant's mid-stem region. Immediately after harvest, glutaraldehyde (GTA) solution was applied to the mid-zone of the cut leaf limb.

2.1.3.2 Scanning electron microscope

The leaves were left with 2.7% GTA in 0.1 M phosphate buffered saline (PBS) for 1 h, after which they were washed three times with PBS, 1 h each (Ciorîță *et al.*, 2021b). The samples were then dehydrated according to the following routine (the first three steps were done at 4°C):

- 30% acetone in ultrapure water: 1 h;
- 50% acetone in ultrapure water: 1 h;
- 70% acetone in ultrapure water: 1 h;
- 100% acetone: 1 h × 3 times.

The samples were immersed for an hour each in a 1:1 mixture of hexamethyldisilazane (HMDS) and anhydrous acetone to retain the structure as close to its unaltered condition as feasible.
The samples were analyzed with a Hitachi SU8230 SEM after being metallized with a 9 nm coating of gold using a Quorum Q150T ES metallizer in LIME-INCDTIM, Cluj-Napoca, Romania.

Equations 1 and 2 allow for the calculation of metrics like trichome density (DT), stomatal density (DS), stomatal index (IS), and stomatal aperture index (IAS) based on the pictures collected (Liu *et al.*, 2019; Royer, 2001):

$$\mathrm{IS}(\%) = \frac{\mathrm{DS}}{\mathrm{DS+E}} \times 100 \quad \text{Equation 1}$$

Where: DS = stomatal density (number of stomata in 1 mm^2), E = epidermal cells density in the same surface unit.

$$\mathrm{IAS}(\%) = \mathrm{DS} \times \mathrm{LS}^2 \times 10^{-4} \quad \text{Equation 2}$$

where: LS = the length of stomatal aperture (calculated for six randomly dispersed stomata).

2.1.3.3 Light microscopy

After harvest, the samples were cut into ~3 mm × 1 mm × 0.5 mm pieces, near a secondary vein. The samples were placed in 2.7% GTA for 1 h, washed with PBS four times of 1 h each, and counter-fixed with osmium tetroxide (OsO_4). The OsO_4 was left on the samples for 1.5 h and then washed with PBS four times, 1 h each.
Dehydration was conducted as following:

- 30% acetone in ultrapure water: 1 h;
- 50% acetone in ultrapure water: 1 h;
- 70% acetone in ultrapure water: 1 h;
- 80% acetone in ultrapure water: 30 min.;
- 90% acetone in ultrapure water: 30 min.;
- 100% acetone 30 min × 3 times.

Epon 810 resin was used for gradual infiltration. The samples were polymerized for 72 h, at 60°C. The blocks were modeled with Leica UC6 ultramicrotome and glass knives. The semithin sections had 200-400 nm thickness. The sections were placed on glass slides, thermally fixed and stained with Epoxy Tissue Stain. Olympus BX51 light microscope was used. These steps took place at EMC-UBB, Cluj-Napoca.
It was possible to determine various aspects of the leaf anatomy using the light microscopy pictures, including the cell tension ratio (RTC) and the spongy parenchyma tension ratio (RS) in accordance with equations 3 and 4 (Liu *et al.*, 2019):

$$\mathrm{RTC}(\%) = \frac{\mathrm{PTT}}{\mathrm{GF}} \times 100 \qquad \text{Equation 3}$$

where: PTT = pallisadic tissue thickness, GF = leaf thickness.

$$\mathrm{RS}(\%) = \frac{\mathrm{STT}}{\mathrm{GF}} \times 100 \quad \text{Equation 4}$$

where: STT = spongy tissue thickness.

2.1.3.4 Transmission electron microscopy

The blocks obtained in subchapter 2.1.3.3, were used to obtain 80-100 nm thick sections, using a DiATOME diamond knife and Leica UC7 from LIME-INCDTIM, Cluj-Napoca. The samples were placed on Cu grids of 100 mesh and stained with uranyl acetate and lead citrate. TEM Jeol JEM 1010, from EMC-UBB, Cluj-Napoca was used for examination.

2.1.3.5 Computational analysis

A computational approach was developed to estimate the ratio between intercellular gaps and cells, in partnership with the Faculty of Mathematics and Informatics at UBB, Cluj-Napoca (Dr. Mircea Gabriel). The intercellular areas could be quantified using semi-thin sections. Each region of interest was colored differently: cellular region - green; intercellular region - gray; epidermis - blue; leaf exterior - yellow. Intercellular spaces were manually determined using an image processing application (Photoshop, version 13.0). Epidermises were not included in the final computation because they are not a component of the leaf mesenchyme. The images were then converted into a Python script (version 3.8.6) that quantified the pixels according to the color they possessed before determining the proportion of green pixels to gray pixels (intercellular space).

2.1.4 Plant extract preparation

Cold repercolation was used for plant extract preparation (Pârvu *et al.*, 2011b). The leaves of *Vinca* and *C. roseus* were used in the process, while the total herbal material was used for *C. majus*. The plant material was washed with distilled water, chopped and weighed. The extracts were obtained by Dr. Marcel Pârvu, within the Mycology Laboratory, UBB-Cluj-Napoca and stored in brown glass containers at 4°C until their use in subsequent experiments.

2.1.5 Phytochemical composition determination

All extracts were analyzed using the Tecan SPARK 10M spectrophotometer and the Agilent 1200 HPLC system, from the Faculty of Chemistry of UBB, Cluj-Napoca. The analyzes were carried out under the guidance of dr. Augustin Moț and together with drd. Cezara Zăgrean-Tuza.

2.1.5.1 High performance liquid chromatography

According to a prior work, chromatographic separation and detection were carried out under regulated pressure and temperature conditions (Andreicut *et al.*, 2018). A quaternary pump that regulates the mobile phase's flow

rate was used to automatically inject the samples. A Zorbax SB-C18 column (250 mm × 4.6 mm, 5 µm particle size) was used for chromatographic separation, and a DAD detector allowed for detection. The column was heated to 30°C, and 8 µL of plant extract was injected at a flow rate of 1 mL/min.

Ultrapure water was solvent A and acetonitrile was solvent B. The standards used were: 3,4-dihidrobenzoic acid, 4-hidroxibenzoic acid, caffeic acid, chlorogenic acid, ferulic acid, p-coumaric acid, syringic acid, berbamine, berberine, galangin, isoquercitrin, jatrorrhizine, kaempferol, myricetin, palmatine, quercetin, quercitrin, rutin, vinblastine and vincamine. Every two seconds, the DAD detector took measurements of the whole spectrum between 210 and 600 nm (Farcaș *et al.*, 2018).

2.1.5.2 Total polyphenols and flavonoids

a. The Folin-Ciocâlteu method was used to calculate the total content of polyphenols: 25 µL of each plant extract was combined with 25 µL Folin-Ciocâlteu reagent and 200 µL of ultrapure water. The solution was incubated for 5 min. Na_2CO_3 was added at 25 µL volume (stock concentration: 10.6 g/100 mL) and incubated for 60 min in the dark. The absorbance was measured at 725 nm, while gallic acid was used as standards in the 2-40 µg/mL concentration range (Blainski *et al.*, 2013).

b. $AlCl_3$ complexation was used to determine the total flavonoid content: 10 µL of each plant extract was combined with 50 µL of 2% $AlCl_3$ and 50 µL of 1 M sodium acetate in 140 µL ultrapure water. After 5 min, 50 µL of 0.1 mM HCl solution was added. After an additional 20 min, the absorbance was measured at 452 nm. Rutin was used as calibration standard at 1.6-50 µg/mL concentration range (Pękal *et al.*, 2014).

2.1.5.3 Total alkaloid content

In this study, the Dragendorff method was adapted and optimized to assess total alkaloid content. The solutions used: (1) $Bi(NO_3)_3$ at a concentration of 43.8 mM and tartaric acid at a concentration of 1.66 M, and (2) KI at a concentration of 2.4 M in ultrapure water. 30 µL of each plant extract and 10 µL of glacial acetic acid were added to 260 µL of this reagent after 5 mL of the first solution and 2 mL of the second solution were combined. At 560 nm, optical density was observed (Sreevidya *et al.*, 2003).

2.1.6 Antioxidant activity determination

The following methods were used to determine the antioxidant activity:

a. DPPH: 10 µL of each extract were combined with 15 µL of DPPH reagent and 285 µL 50% ethylic alcohol. The absorbance was measured in the beginning and after 20 min at 517 nm. Rutin was used as standard (stock 83 mg/mL) (Sharma *et al.*, 2009).

b. REAC: the ABTS anionic radical was prepared by combining 5 mM ABTS reagent with 59 nM *Cucurbita pepo* peroxidase and 1.3 mM hydrogen peroxide in 50 mM sodium acetate buffer solution, at 5.5 pH. 290 µL of this solution were mixed with 10 µL plant extract. The absorbance was

measured after 30 min at 730 nm. Rutin was used as standard at 3-23 μg/mL concentration range (Alam *et al.*, 2013).

c. CUPRAC: 2 mM neocuproine solution, 1 mM $CuSO_4$ pentahydrate and 1 M ammonium acetate (pH 7) were incubated together for 10 min. From this solution, 190 μL was incubated with 100 μL of ultrapure water and 10 μL of each extract. The absorbance was measured after 10 min. at 450 nm and the calibration curve was made using rutine standard in the concentration range 3-14 μg/mL (Ozyurek *et al.*, 2011).

d. Lipid peroxidation: 0.2 mg/mL liposomes in PBS (pH 7.4) were sonicated for 30 min. to homogenize the solution. From this solution, 290 μL was incubated with 10 μL of the analyzed plant extract, and the reaction was triggered by the addition of cytochrome C, in a final concentration of 2 μM. The kinetics of the reaction was measured at 235 nm, and the standard used was rutin in the range of 0.067-2.3 μg/mL concentrations (Moț *et al.*, 2016).

2.1.7 Antibacterial activity determination

It is advised that the antibacterial potential of an improved or newly synthesized chemical be assessed in accordance with the current EUCAST regulations ("European Committee on Antimicrobial Susceptibility Testing," 2020). The antibiogram or the diffusimetric approach, then, is the accepted procedure for determining how susceptible a particular bacterial strain is to a chemical (Matuschek *et al.*, 2014). Using the plate microdilution method, the minimum inhibitory concentration (MIC) is determined (EUCAST, 2020c). We employed Mueller-Hinton (MH) agar growth medium for the diffusimetric approach, and the strains were inoculated at a typical turbidity of 0.5 McFarland.

Depending on the strain, the plates were incubated for 18 ±2 hours at 35°C ±1°C in an aerobic or anaerobic condition (EUCAST, 2020a). The interpretation was made based on the tables that the same source gave (EUCAST, 2020b).

A Gram-negative (*Escherichia coli*, ATCC 25922) and a Gram-positive (*Staphylococcus aureus*, ATCC 25923) strain were used in the experiments. The antibacterial activity was determined by the diffusimetric method and by the microdilution method (Carpa *et al.*, 2014).

2.1.7.1 Diffusimetric method

E. coli and *S. aureus* were incubated with MH media for 24 h in Petri dishes. Plates were swabbed with a clean cotton swab and incubated at 37°C for one hour (Jyoti *et al.*, 2018). Then, wells with a diameter of 6 mm were cut in the MH agar medium-coated plates with infiltrating bacterial strains. These wells were then loaded with 150 μL of the examined plant extract and small, sterile cotton balls (Valgas *et al.*, 2007). A blank of 30% ethyl alcohol and ciprofloxacin positive control (0.1%) were included on the plates. Samples were evaluated after being incubated for 24 hours at 37°C.

2.1.7.2 Microdilution method

E. coli and *S. aureus* 24 h bacterial cultures were adjusted to 0.5 McFarland standard in PBS or 0.85% physiological serum. The 96 well plates were inoculated as following: 100 µL MH media/well, first row of wells were then inoculated with 100 µL plant extract and two-fold dilutions were afterwards conducted. The final concentrations were from 0.09-50%. The bacterial strains were added at the end, 10 µL each, of 5×10^5 CFU/mL final concentration (colony forming units). An untreated control and a ciprofloxacin 4.5% positive control were both included on each plate. To interpret the findings, separate controls using alcohol and plant extracts in a media devoid of microorganisms were carried out. The plates were incubated for 24 hours at 37 °C. Using the Bio-Tek EPOCH spectrophotometer and Gen5 software from INCDTIM, Cluj-Napoca, absorbances were read at a wavelength of 600 nm.

Bacterial inhibition was expressed as a percentage calculated according to Equation 5 (ISO10993-5:2009(E), 2009):

$$\text{Inhibition (\%)} = \frac{\text{absorbance (nm)}}{\text{untreated control absorbance (nm)}} \times 100 \qquad \text{Equation 5}$$

2.1.7.3 Morphological modification induced in bacteria by the used plant extracts

A To ascertain how the plant extracts affect the bacterial cells of *E. coli* and *S. aureus*, morphological investigation by SEM was conducted. Sample preparation followed a methodology that was improved for this investigation (Erlandsen *et al.*, 2004). In order to centrifuge the bacteria for five minutes at 5000 revolutions per minute (rpm) at room temperature, the bacteria were treated for 24 hours at the CMI established using the procedure given in section 2.1.8. The bacterial pellet was then resuspended in 0.5% alcian blue solution, 2% GTA solution, and 2% PFA (paraformaldehyde) solution in 0.15 M PBS after the supernatant was removed. Three PBS washes were done after the seven hours of fixation. Acetone was used to dehydrate the subjects at escalating concentrations (30%, 50%, 70%, 80%, 90%, and 100%). After that, samples were post-fixed with HMDS in acetone:HMDS ratios of 1:1 and 1:0 for 1 hour. Each phase of the process was followed by centrifugation at 4 °C (5 min. at 5000 rpm). 5 µL of the bacterial suspension was poured onto formvar-coated copper grids for screening (200 mesh).

The grids were attached to aluminum stubs, gold-plated, and then analyzed with a Hitachi SU8230 SEM. (Ciorîță *et al.*, 2021c; Erlandsen *et al.*, 2004).

2.1.7.4 Computational analysis

To determine the degree of alteration in the dimensions of *E. coli* bacilli using computational analysis, the extract of *V. minor* was used (Belean *et al.*, 2020). Therefore, measurements were made of bacteria from the untreated control, bacteria treated with 3% concentration of plant extract (the MIC value established by the prior analyses), and bacteria treated with 25% concentration of plant extract (the highest concentration tested in the beginning analyses). Dr. Gutt Robert, INCDTIM, developed a script in the MATLAB application that allowed for the automatic quantification of *E. coli* bacteria based on the SEM images of the bacteria. In the lower right corner of

the obtained images is a scale that represents the actual size of the images. It is simple to calculate the number of pixels in the image that correspond to the specified unit of measurement because the position and size of the gradations are fixed. The "Optical Character Recognition" (OCR) procedure is used to identify the value and the unit of measurement associated with the image after the program selects the area of the image where the unit of measurement is present. The scale from the image is chosen in the second section of the program, and by summing the columns that correspond to the vertical axis, a matrix is created in which the highest values match the scale's gradations. The number of pixels that make up a gradation is determined by the matrix's first two maxima (Fig. 10).

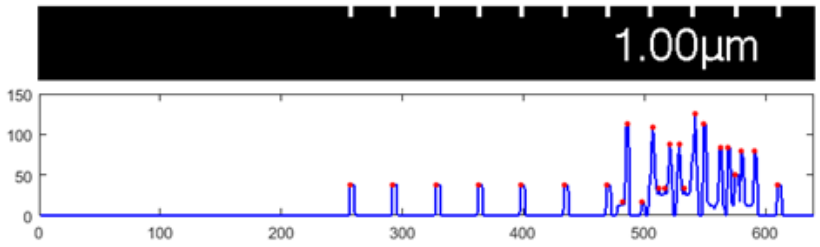

Figure 10. Determining the number of pixels associated to one measuring unit.

For the purpose of defining the maximum sizes of the bacteria, a precise and clear outline is necessary. However, this stage is also the most challenging because numerous parameters need to be modified in order to get the right contour. The photos' contrast and brightness make automation more challenging, thus in order to solve these issues, the intensities of the photographs are normalized in comparison to a reference image, and this feature is taken into consideration when developing the code (Belean *et al.*, 2020). The contour of the bacterium (Cbac) is represented by the zero-level set of the level function (LSF) defined by ϕ (x, y, t) for each rectangular region Rbac (area of interest enclosing a single bacteria), using equation: $C_{\mathrm{bac}} = \{(\mathrm{x}, \mathrm{y}) : \phi\ (\mathrm{x}, \mathrm{y}, \mathrm{t}) = 0\}$.

Identifying the contour: the partial differential equation (PDE), also known as the level set evolution problem, is transformed from Cbac to finding the solution. F is the velocity function that governs the motion of the curve.: $\frac{\partial \phi}{\partial t} = F|\nabla \phi|$ (Li *et al.*, 2010).

The selection of the Rbac region of interest, which encloses each bacterium, determines the rectangular contour represented by the function ϕ (x, y, 0), which is the beginning condition for the LSF. Thus, the edge separating the bacterium from its local background is represented by the resulting LSF function ϕ (x, y, t), where t is the number of iterations (Fig. 11 a). The zero level ϕ(x, y, t) set for each Rbac is established (Belean *et al.*, 2020; Li *et al.*, 2010).

The binary picture obtained from the zero level of the LSF may have some spots or lines as a result of the inhomogeneity that may be present on the surface of the bacterial membrane or on the image's background. Their removal is accomplished using an established method in image processing to get

rid of artifacts larger than a predetermined threshold. To determine the bacterium's length or width, the final image is used (Fig. 11 b-c).

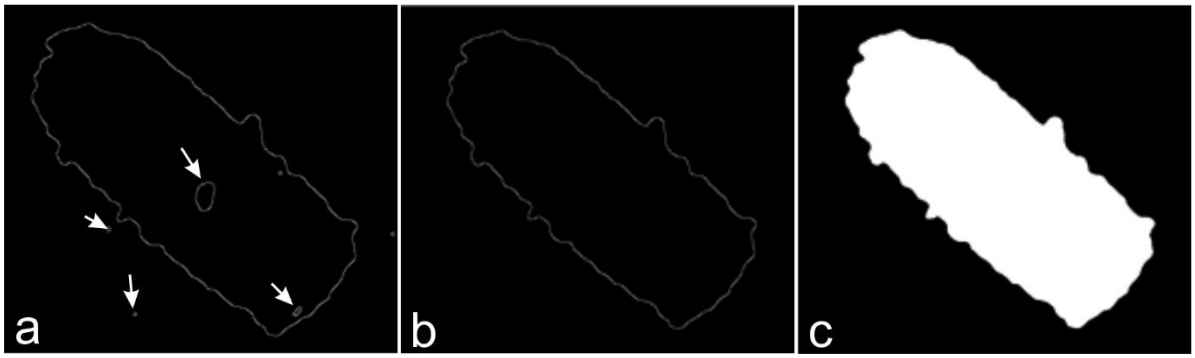

Figure 11. *E. coli* bacterial cell: **(a)** bacterial contour estimation; **(b)** bacterial contour after resolving the artefacts, **(c)** binary image of one bacterial cell.

2.1.8 Cytotoxicity determination

International Standard ISO 10993-5/2009 states that one or more quantitative and/or qualitative techniques that evaluate cellular degeneration at the morphological level, measure cellular degeneration and growth, and evaluate specific aspects of cellular metabolism can be used to determine the cytotoxicity of a compound in vitro (ISO10993-5:2009(E), 2009).

Cell viability is measured by the 3(4,5-dimethylthiazol-2-yl)-2,5-diphenyltetrazolium bromide (MTT) cytotoxicity assay. The MTT reagent is turned from yellow to blue-violet, and the quantity of live cells can be determined by correlating the color's intensity with spectrophotometric measurements. The tested substance is not cytotoxic for absorbance values equal to 80% of cell viability, weakly toxic for absorbance values between 60% and 80%, moderately toxic for absorbance values between 40% and 60%, and extremely toxic for absorbance values below 40% (ISO10993-5:2009(E), 2009).

The lactate dehydrogenase (LDH) test can be used to check the integrity of cell membranes. Cytotoxicity can be determined by spectrophotometrically detecting the amount of LDH released by damaged cells. The underlying idea is based on LDH's ability to catalyze the reaction: $NADH + piruvate \xrightarrow{LDH} NAD^+ + lactate$, where NADH is reduced to β-nicotinamide adenine dinucleotide (Han *et al.*, 2011). Thus, the degree of cell inhibition, necrosis, and/or apoptosis can be assessed depending on the equation employed to measure the concentration of LDH in the culture medium in which the treated cells were placed (Macavei *et al.*, 2016).

Nitric oxide (NO) measurement in the culture media was another technique used to detect in vitro cytotoxicity. NO is engaged in a variety of physiological and pathological processes, but its presence can signal both the suppression of tumor growth by triggering cell apoptosis and the inhibition of cell death by apoptosis (Levytskyy *et al.*, 2004). It is advised to correlate the outcomes of additional cytotoxicity tests with the results of the NO detection tests as a consequence (such as MTT and LDH). The Griess reaction creates a molecule that can be read at a wavelength of 540 nm when N_2O_3 (the nitrosating agent) created by the autoxidation of NO, bonds to sulfanilamide and produces a diazonium ion (Bryan *et al.*, 2007).

Human melanoma (A375, ATCC CRL-1619) and immortalized normal human cells (HaCaT keratinocytes, CLS-300493) were used to test the cytotoxicity of plant extracts in vitro. The *V. minor* extract was tested four times (at 24, 48, 72, and 96 hours), and the studies with the other plant extracts from this study were started based on the findings with this extract. Therefore, HaCaT cells and A375 cells received treatments with the plant extracts for 48 and 72 hours, respectively.

2.1.8.1 Cell viability assay

For 24 hours, cell cultures were attached in an anaerobic environment at 37°C and 5% CO_2 on 96-well culture plates. A375 cells and HaCaT cells were injected at 10^4 cells per well and 12×10^3 cells per well, respectively (Ciorîță *et al.*, 2020; Macavei *et al.*, 2016). Following attachment, the medium in the wells was replaced with medium containing plant extract at progressively higher concentrations (0.09%, 0.5%, 1%, 2%, and 3%) and placed back into the incubator for 48 or 72 hours.

The plant extract culture medium was withdrawn once the experiment's allotted time had passed, and 100 µL of MTT solution (with a concentration of 0.5 mg/mL/well) was then added. The plates were placed back into the incubator for 1.5 hours, as directed by ISO 10993-5:2009(E) (ISO10993-5:2009(E), 2009). Cells were lysed using acidified iso-propanol (25 mM HCl), and the absorbance of the resultant substance was assessed using a Bio-Tek EPOCH plate reader and Gen5 Plate Reader software. Each plate had untreated cells for the positive control, sterility controls, background signal (such as plain medium, medium plus extracts, etc.), ethyl alcohol controls, and a final concentration of 2% of Tween 20 detergent for the negative control. Each concentration was tested six times.

Cell viability was calculated according to Equation 6 (ISO10993-5:2009(E), 2009), and IC_{50} was calculated according to Equation 7:

$$\text{Viability (\%)} = \frac{\text{absorbance (nm)}}{\text{untreated control absorbance (nm)}} \times 100 \qquad \text{Equation 6}$$

$$x = \frac{y-c}{m} \qquad \text{Equation 7}$$

where x = median concentration, y = 50%, m = the coefficient calculated following the exponential calibration of the data, and c = calibration constant.

2.1.8.2 Lactate dehydrogenase release

Plant extract culture medium resulted from the MTT assay was analyzed to investigate cell membrane integrity. In a new 96-well plate, the following solutions were added: 50 µL plant extract medium, 50 µL 50 mM lithium lactate, 50 µL 200 mM Tris at pH 8, and 50 µL NAD (ionitrotetrazolium violet, phenazine methosulfate and nicotinamide-dinucleotide). The absorbance of LDH was measured at a wavelength of 490 nm and the value was calculated according to Equation 8:

$$\text{LDH (\%)} = \frac{\text{(sample absorbance)}-\text{(untreated control absorbance)}}{\text{(negative control absorbance)}-\text{(untreated control absorbance)}} \times 100 \quad \text{Equation 8}$$

2.1.8.3 Griess assay

The concentration of NO was measured by the Griess reaction of the culture medium with plant extract from the MTT assay. The nitrosating agent N_2O_3, derived from NO and generated from the autoxidation of NO, reacts with sulfanilamide to produce the diazonium ion. This then couples with N1-NAP and forms a compound that absorbs at a wavelength of 540 nm. A volume of 50 µL of extract culture medium was incubated with 50 µL of sulfamylamide for 10 min. in the dark. N1-NAP was then added and incubated for an additional 10 min. in the dark. The samples were subsequently read at a wavelength of 540 nm.

2.1.8.4 Ultrastructure modification induced in HaCaT and A375

In order to observe the cells' caused alterations at the ultrastructural level, they were prepared for TEM inspection in accordance with a methodology that had been made particularly effective in a prior study (Macavei *et al.*, 2016). In order to do this, HaCaT and A375 cells were cultivated on glass slides for 24 hours, reaching a confluence of 3×10^4 cells per slide, and then incubated with plant extracts at a final concentration of 3% for the same amount of time under anaerobic circumstances. After this time, the cells were fixed with 3% GTA in 0.1 M PBS for 1.5 h before the culture media was replaced. The samples were then fixed with OsO_4 for one hour following four subsequent PBS washes that were separated by 15 minutes between each stage.

The samples were dehydrated with increasing concentrations of acetone (30%, 50%, 70%, 80%, 90%, 100%, 15 min each stage) after a further series of four successive PBS washes lasting 15 minutes each, and then they were infiltrated with Epon 812 in increasing concentrations (1:2, 1:1, 1:0 with acetone). The resulting coverslips were then put on silicone capsules containing pure Epon 812, totally submerging the cells in the resin (Fig. 12), and polymerized at 60°C for 72 hours.

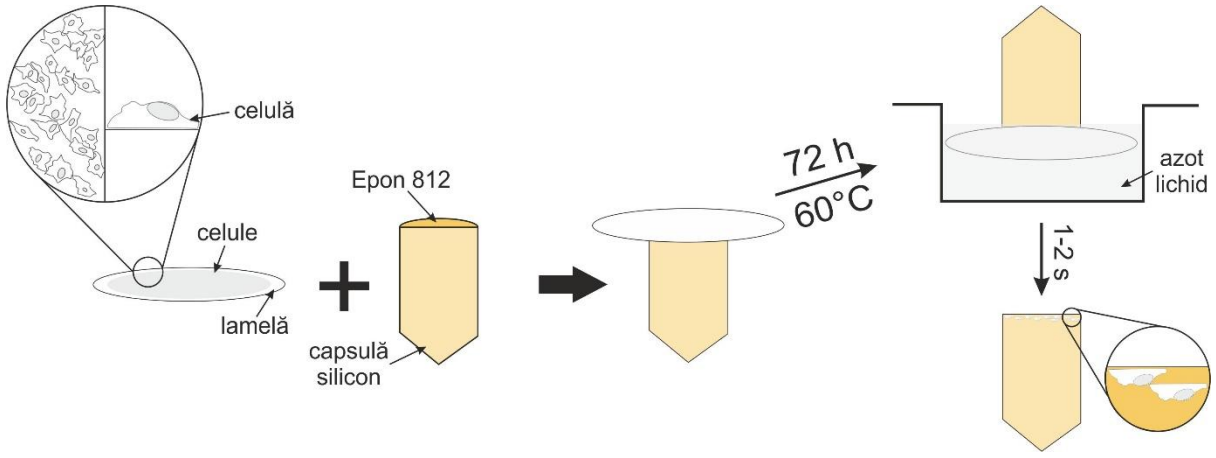

Figure 12. Schematic representation of the method of processing cells for examination by TEM – mounting the glass slide on the silicone capsule and the step of detaching it. Once the cells are completely dehydrated and still attached to the glass slide, it is placed face down (with the cells in relief) on the silicone capsule containing the Epon 812. The resin should slightly extend beyond the capsule's boundaries so that the cells are completely immersed in the resin. After 72 h of polymerization at 60°C, detach the glass slide from the silicone capsule by

thermal shock. At the end the cells will be trapped in the resin block which can later be processed to obtain ultrafine sections to be examined by TEM.

Following this break, the silicone capsule's glass coverslip was removed by creating a thermal shock (immersion in liquid nitrogen for 1-2 seconds), and the resin blocks containing the treated cells were sectioned and contrasted in accordance with the subsection's 2.1.4.4 protocol. Samples were analyzed using a Jeol JEM 1010 TEM (Ciorîță *et al.*, 2021c).

2.1.9 Reagents and kits

Table 7 presents the list of used substances, reagents, and kits:

Table 7. The complete list of reagents used in this study

No.	Reagent	No.	Reagent	No.	Reagent	No.	Reagent	No.	Reagent	No.	Reagent
1	3(4,5-dimetiltiazol-2-yl)-2,5-difeniltetrazoliumbromid	13	Gallic acid	25	Ciprofloxacin	37	Isoquercitrine	49	Neocuproin	61	DPPH
2	Ammonium acetate	14	p-coumaric acid	26	Cytochrome C	38	Isopropanol	50	Nicotinamid-dinucleotid	62	Folin-Ciocâlteu
3	Sodium acetate	15	Syringic acid	27	Lead citrate	39	Jatrorrhizine	51	Bismuth nitrate	63	Rutin
4	Uranyl acetate	16	Tartaric acid	28	Aluminum chloride	40	Kaempferol	52	Palmatine	64	Foetal serum
5	Acetone	17	Agar-agar	29	Sodium chloride	41	Lithium lactate	53	Paraformaldehyde	65	Sulfanilamide
6	3,4-dihidrobenzoic acid	18	Alcian blue	30	Dinitrogen trioxide	42	L-glutamine	54	Penicilin-streptomicin	66	Copper sulfate
7	4-hidroxibenzoic acid	19	Ethylic alcohol	31	Epon 812	43	DMEM	55	Potassium permanganate	67	Phosphate buffered saline
8	Acetic acid	20	Methyl alcohol	32	Galangine	44	Mueller-Hinton	56	Hydrogen peroxide	68	Osmium tetroxyde
9	Caffeic acid	21	Ultrapure water	33	Glutaraldehide	45	Nutrient	57	*Cucurbita pepo* peroxidase	69	Tris
10	Chlorohydric acid	22	Berbamine	34	Hexametildisilazane	46	Phenazine methosulfate	58	Quercetin	70	Vinblastine
11	Chlorogenic acid	23	Berberine	35	Potassium iodine	47	Miricetin	59	Quercitrin	71	Vincamine
12	Ferulic acid	24	Sodium carbonate	36	Ionitrotetrazolium violet	48	N-(-1-naftil)-ethylenediamine	60	ABTS		

2.2 Green nanotechnology - Ag-MnO_2 nanoparticles

Ag-MnO_2 nanoparticle synthesis and interpretation were conducted at INCDTIM, Cluj-Napoca.

2.2.1 Green synthesis

According to the given methodology (Ciorîță *et al.*, 2020), Ag-MnO_2 nanoparticles (NPs) were produced in two phases. Thus, by combining 8 mL of plant extract with 200 mg of $KMnO_4$ and 16 mL of ultrapure water, MnO_2 NPs were produced in the first step. The solution's transformation from reddish purple to dark brown after one hour of sonication showed evidence of NP production (Fig. 13). The NPs were washed with ultrapure water and ethanol using several centrifugations at 7000 rpm, and then they were dried for 24 hours at 60°C.

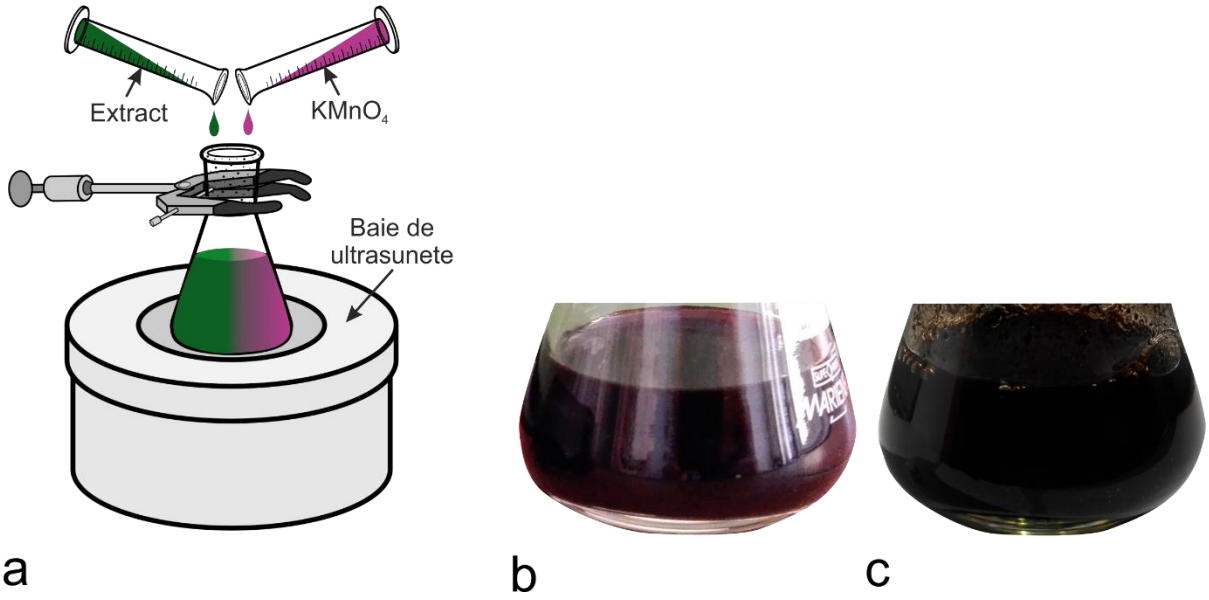

Figure 13. The color change of $KMnO_4$ and plant extract from red-purple to brown, phenomenon that indicates the successful formation of nanoparticles; **(a)** schematic representation of the stage preceding the formation of nanoparticles, **(b)** $KMnO_4$ solution in the beginning, **(c)** $KMnO_4$ solution after one hour.

In the second step, Mn NPs were mixed with $AgNO_3$ (5 mM) and plant extract. The solution was placed on a magnetic agitator for six hours at a speed of 1000 rpm and room temperature. The stirring and cleaning processes took place under the same conditions as those described in phase one. Three types of NP were obtained: CmNPs (*C. majus* extract), VmNPs (*V. minor* extract), and MNPs (1:1 (*v:v*) extract mix).

2.2.2 Physical characterization of nanoparticles

2.2.2.1 S/TEM, EDX, XRD, and FTIR

Din S/TEM was used to characterize the NPs from a morphological perspective, and the resulting images were also used to analyze the nanoparticles' size distribution. The distribution of elements in the three types of NPs was evaluated by elemental analysis of the type EDX (energy-dispersive X-ray spectroscopy), and the structure of the nanoparticles was determined by Fourier Transform Infrared spectroscopy (FTIR) and X-ray Diffraction (XRD) (Ciorîță *et al.*, 2020).

2.2.3 Biological characterization of nanoparticles

2.2.3.1 Antimicrobial activity

The diffusimetric approach described in section 2.1.8. was used to assess the antibacterial activity on two bacterial strains (*E. coli* and *S. aureus*) and the antifungal activity on a strain of *Candida albicans* (ATCC 90028).

2.2.3.2 Cytotoxicity

A375 and HaCaT were used to test the cytotoxic effect using the MTT, LDH, and NO assays, in accordance with the methods outlined by Ciorîță *et al*. (2020) and in subchapter 2.1.9. Cells were cultured for 24 hours in a medium containing nanoparticles at concentrations ranging from 1 to 1000 g/mL. Additionally, TEM and EDX were used to assess the ability of nanoparticles to be taken up by human cells. Therefore, 3×10^4 confluent fresh cell cultures were allowed to adhere to glass coverslips for 24 hours. Following this, 1000 g/mL of nanoparticles were introduced, and the cells were incubated once more for 24 hours. Only CmNPs and MNPs were evaluated because they had the biggest and smallest sizes, respectively. Samples were prepared in accordance with section 2.1.9.4. Additional EDX analysis was carried out to determine the nature of the electron-dense deposits observed within the cells.

2.3 Statistical analyses

Student *t* Test, Analysis of Variance (ANOVA), Principal component analysis (PCA), Tukey Test, Pearson and Spearman correlation tests were performed using the Origin Lab software.

3 Results and discussions

3.1 *Vinca* and *Catharanthus roseus* leaf morphology

Although each type of microscope has benefits and drawbacks, imaging techniques used to analyze various samples help us better understand how the living world functions and how organic and inorganic matter interact. Therefore, a combination of several pieces of equipment, each intended to perform a specific task (representing the surfaces, anatomies, and ultrastructures, as well as the interactions between the elements of the studied specimen), is suggested in order to obtain the most accurate representation of a functional assembly.

The presence or lack of trichomes and stomata on the surface of the leaf blade were highlighted by the use of SEM. With the exception of *V. minor*, the hairs present on the adaxial (superior) face are gathered on the midrib, on the secondary ribs (*V. herbacea* and *C. roseus*), and on the margin (postero-anterior orientation) (Fig. 14). The top edge of the leaf limbs of *V. minor* has protuberances that resemble trichomes in their early stages of development (Fig. 14b), and the trichomes on the surface of the leaf limbs of *C. roseus* are also dispersed randomly (Fig. 14g).

Details on the trichomes reveal that, according on the species, they have various ornamentation (Fig. 15). Stomata were also observed on the adaxial surface, clustered along the veins (Fig. 15). Stomata are absent from the adaxial face of *V. minor*. Another significant finding was the contrast between the epidermal cells, which in *V. minor*, *V. major*, and *V. major* var. *variegata* appeared like puzzle pieces, and those in *V. herbacea* and *C. roseus*, had a papillary look (Fig. 15).

The abaxial (lower) surface of the leaves shows epidermal cells with a puzzle-piece appearance for all species analyzed, and stomata are randomly distributed over the entire surface (Fig. 16). *C. roseus* also shows hairs on the abaxial side (Fig. 16i), and their density is higher than on the adaxial side (Table 8).

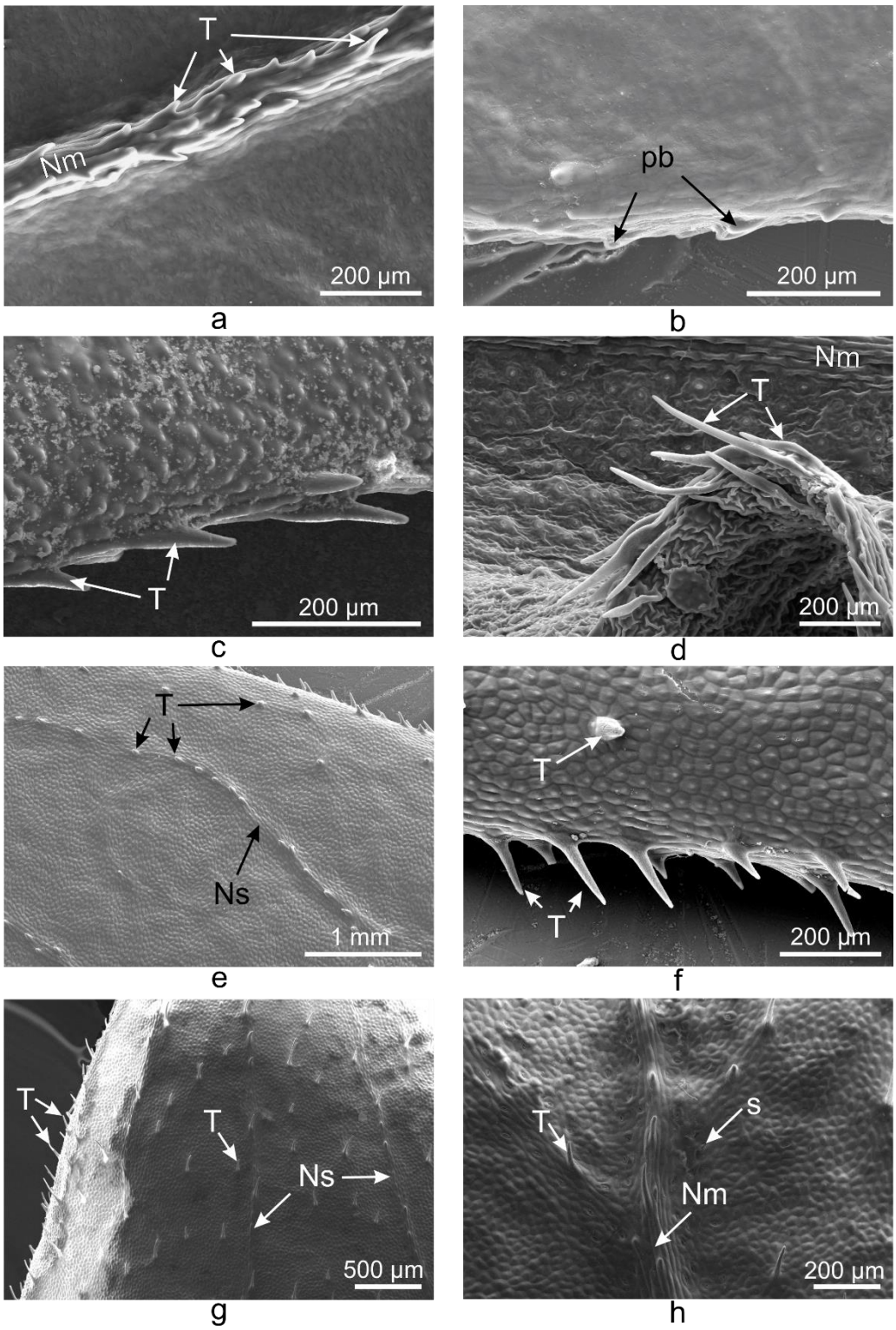

Figure 14. Distribution of trichomes on the adaxial surface and on the edge of the leaf blade of *Vinca* and *C. roseus* plants. **(a)** distribution and orientation of trichomes on the central vein of the *V. minor* leaf; **(b)** the presence of protuberances on the edge of the *V. minor* leaf; **(c)** distribution and orientation of trichomes on the edge of the *V. major* and **(d)** *V. major* var. *variegata* leaves; **(e)** the distribution of trichomes on the secondary veins of the *V. herbacea* leaf and **(f)** on the margin; **(g-h)** the distribution of trichomes over the entire surface of the *C. roseus* leaf; Nm – midvein, Ns – secondary vein, pb – protuberances, s – stomata, T – trichome (Ciorîță *et al.*, 2021b).

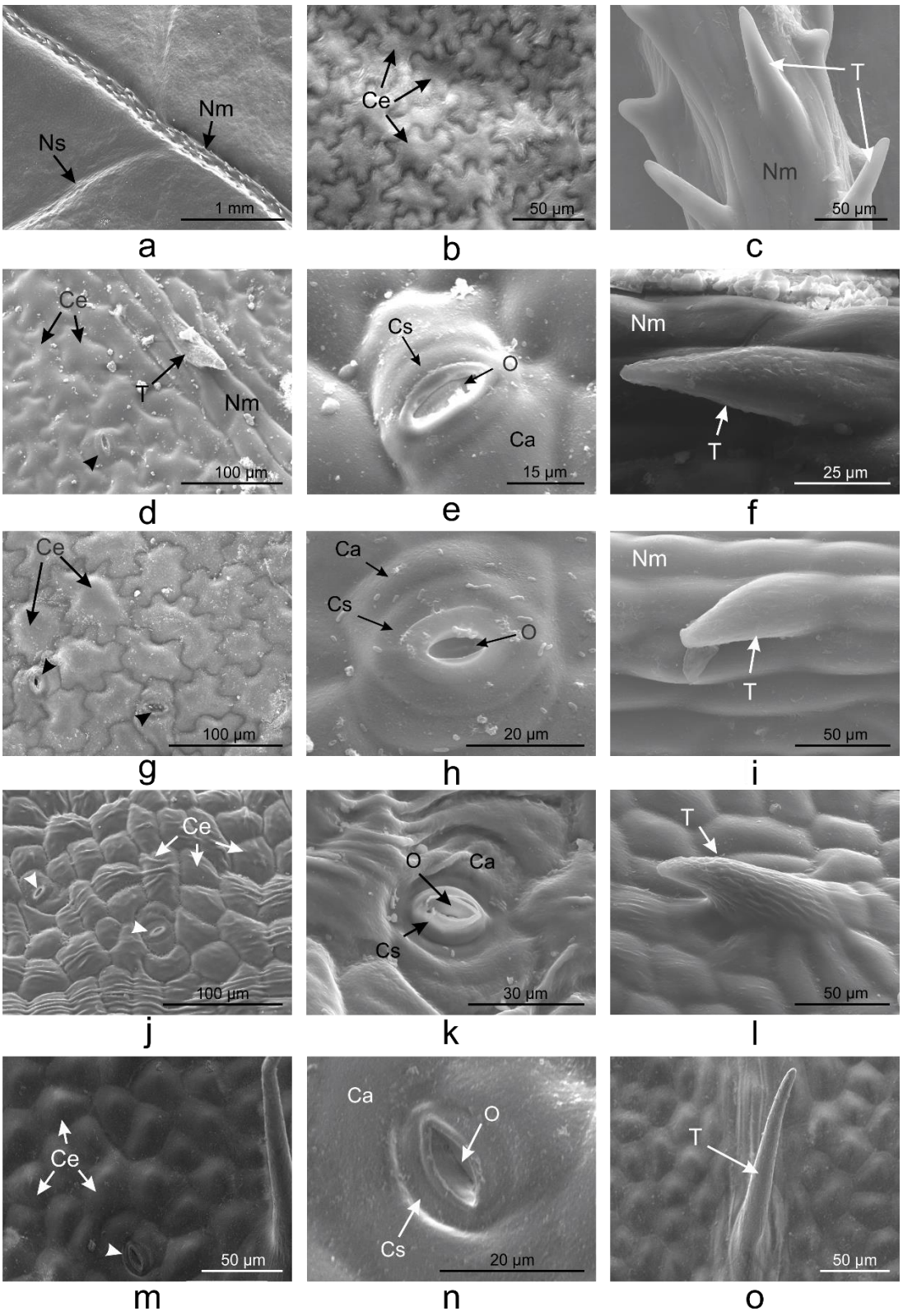

Figure 15. The distribution and appearance of trichomes, the organization of epidermal cells and the different shapes of stomata on the adaxial surface of the *V. minor* **(a-c)**, *V. major* **(d-f)**, *V. major* var. *variegata* **(g-i)**, *V. herbacea* **(j-l)**, and *C. roseus* **(m-o)** leaves' blade; Ca – subsidiary cell, Ce – epidermal cell, Cs – guard cell, Nm – midvein, Ns – secondary vein, O – stomatal aperture, T – trichome, arrowhead – stomata (Ciorîță *et al.*, 2021b).

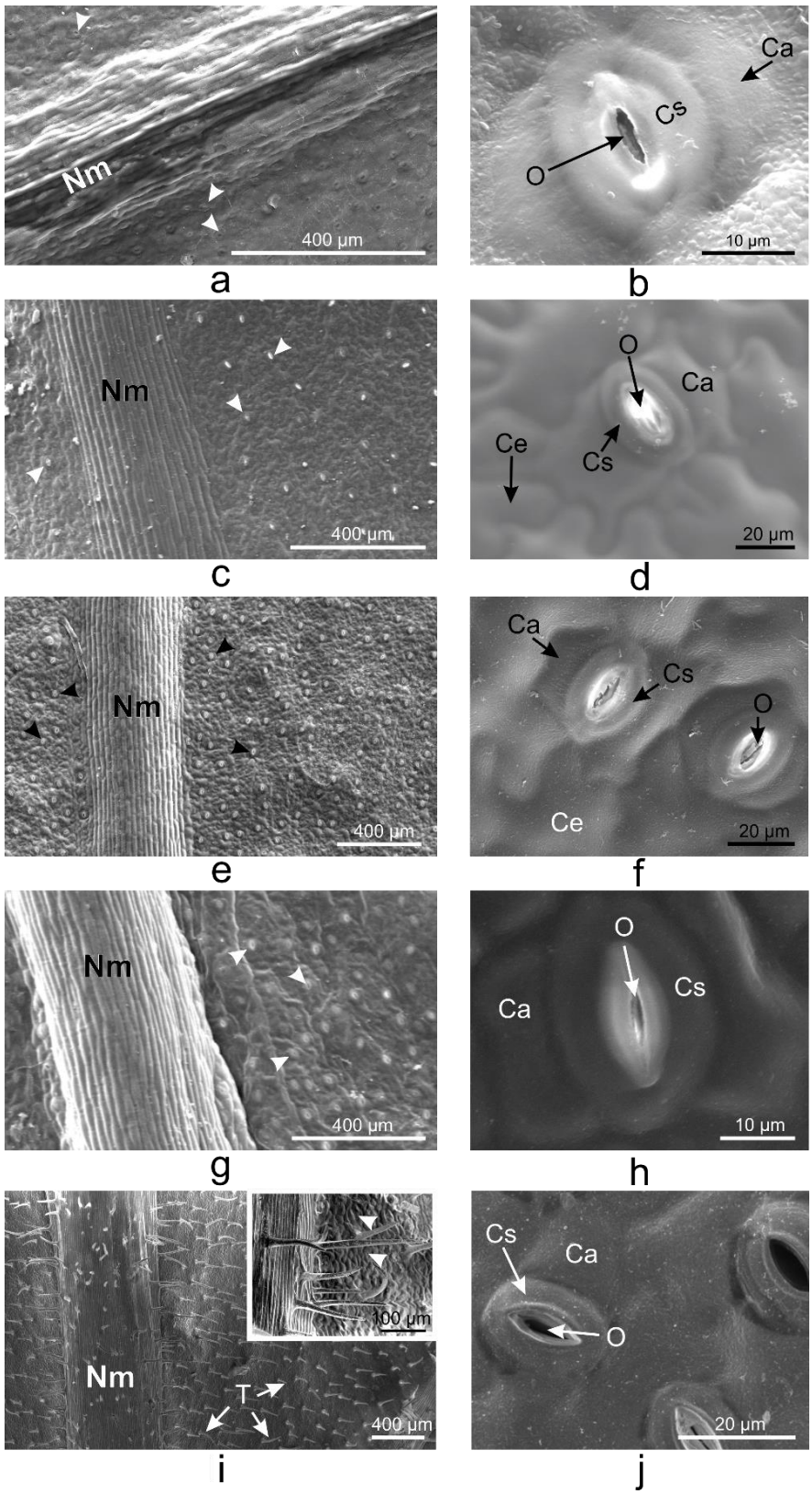

Figure 16. The distribution and appearance of trichomes, the organization of epidermal cells and the different shapes of stomata on the abaxial side of the *V. minor* **(a-b)**, *V. major* **(c-d)**, *V. major* var. *variegata* **(e-f)**, *V. herbacea* **(g-h)**, and *C. roseus* **(i-j)** leaves' blade; Ca – subsidiary cell, Ce – epidermal cell, Cs – guard cell, Nm – midvein, Ns – secondary vein, O – stomatal aperture, T – trichome, arrowhead – stomata (Ciorîță *et al.*, 2021b).

In the taxonomy of medicinal plants, the aspects described in this research paper play a very important role (El-Fiki *et al.*, 2019; Venkateshwar *et al.*, 2013), as connections have been established between the cell walls of epidermal cells and the content in natural compounds (Abouzeid *et al.*, 2019b). Epidermal cells have a specialized role in the biosynthesis and accumulation of natural compounds such as alkaloids (Murata *et al.*, 2008), terpenes, and flavonoids (Murata *et al.*, 2008; Roepke *et al.*, 2010).

The epidermis of the species covered in this study has a single row of pavement cells as well as specialized elements like stomatal complexes and protective trichomes (Murata *et al.*, 2008). In accordance with factors such as the age of the leaves, placement on the stem, CO_2 emissions, frequency of solar radiation, humidity, pollution, etc., these specialized epidermal structures can vary both intra- and interspecifically (Royer, 2001; Vofely *et al.*, 2018).

In contrast to the other leaves examined, *V. herbacea* and *C. roseus* had different epidermal cells on the adaxial face. Similar findings were previously reported with this difference between *V. minor* and *V. herbacea* (Gagua *et al.*, 2012). Although it is common to see this kind of arrangement in the shape of puzzle pieces, no clear explanation has yet been found. According to a number of theories, this aspect strengthens the leaf surface, permits the proper framing of specialized structures (stomata and trichomes), enhances the flow of chemical signals between cells, and relieves mechanical stress brought on by the turgor of subepidermal cells (Sampathkumar *et al.*, 2014; Sapala *et al.*, 2018; Vofely *et al.*, 2018).

In an attempt to find an explanation, but also to define these parameters in the studied species, stomatal density (DS), stomatal index (IS), stomatal aperture index (IAS) and trichome density were calculated for both sides of the leaf (DT), each value varying by species (Table 8).

Table 8. Morphological parameters measured on both adaxial and abaxial faces of the leaves of *Vinca* and *C. roseus* plant species (Ciorîță *et al.*, 2021b)

Species	DS*		IS (%)*		LS (µm)		IAS (%)		DT*	
	Ad	Ab	Ad	Ab	Ad	Ab	Ad	Ab	Ad	Ab
V. minor	0	223	0	25.3	0	9.57 ±0.6	0	2.04	31	0
V. major	10	49	4.5	23.2	14.84 ±1.1	19.75 ±0.4	0.22	1.91	14	0
V. major var. *variegata*	12	68	4.2	20.9	12.33 ±1	12.24 ±1.4	0.18	1.01	25	0
V. herbacea	16	60	4.4	25	12.56 ±1	13.05 ±1.2	0.25	1.02	23	0
C. roseus cv. Pacifica	17	175	4.7	25	11.93±0.5	12.25 ±0.2	0.24	2.62	9	32.3

Ad = adaxial (superior), Ab = abaxial (inferior), DS = stomatal density, IS (%) = stomatal index, LS = stomatal aperture length, IAS (%) = stomatal aperture index, DT = trichome density; '*' measurements conducted in 1 mm^2 surface.

The density of trichomes on the adaxial surface differs for each species examined. The production, storage, and secretion of phytocompounds by secretory and glandular cells play a part in defense. Only tector trichomes were seen in the species described, however they play a part in mechanical defense and reducing water loss (Murata *et al.*, 2008).

Stomata are crucial plant physiology components that are involved in the processes of respiration and transpiration (Csiky *et al.*, 2013; Murata *et al.*, 2008; Petra *et al.*, 2020; Segev *et al.*, 2015; Zhu *et al.*, 2018). Stomatal sizes and shapes vary widely inter- and intraspecific (Bertolino *et al.*, 2019)determinate and several significant negative correlations were determined between stomatal density and stomatal shape (area, perimeter, axes) for different plants (Hong *et al.*, 2018). The number of stomata might rise as we ascend the stem's axis as well as from the leaf's petiole to its apex (Zhu *et al.*, 2018). As a result, it is advised to use the stomatal index as a benchmark for comparing different species because it is specific to each one and the difference in values can only be explained by internal causes (Segev *et al.*, 2015). Stomata were seen on both sides of the leaf (except for *V. minor*, with stomata only on the lower side), with a significantly lower index (~ 4%), compared to the lower side (20-25%). This makes all species hypostomatous (Ticha, 1985), with the lowest stomatal index for *V. minor*, followed by *V. herbacea* and *C. roseus* cv. Pacifica. The stomatal aperture index was high for *C. roseus* cv. Pacifica (2.62%), followed by *V. minor* (2.04%) and the others with under 2% (Table 8).

Given the physiological significance of stomata and trichomes for leaves, a significant negative correlation (r=-0.73) between their densities was found (Fig. 17). This feature suggests that the number of trichomes rises while the stomatal index falls, which controls the transpiration process (Bertolino *et al.*, 2019).

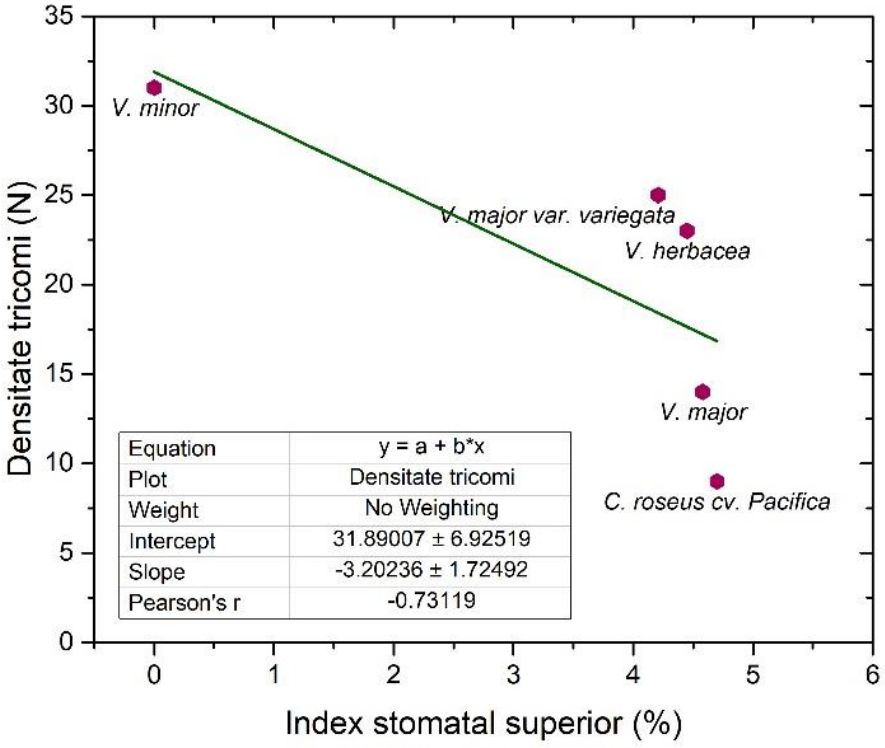

Figure 17. Linear fit of the trichomes' density and stomatal index on the adaxial side of the examined *Vinca* (*V. minor*, *V. major*, *V. major* var. *variegata*, *V. herbacea*) leaves and *C. roseus* cv. Pacifica leaf (Ciorîță *et al.*, 2021b).

The morphology and anatomy of the leaves used in extract preparation are two important characteristics for *Vinca* species (Csiky *et al.*, 2013; Ochirova *et al.*, 2018; Petra *et al.*, 2020; Samiyarsih *et al.*, 2019), along with the solvent used or the time of year the plant organs are harvested (Bahadori *et al.*, 2012; Barrales-Cureño *et al.*, 2019; Farahanikia *et al.*, 2011). Studies on climbing plant species *Vinca major*, *Hedera nepalensis* var. *sinensis* and *Trachelospermum jasminoides* (Shi *et al.*, 2020) or *Arabidopsis thaliana* (Weraduwage *et al.*, 2015) have revealed a relationship between dry mass content, leaf area, and biomass accumulation. The stomatal index for the leaves of *Vinca* and *C. roseus* plants has different values and can produce the variability of the chemical composition of the extracts. A high stomatal index is directly correlated with the rate of photosynthesis, as was also indicated for other plant species (Opriș *et al.*, 2019; Segev *et al.*, 2015).

According to Petra *et al*. (2020) the stomatal density of *V. major* var. *variegata* varied with light intensity and ranged between 88 and 119 stomata/mm^2 (Petra *et al.*, 2020). According to Ochirova *et al*. (2018) *V. minor* has 350 stomata per square millimeter (Ochirova *et al.*, 2018). Additionally, there are no reports of stomata on the upper face of *V. herbacea* in the literature (Gagua *et al.*, 2012). As a result, three of the ten leaves in the examined batch were also found to have stomata on the upper side. The plants from which the leaves were taken might have various adaptations to the current environmental variables, which helps to explain this aspect (Royer, 2001). Although phenotypic and leaf development are typically controlled by genetics, environmental variables can also have a role (Ruan, 2012). The synthesis methods of primary and secondary metabolite products, such as sugars, which have been demonstrated to be in charge of the growth and development of leaves in *V. minor* and *C. roseus* plants, are linked to a number of the reported morphological distinctions between *Vinca* species (Chen *et al.*, 2017). In plants, morphological characteristics of aerial organs are frequently employed to identify species (Chen *et al.*, 2017; Csiky *et al.*, 2013; Ochirova *et al.*, 2018; Petra *et al.*, 2020), and these characteristics can be seen in *Vinca* leaf morphology as well. The leaf phenotype can differ intraspecifically across plants and occasionally even within the same individual, which has an impact on processes including photosynthesis, water and thermal balances, and interactions with other species (Kidner *et al.*, 2010).

3.2 *Vinca* leaf anatomy

Light microscopy could be used to see how the leaf mesophyll is organized using the obtained semi-thin sections. Only the leaves of the species *V. minor*, *V. major*, *V. major* var. *variegata* and *V. herbacea* were examined by light microscopy because the species of the genus *Vinca* have undergone less anatomical study than *C. roseus*. Under the upper epidermis of the leaf limb, all species exhibit a simple palisade tissue that is more or less developed, as well as spongy tissue beneath the lower epidermis (Fig. 18).

In contrast to other species, *V. major*'s mesophyll is organized rather uniformly, and its cuticles are thin compared to other species. These traits are common in ornamental houseplants (Fig. 18c).

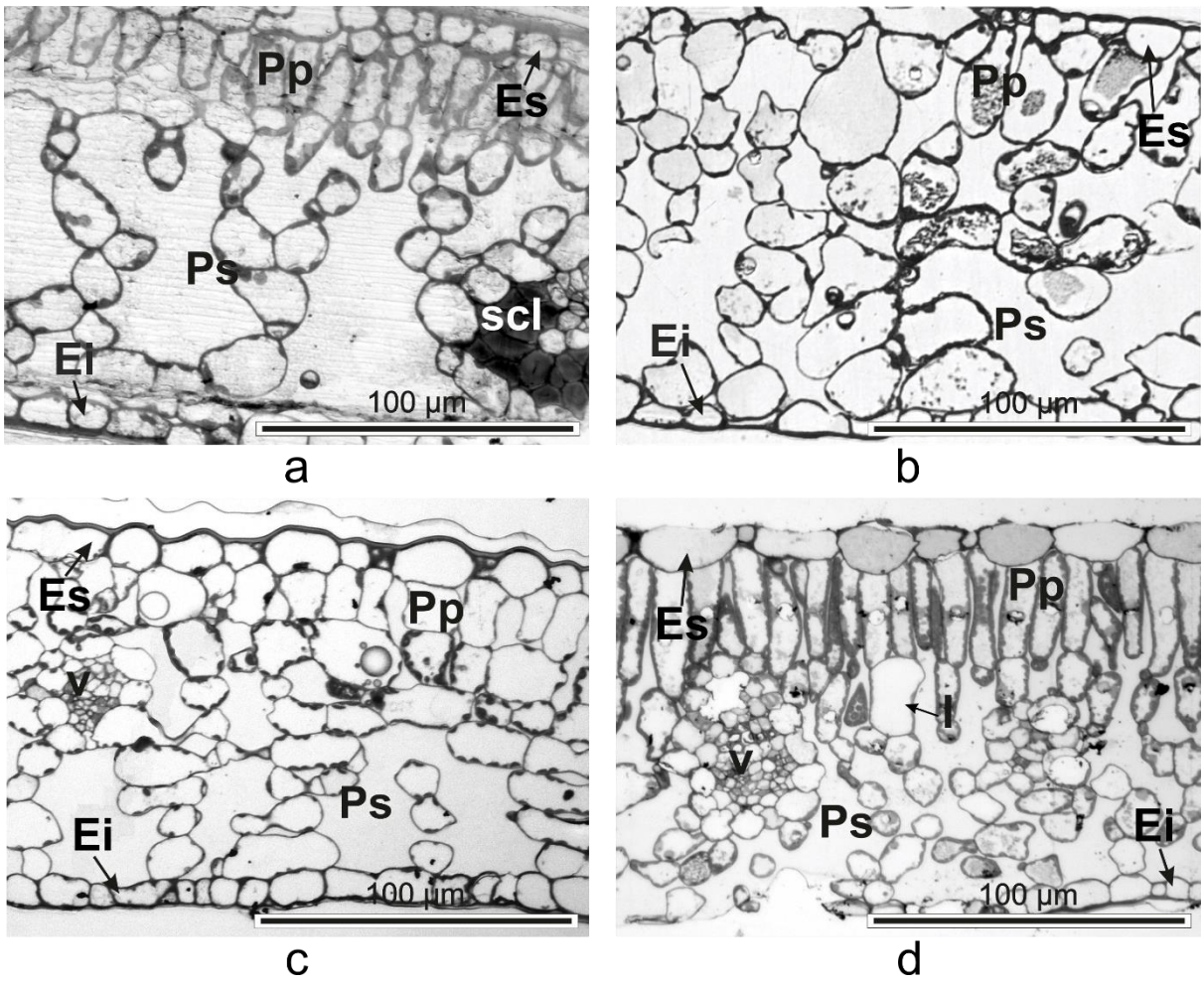

Figure 18. Semithin cross-sections of *Vinca* leaves showing the organization of the mesophyll between the upper epidermis (Es) and lower epidermis (Ei) as determined through light microscopy. **(a)** *V. minor*, **(b)** *V. major*, **(c)** *V. major* var. *variegata*, **(d)** *V. herbacea*; Ei = lower epidermis, Es = upper epidermis, I = idioblast, Pp = pallisadic parenchyma, Ps = spongy parenchyma, scl = sclerenchyma, v = vascular bundle (Ciorîță *et al.*, 2021b).

Parameters such as cellular tension ratio (RTC) and spongy parenchymal tension ratio (RS) were measured based on images obtained by light microscopy (Table 9).

Table 9. Anatomic parameters of *Vinca* species (Ciorîță *et al.*, 2021b)

Species	GF (µm)	PTT (µm)	STT (µm)	RTC (%)	RS (%)
V. minor	85.47 ±2.6	12.58 ±0.7	52 ±0.5	14.72	60.84
V. major	136.85 ±1.4	0	124 ±0.5	0	90.61
V. major var. *variegata*	97.09 ±1.5	14.57 ±4.4	67.29 ±1.7	15.01	69.31
V. herbacea	133.38 ±2.2	36.66 ±2.2	68.42 ±3.7	27.48	51.3

GF = leaf blade thickness, PTT = pallisadic tissue thickness, STT = spongy tissue thickness, RTC (%) = cell tension report, RS (%) = spongy tissue tension report.

The leaf of *V. herbacea* (27.4%) has the highest cell tension ratio, followed by the leaves of *V. major* var. *variegata* (15.01%) and *V. minor* (14.7%). This ratio varies by species and is determined by the level of pallisadic tissue growth (Liu *et al.*, 2019) (Samiyarsih *et al.*, 2019). When plants are grown in areas that receive sunshine, their number of pallisadic cells increases, while when they are grown in the shade, it decreases (Gotoh *et al.*, 2018; Ochirova *et al.*, 2018; Petra *et al.*, 2020). Palisade cell phenotypic regulation by phototropins, a crucial factor in photosynthesis, determines palisade cell form and chloroplast motions (Gotoh *et al.*, 2018). In comparison to the other investigated species, the palisade tissue of *V. major* (growing in greenhouse conditions) was extremely underdeveloped (Fig. 18, Table 9).

According to a recent study (Petra *et al.*, 2020), plants cultivated at altitude have a double layer of palisade tissue in contrast to plants grown at ground level, which is an explanation that also applies to the situation we observed. A double palisade tissue for *V. minor* and a single palisade tissue for *V. herbacea* are both described in another study (Gagua *et al.*, 2012). Therefore, the variation in the chemical makeup of these plants can also be explained by the fact that the pallisadic tissue, the unit directly in charge of performing photosynthesis, varies between species of the genus *Vinca* (Gotoh *et al.*, 2018).

The spongy tissue has multiple layers of circular or ovoid cells that are either closely packed together or separated by broad intercellular spaces. These characteristics may be determined by external stimuli or inherent characteristics (Gagua *et al.*, 2012; Ochirova *et al.*, 2018; Petra *et al.*, 2020). The mesophyll for the plants grown in greenhouses (*V. major* and *V. major* var. *variegata*), was rather uniform (Fig. 18), echoing the findings of Petra *et al*. (2020).

A computational study of the images produced by semi-thin sectioning was done to determine the ratio between the intercellular gaps of the mesophyll present in the anatomy of the *Vinca* leaf (Fig. 19).

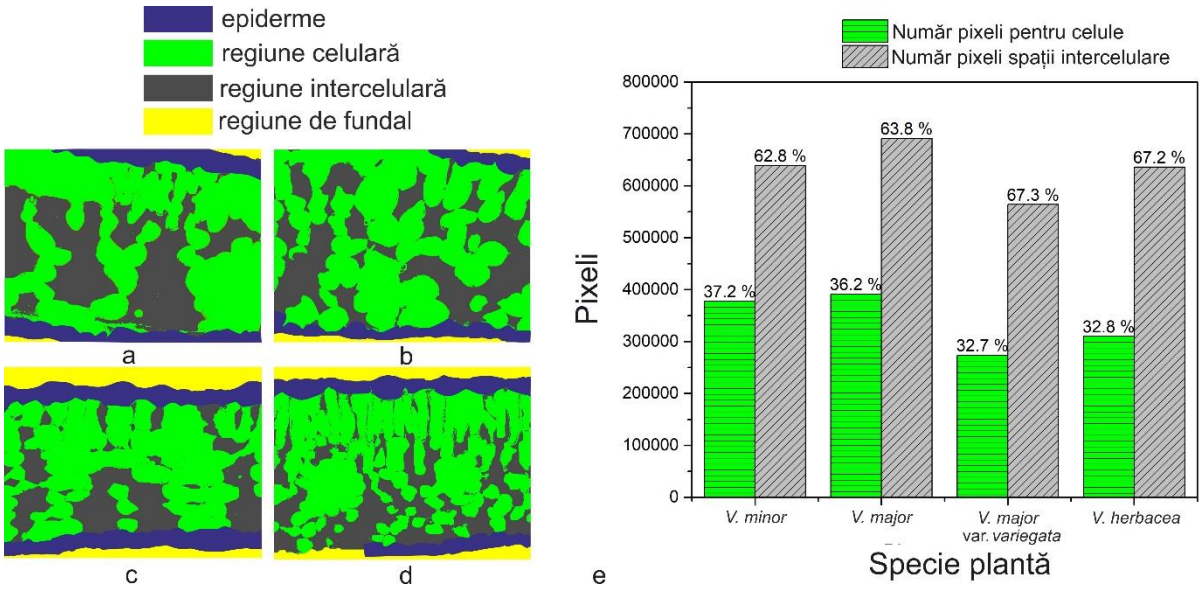

Figure 19. Computational estimation of the intercellular space of the *Vinca* mesophyll; **(a)** *V. minor*, **(b)** *V. major*, **(c)** *V. major* var. *variegata*, **(d)** *V. herbacea*, **(e)** graphical representation of the estimated number of cell pixels and inter-cell pixels as calculated using the Python scrip (Ciorîță *et al.*, 2021b).

Following this analysis, it was showed that only 37% of the leaf of *V. minor*, 36% of *V. major*, and 32% of *V. major* var. *variegata* and *V. herbacea* are occupied by cells. These findings suggest that these factors may be directly to blame for the variation in chemical composition seen in these plants' extracts (Ciorîță *et al.*, 2021b; Ciorîță *et al.*, 2021c). These variations could also affect the rate of photosynthesis (Huang *et al.*, 2019).

The correctness of the mathematical model that is produced in comparison to the conditions seen in reality is the primary goal of the computational technique used. Other semi-automatic techniques for dividing up a portion into distinct zones have been reported over time, including computer vision (Kulwa *et al.*, 2019; Minaee *et al.*, 2020) and machine learning (Xue *et al.*, 2019; Xue *et al.*, 2017b).

Although the results we obtained are within normal bounds, computational mistakes were also noted because our ultimate goal was to segment the intercellular space as accurately as feasible but not perfectly. In other words, even though the results were valid from a mathematical standpoint, the data's scientific accuracy may have been affected because this method cannot faithfully replicate reality.

Our findings can, however, be connected. Wide intercellular spaces may be directly associated to a high stomatal index, supporting our data, according to recent research (Lundgren *et al.*, 2019; Samiyarsih *et al.*, 2019). These studies also show the relationship between intercellular gaps and the number of functional stomata.

3.3 *Vinca* and *C. roseus* leaf ultrastructure

The leaf ultrastructure of the four *Vinca* species and the *C. roseus* cv. Pacifica species was determined through TEM analysis (Fig. 20).

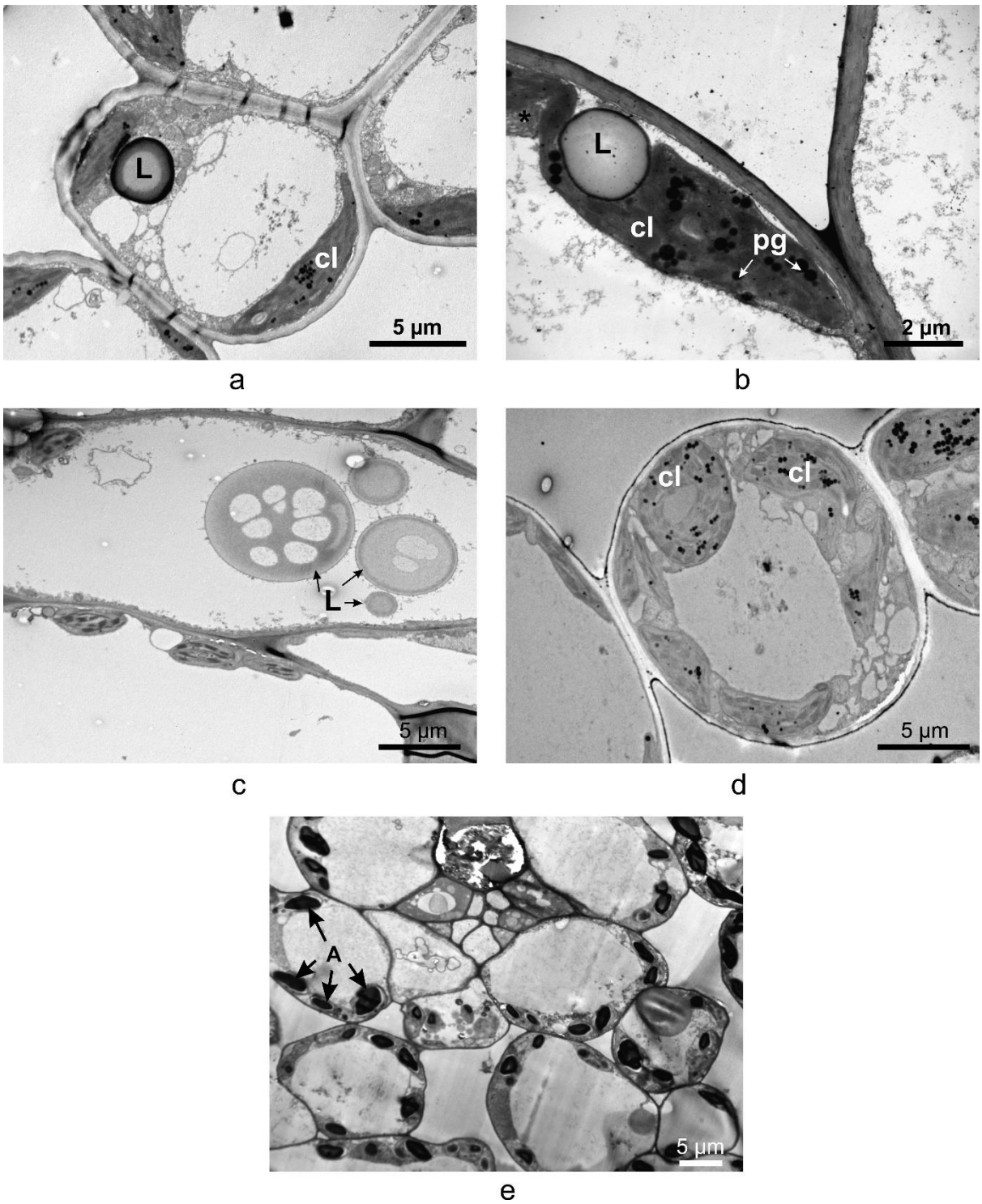

Figure 20. TEM micrographs of the cells located in the spongy parenchyma of **(a)** *Vinca minor*, **(b)** *V. major*, **(c)** *V. major* var. *variegata*, **(d)** *V. herbacea* and **(e)** *C. roseus* cv. Pacifica leaves; A = starch granules, cl = chloroplast, L = lipid droplets, pg = plastoglobuli (Ciorîță *et al.*, 2021b).

The presence of large lipid droplets in *V. major* and *V. major* var. *variegata* may be an indication of the emergence of a compensatory mechanism developed by the plant as a result of an adaptation to greenhouse conditions. Lipids can be used by plants in processes involving energy production when they are deficient (Fan *et al.*, 2019). Additionally, the lipid droplets found in the investigated plants can be used to directly correlate the variability of the chemical composition (Fan *et al.*, 2019).

Next, TEM was used to define the upper and lower epidermis' cell walls for the first time (Fig. 21).

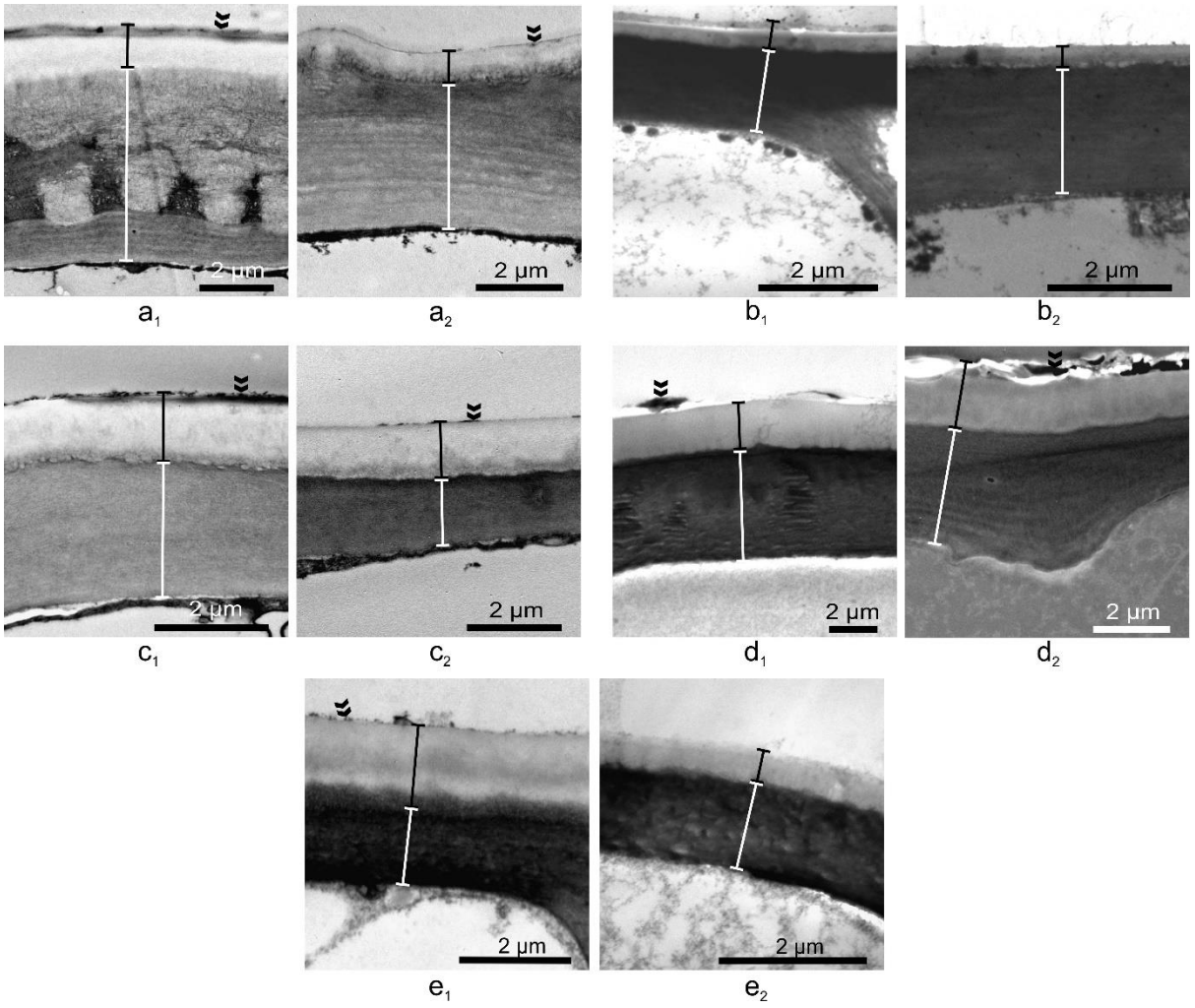

Figure 21. TEM micrographs of the upper and lower epidermises of **(a)** *V. minor*, **(b)** *V. major*, **(c)** *V. major* var. *variegata*, **(d)** *V. herbacea* and **(e)** *C. roseus* cv. Pacifica leaves; 1 = upper epidermis, 2 = lower epidermis, black delimitation = cutin layers, white delimitations = epidermal cells' cell wall, double arrowhead = epicuticular waxes (Ciorîță *et al.*, 2021b).

The thickness of the cell walls in the two epidermises of the leaf limb was another issue that the TEM was used to examine (Fig. 22).

The upper epidermises of *V. minor* and *V. herbacea* exhibit accumulations. The epidermis of these two species was likewise the thickest. The leaf epidermis of *V. major* was determined to be the thinnest (2.08 µm ±0.02 µm upper epidermis and 2.8 µm lower epidermis) when compared to the other investigated species, as seen in the semi-thin sections.

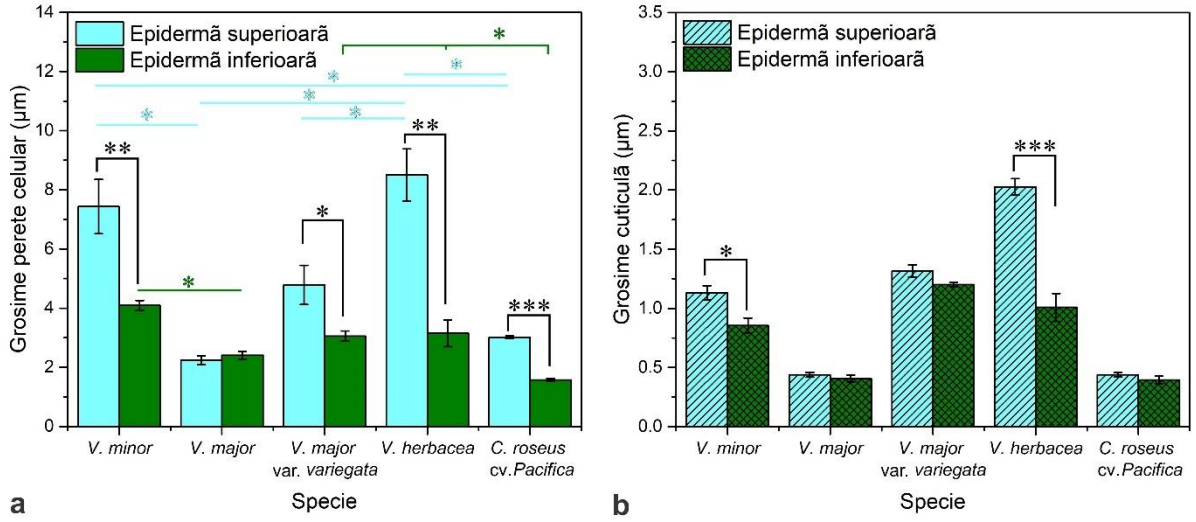

Figure 22. Graphic representation of epidermal cells' cell wall thickness of lower and upper epidermis **(a)** and cuticles **(b)** of the *Vinca minor*, *V. major*, *V. major* var. *variegata*, *V. herbacea*, and *C. roseus* cv. Pacifica plant species; ***$p<0.0001$, **$p\leq0.005$, *$p\leq0.05$ (Ciorîță *et al.*, 2021b).

With the exception of *V. major*, all species have intraspecific variations in cell wall thickness (upper versus lower epidermis), and *V. minor* and *V. herbacea* have intraspecific variations in cuticle thickness. The only interspecific difference that was found to be significant ($p\leq0.05$) was the thickness of the cell wall. *Vinca* leaves have a very complex chemical composition, with many layers of cutin covering the outer cuticle (Fernandez *et al.*, 2016; Guzman *et al.*, 2014; Xue *et al.*, 2017a).

These cutin layers morphologically resemble the leaves of *Pyrus communis* and *Populus bolleana* plants, and they are found in *V. minor*, *V. major* var. *variegata*, *V. herbacea* and *C. roseus* cv. Pacifica (Guzman *et al.*, 2014). Important defense against infections, variations in temperature, salinity, or light intensity is provided by epicuticular cutin layers (Xue *et al.*, 2017a).

3.4 Characterization of the obtained hydroalcoholic plant extracts

Natural compounds from plants have a multivalent use, being used in industries such as pharmaceutical, food or chemical. The extraction process thus becomes an important pillar, preceding the isolation and purification stages, in which the correct choice of the method used for extraction plays an important role (Pârvu *et al.*, 2011a; Pârvu *et al.*, 2008; Pârvu *et al.*, 2013).

The extraction techniques can be categorized based on a number of factors (extraction time, solvent consumption, completed product, or method complexity itself), but the majority of them will be contrasted with those pioneers in the area who created them first (Azmir *et al.*, 2013; Jones *et al.*, 2006).

The cold repercolation approach, which combines the two earlier procedures, is frequently employed for thermosensitive extracts (Jones *et al.*, 2006). The percolation theory was created by Broadbent and Hammersley in 1957 and is based on the likelihood that an object immersed in water (or alcohol, gas, plasma, etc.) will become

completely saturated within a specified period of time (Grimmett, 1999; Handa *et al.*, 2008; Stauffer *et al.*, 1994). The plant material is crushed and washed before being added to a percolator, where a known amount of solvent is then added (Pârvu *et al.*, 2011a; Zhang *et al.*, 2005).

The following plant extracts were obtained:

- *C. majus* ➔ 1:1 (g:mL) with 30% ethanol;
- *V. herbacea* ➔ 1:2 (g:mL) with 30% ethanol;
- *V. minor* ➔ 1:1.2 (g:mL) with 30% ethanol;
- *V. major* ➔ 1:1.4 (g:mL) with 30% ethanol;
- *V. major* var. *variegata* ➔ 1:1.5 (g:mL) with 30% ethanol.

3.4.1 Phytochemical composition

Different qualitative or quantitative techniques are used to assess the phytochemical composition of plant extracts. High-performance liquid chromatography (HPLC) is one technique that can be used to examine and separate mixtures of substances into their constituent parts. The mobile phase is pushed under pressure through columns that make up the stationary phase, and the entire assembly is entirely automated. By using this technique, it is feasible to evaluate solutions or extracts from intricate plants that can be broken down into their constituent parts and subsequently isolate them (Dong, 2006).

The main types of polyphenolic chemicals produced by plants include hydroxycinnamic acids, flavonoids, tannins, and anthocyanins (Ainsworth *et al.*, 2007). The Folin-Ciocâlteu method, invented in 1927, is one colorimetric technique used to measure the amount of phenols in extracts (Everette *et al.*, 2010). The reaction is based on the reduction of molybdenum and oxidation of polyphenols, which results in the complex's color change from yellow to blue. The solution is then spectrophotometrically evaluated at specific wavelengths (Ainsworth *et al.*, 2007).

Rutin-specific detection of total flavonoids is possible through the complexation of polyphenols with $AlCl_3$. In a process that changes the color from yellow to red, aluminum interacts with polyphenols and forms complexes with two ligands (Pękal *et al.*, 2014).

Alkaloids and flavonoids belong to the group of organic chemicals that provide extracts their medicinal potential. However, plants produce alkaloids as a defensive mechanism, thus the effect is poisonous to both the pathogen and the plant. Because of this, alkaloids are only synthesized in small amounts, and some of them, such as nicotine, atropine, and aristolochic acids, can be quite dangerous to humans as well (O'Connor, 2008; Sreevidya *et al.*, 2003; Ziegler *et al.*, 2008).

Methods for measuring total alkaloid content frequently use the Dragendorff reagent, however its specificity is limited to certain classes (Sreevidya *et al.*, 2003). Therefore, a key goal of this doctoral thesis was the optimization of the technique for detecting indole alkaloids from *Vinca* species. Thus, indole alkaloids could be detected

without using other methods by adding tartaric acid, increasing the amount of glacial acetic acid, and measuring the whole chemical generated after precipitation with bismuth (Chaudhary *et al.*, 2010; Shaheen *et al.*, 2019).

3.4.1.1 HPLC analysis

HPLC was used to determine the chemical makeup of the extracts of *Vinca minor*, *Vinca major*, *Vinca major* var. *variegata*, *Vinca herbacea*, and *Catharanthus roseus* cv. Pacifica (Fig. 23, Table 10). Chlorogenic acid levels in all extracts were high, and *V. herbacea* had a high rutin content. Vinblastine was only found in *C. roseus* cv. Pacifica, and the alkaloid vincamine was found in all extracts (except *V. herbacea*).

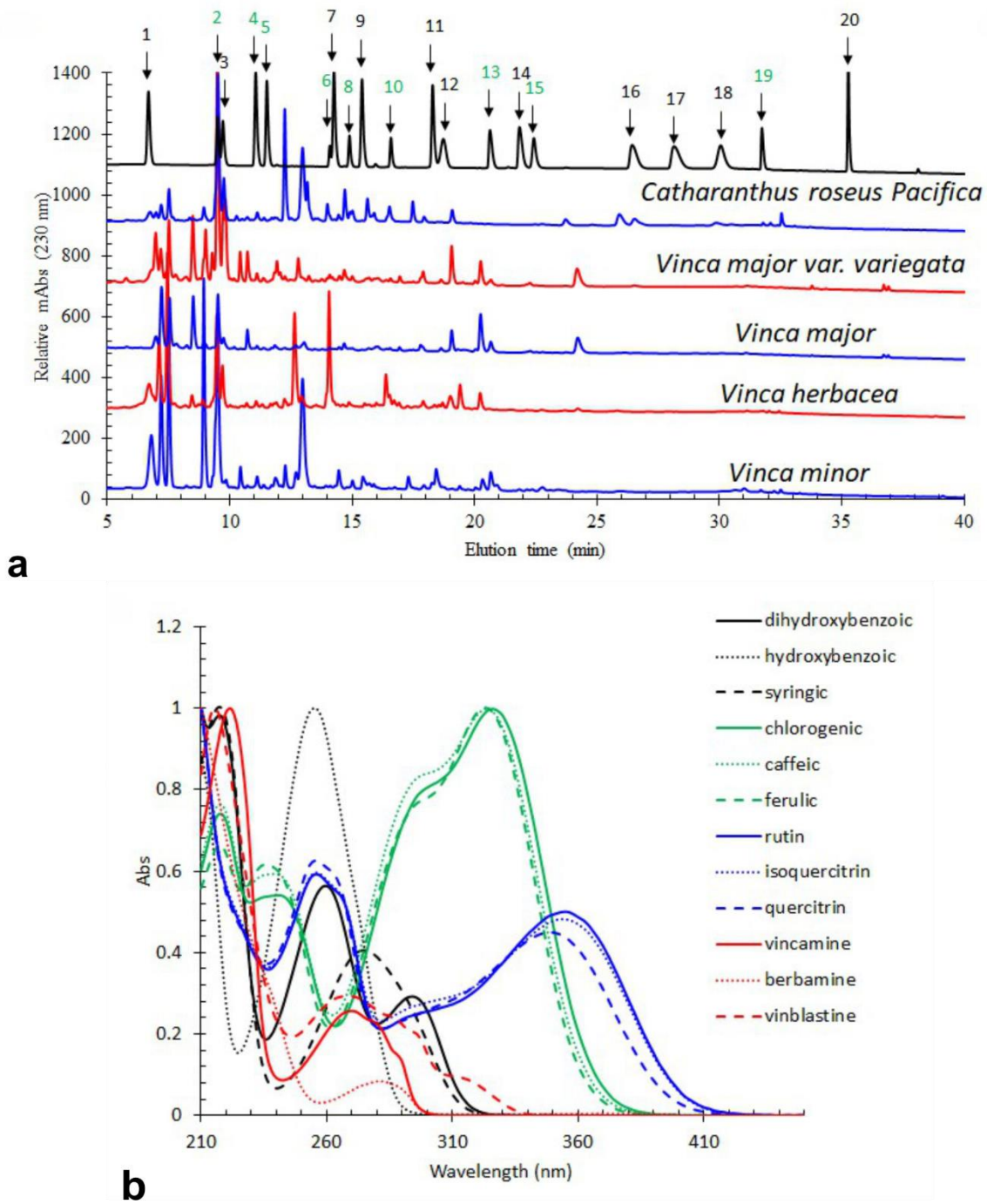

Figure 23. (a) HPLC-DAD chromatograms of *Vinca minor*, *V. major*, *V. major* var. *variegata*, *V. herbacea*, and *Catharanthus roseus* cv. Pacifica plant extracts measured at 230 nm. Analytical standards used: 1 –3,4-

dihidroxibenzoic acid, 2 –chlorogenic acid, 3 – 4-hidroxibenzoic acid, 4 – caffeic acid, 5 –syringic acid, 6 – rutin, 7 – p-coumaric acid, 8 – isoquercitrin, 9 – ferulic acid, 10 – quercitrin, 11 – miricetin, 12 – berbamine, 13 – vincamine, 14 – jatrorrhizine, 15 – quercetin, 16 – palmatine, 17 – berberine, 18 – kaempferol, 19 – vinblastine, 20 – galangin. The identified compounds are marked in green. **(b)** UV molecular spectra registered by the DAD detector for each phytoconstituent (grey – hydroxybenzoic acid, green – cinnamic acid, blue – flavonoids, red – alkaloids) (Ciorîță *et al.*, 2021c).

Table 10. The main phytoconstituents concentration in *Vinca* and *C. roseus* plant extracts (Ciorîță *et al.*, 2021c)

Compound	Compound concentration (μg/g)				
	Vm	VM	VMv	Vh	Crp
Chlorogenic acid	4112±13	675±160	932±260	1538±200	2959±240
Caffeic acid	229±2	13±2	182±23	13±1	13±1
Rutin	73±1	11±1	94±10	2528±160	44±2
Isoquercitrin	12±1	12±1	38±4	87±4	82±7
Quercitrin	52±4	11±1	45±8	109±10	86±6
Vincamine	65±1	42±3	31±2	n.d.	4±1
Quercetin	21±2	14±2	28±2	20±3	21±2
Vinblastine	n.d.	n.d.	n.d.	n.d.	6.8±2

*Vm = *V. minor*, VM = *V. major*, VMv = *V. major* var. *variegata*, Vh = *V. herbacea*, Crp = *C. roseus* cv. 'Pacifica'; n.d. – not detected.

The alkaloids' greatest absorption peak, which ranged between 240 and 310 nm, displayed different spectrum properties. To sort and identify the components connected to the unidentified spectral peaks, a principal component analysis (PCA) was initiated. Thus, the detected groups belonged to hydroxycinnamic acids and flavonoids, while alkaloids were the most prevalent category in the undetermined chemicals (Fig. 24). The extract from *V. minor* contained the highest amount of alkaloids, and the HPLC results were then compared to those from colorimetric assessments of the total alkaloid content.

3.4.1.2 Total polyphenol and total flavonoid contents determination

Utilizing colorimetric techniques, the total amount of polyphenols and flavonoids was also determined (Fig. 25). The highest concentration of polyphenols was found in *V. herbacea*, followed by *V. major* var. *variegata* and *C. roseus* cv. Pacifica (Fig. 25a).

V. major var. *variegata* (Fig. 25b) had the highest flavonoid concentration, followed by *C. roseus* cv. Pacifica and *V. herbacea*. In comparison to the other extracts, the polyphenol and flavonoid contents of both *V. minor* and *V. major* were comparatively low.

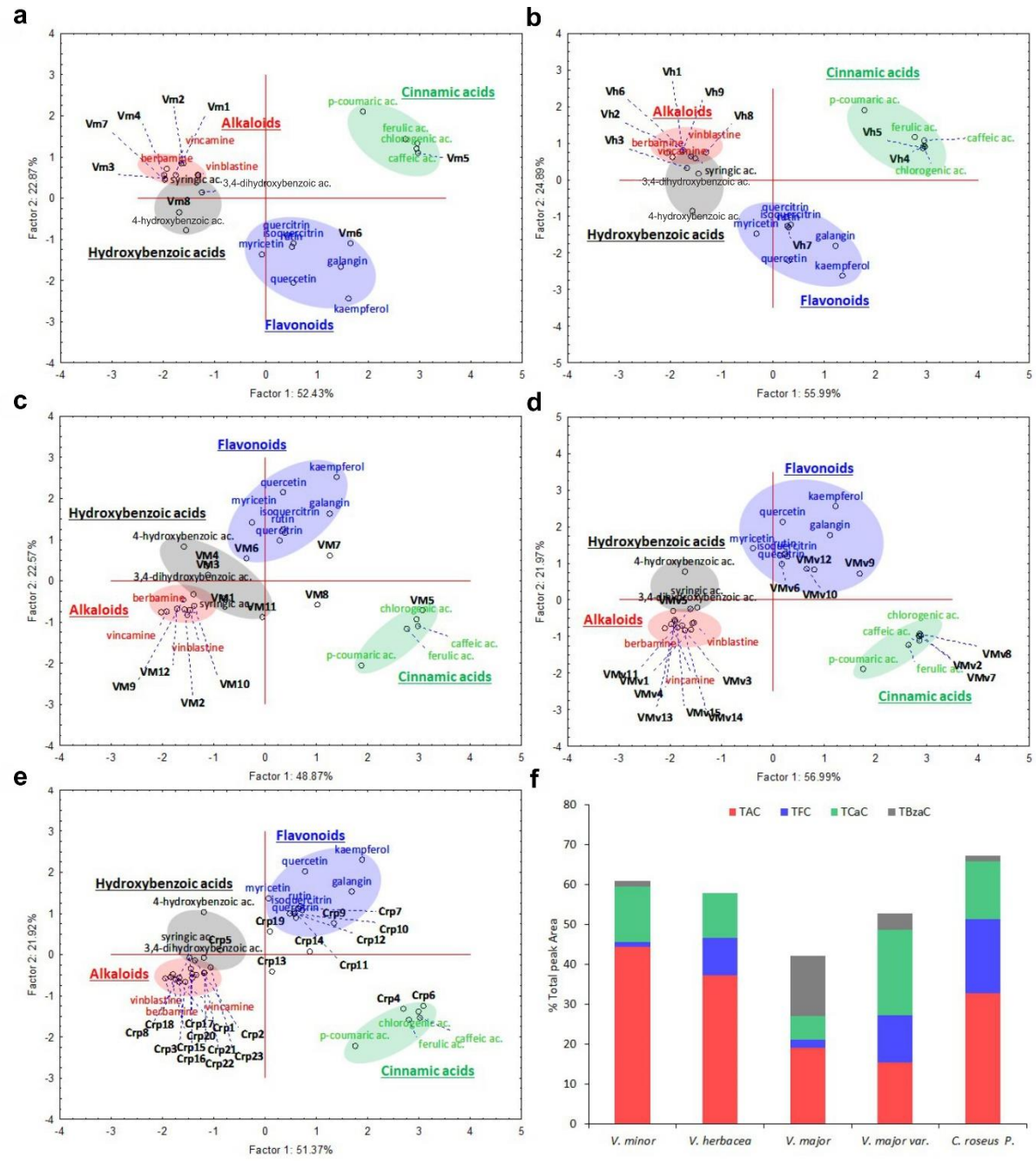

Figure 24. Chemo-mapping of the major chromatographic peaks—phytoconstituents classification—based on spectral similarities for each studied extract using PCA. PCA was applied on exported UV DAD spectra, for each chromatographic peak. Shown here are the scatterplots of the scores for the first two principal components for (**a**) *V. minor*, (**b**) *V. herbacea*, (**c**) *V. major*, (**d**) *V. major* var. *variegata* and (**e**) *Catharantus roseus* cv. Pacifica. Groups with high similarity are clustered in specific color for each phytoconstituent group or class (grey-hydroxybenzoic acids, green-cinnamic acids, blue-flavonoids, and red-alkaloids); (**f**) Total standard (vincamine for TAC, quercetin for TFC, cynnamic acid for TCaC and benzoic acid for TBzaC) equivalent content (%) for each extract for 230 nm chromatogram, after PCA classification. TAC-total alkaloid content, TFC-total flavonoid content, TCaC-total cinnamic acids content, TBzaC-total hydroxybenzoic acids content, Vm = *V. minor*, VM = *V. major*, VMv = *V. major* var. *variegata*, Vh = *V. herbacea*, Crp = *C. rosuesu* cv. Pacifica (Ciorîță *et al.*, 2021c).

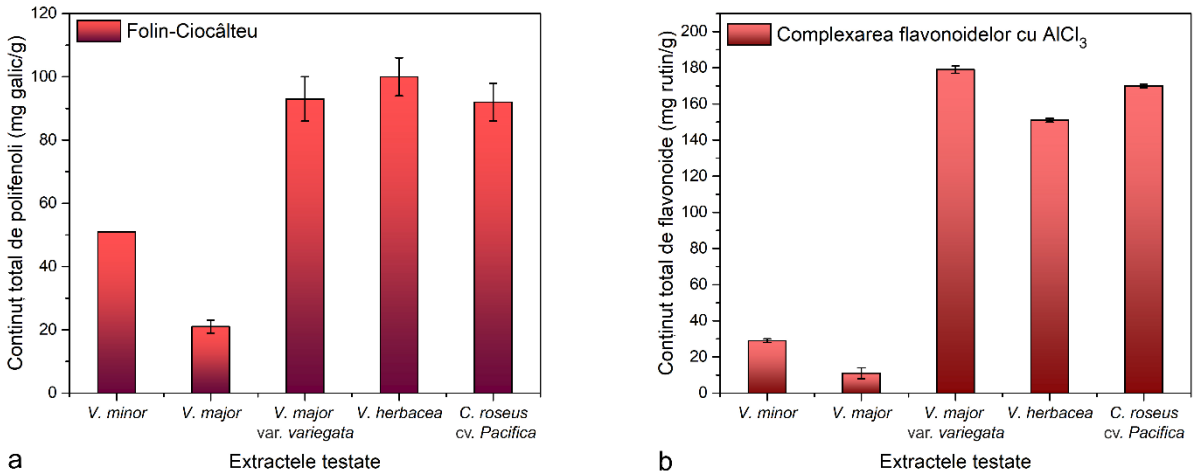

Figure 25. Total polyphenols and flavonoids content in *Vinca minor*, *V. major*, *V. major* var. *variegata*, *V. herbacea*, and *Catharanthus roseus* cv. Pacifica plant extracts, determined through Folin-Ciocâlteu **(a)** and $AlCl_3$ **(b)** methods.

3.4.1.3 Total alkaloid content determination

Using Dragendorff colorimetric assay, the total alkaloid content (TAC) was determined through UV-Vis. Vinblastine was used for calibration with a linearity determined for 60 concentration units (Fig. 24 a). *V. minor* had the highest TAC (332 ±33 vinblastine/g), followed by *C. roseus* cv. Pacifica (278 ±15 vinblastine/g), *V. herbacea* (195 ±9 vinblastine/g), *V. major* var. *variegata* (101 ±6 vinblastine/g), and *V. major* (35 ±11 vinblastine/g) (Fig. 26c). The outcomes were contrasted with those from the HPLC analysis. Strong correlation (r = 0.99) between the two techniques was observed, indicating the effectiveness of the improved Dragendorff protocol in this study (Fig. 26b). The plants used in this study are regarded as medicinal plants due to their abundance of alkaloids and polyphenolic chemicals that have a variety of pharmacological effects (Cheng *et al.*, 2016; Cheng *et al.*, 2014; Grujić *et al.*, 2015; Grujić *et al.*, 2014; Gülçin *et al.*, 2012; Islam *et al.*, 2019; Liao *et al.*, 2013). The improved Dragendorff method, which solely offers numerical data, was used to calculate the total alkaloid content. The Dragendorff and HPLC techniques utilized here were complementary in identifying the overall alkaloid content, making the procedure useful for further specialized research. Along with alkaloids, plants also have flavonoids, hydroxybenzoic, hydroxycinnamic, and chlorogenic acids, which are renowned for helping to protect the plant from environmental stresses (Choi *et al.*, 2004; Mierziak *et al.*, 2014).

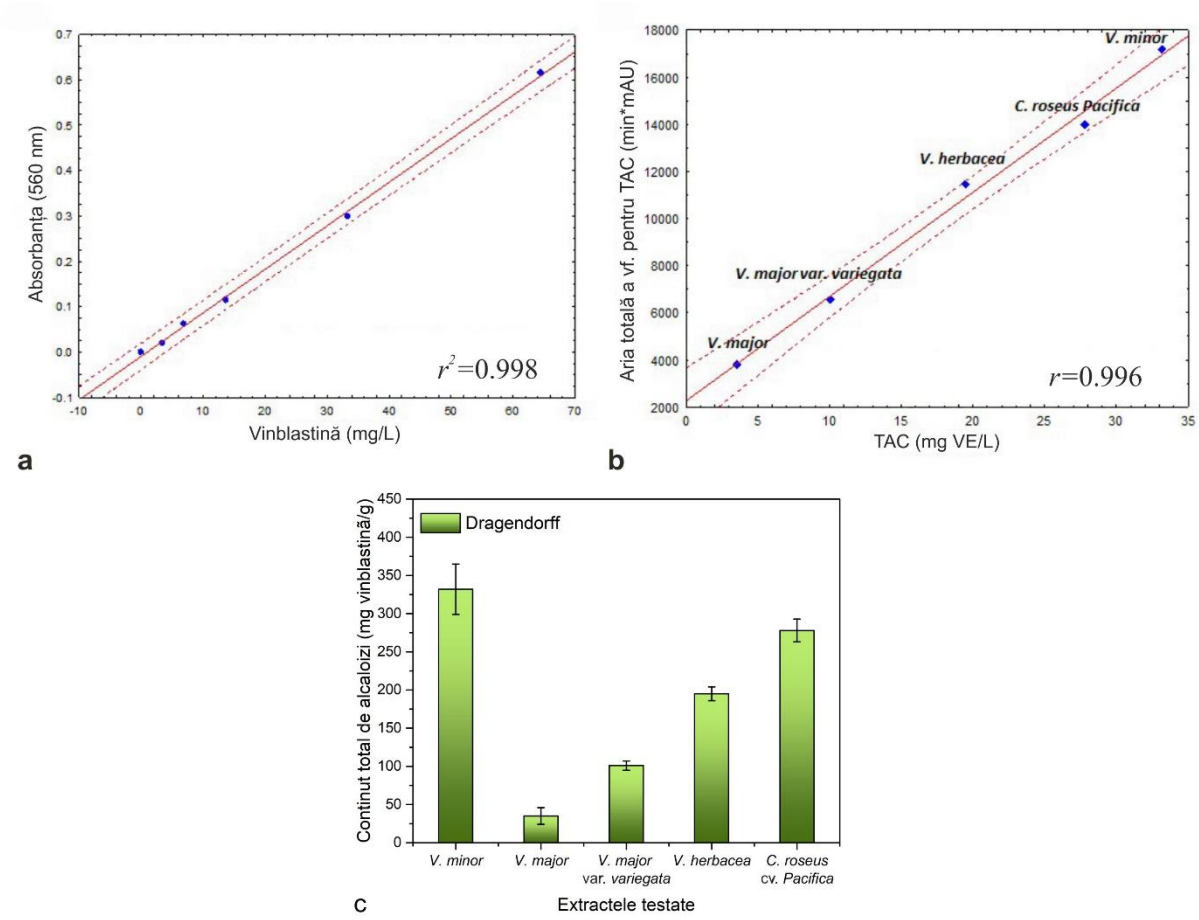

Figure 26. (a) Calibration curve for the Dragendorff assay and compared to vinblastine standard, **(b)** graphical correlation of the total alkaloid content determined through Dragendorff assay and HPLC method, **(c)** graphical representation of the Dragendorff assay results (Ciorîță *et al.*, 2021c).

3.4.2 Antioxidant activity determination

The antioxidant potential of *Vinca minor, V. herbacea, V. major, V. major* var. *variegata,* and *Catharanthus roseus* cv. Pacifica was determined thorough REAC, DPPH, CUPRAC, and lipid peroxidation inhibition methods.

3.4.2.1 DPPH method

Blois created the technique in 1958 with the intention of quickly and accurately measuring a compound's antioxidant activity (Kedare *et al.*, 2011). Purple is the hue of the stable free radical 1,1-diphenyl-2-picrylhydrazyl (DPPH). DPPH transforms into a neutral molecule and gradually loses its color when it interacts with a substance that acts as a hydrogen atom donor. At 517 nm, color fading can be observed. The DPPH decolorization time will be shortened the better a molecule is a hydrogen atom donor (Sharma *et al.*, 2009).

3.4.2.2 ABTS•⁺/REAC method

Blue-green 2,2'-azino-bis(3-ethylbenzothiazoline-6-sulfonic acid), often known as ABTS, is the hue of trolox-equivalent antioxidant capacity (TEAC). The reagent loses its color after coming into contact with one or more antioxidant chemicals. The decolorization duration will be shortened the stronger the antioxidant compound,

according to other studies (Müller *et al.*, 2011; Nenadis *et al.*, 2011; Re *et al.*, 1999). The color change can be observed at 730 nm. Rutin was the standard employed in the studies conducted for this study report; as a result, this procedure was given the name REAC.

3.4.2.3 CUPRAC (Cupric ion reducing antioxidant capacity) method

When powerful antioxidants are present, Cu (II) from bis-neocuproin is converted to Cu (I) (polyphenols, but also alkaloids). The development of a combination between Cu(I) and the quinones produced by the antioxidant chemicals is what gives the substance its apparent yellow color. The more the yellow complex absorbs light at a wavelength of 450 nm, the more potently antioxidant the substance is. (Akar *et al.*, 2019; Ozyurek *et al.*, 2011).

3.4.2.4 Lipid peroxidation inhibition method

Lipid peroxidation occurs more quickly when cytochrome C is present. Following the enzyme's reaction with the peroxyl radicals it produces, some substances with antioxidant activity can postpone its occurrence. The delayed peroxidation will have a sigmoidal kinetic profile, and the longer an antioxidant compound's liposome peroxidation inhibition time is. (Buege *et al.*, 1978; Moț *et al.*, 2016).

The *V. herbacea* extract showed strong antioxidant activity using all four techniques used to measure antioxidant activity (Fig. 27). The *V. minor* extract is the least effective antioxidant when it comes to preventing lipid peroxidation, and among all the extracts examined in this study, the *V. major* extract was the least effective antioxidant in the majority of initial analyses. Thus, in terms of overall antioxidant activity, *V. herbacea* extract tops the list, followed by *V. major* var. *variegata*, *C. roseus* cv. Pacifica, *V. minor*, and *V. major*.

The antioxidant potential is determined by the phytoconstituents present in the extract used, such as vincamine (Wu *et al.*, 2018), chlorogenic acid (Foddai *et al.*, 2017), and other phenolic compounds (Stagos, 2020). The results obtained by us are consistent with previous studies where the antioxidant activity was determined for *V. minor* (Grujić *et al.*, 2014), *V. herbacea* (Șimșek Sezer *et al.*, 2018), *V. major* (Cheng *et al.*, 2016), and *C. roseus* (Ferreres *et al.*, 2008; Mardani-Nejad, 2017). Moreover, the total polyphenol/flavonoid content was directly correlated with the observed antioxidant activity ($r > 0.9$).

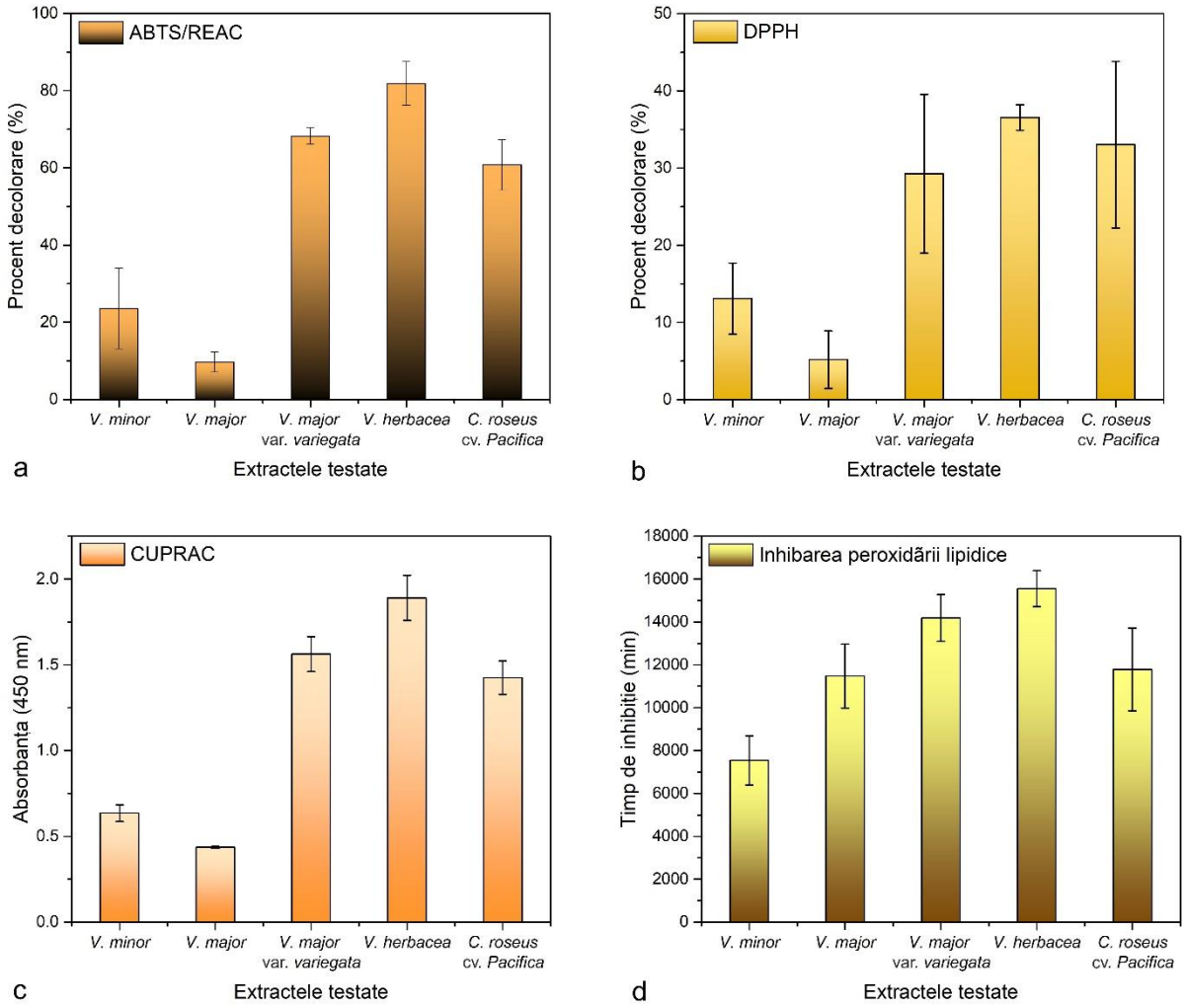

Figure 27. The antioxidant activity determined in *Vinca* and *C. roseus* cv. Pacifica plant extracts through: **(a)** REAC, **(b)** DPPH, **(c)** CUPRAC, and **(d)** lipid peroxidation inhibition methods.

3.4.3 Antibacterial activity determination

3.4.3.1 Diffusimetric method

Preliminary analyzes by the diffusimetric method were carried out to establish the potential of the extracts to inhibit the growth of Gram-positive bacterial strains (*Staphylococcus aureus*) and Gram-negative (*E. coli*) (Fig. 28). In principle, *E. coli* bacteria were more sensitive than *S. aureus* under the action of *Vinca* and *C. roseus* plant extracts, but statistically significant differences were determined only in the case of strains treated with extract of *V. major* var. *variegata* (Fig. 28).

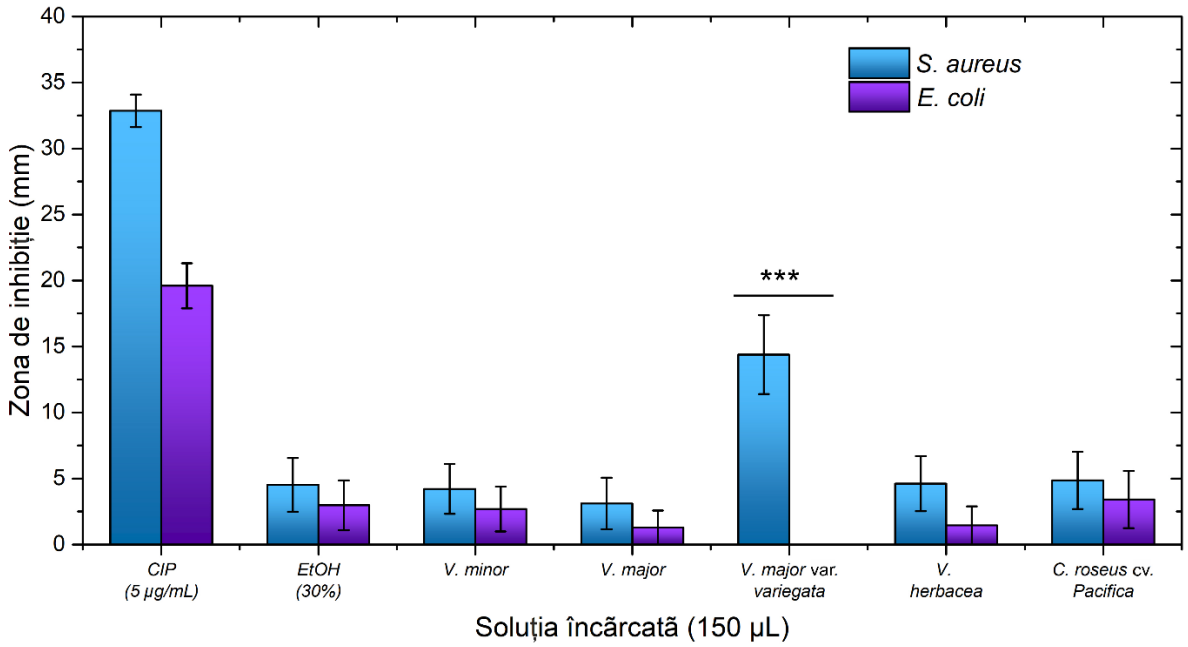

Figure 28. Antibacterial effect of *Vinca minor*, *V. major*, *V. major* var. *variegata*, *V. herbacea*, and *Catharanthus roseus* cv. Pacifica plant extracts, determined through the diffusimetric method against *E. coli* and *S. aureus* bacterial strains (Ciorîță *et al.*, 2021c).

3.4.3.2 Microdilution method

It was feasible to determine, depending on the concentration and the species, how the extracts affected the bacterial strains of *E. coli* and *S. aureus* using the microdilution method. The lowest extract concentration at which bacterial growth is stopped is known as the minimum inhibitory concentration (MIC). For *V. minor* and *V. major* var. *variegata*, MIC could be established at concentrations lower than 50%, and bacterial growth was suppressed for the remaining extracts at 25% or 50% plant extract concentration in the mediu (Fig. 29).

The bacterial strains reacted differently to the extracts depending on the peptidoglycan's composition. In this way, *V. herbacea* promoted the growth of *E. coli* cultures while inhibiting the growth of *S. aureus* cultures. The high quantity of rutin (258 µg/g) found in this extract is an essential factor, and other researchers that examined the effects of rutin on Gram-positive and Gram-negative bacteria obtained similar outcomes (Bharathi *et al.*, 2018; Dubey *et al.*, 2013; Ganeshpurkar *et al.*, 2017). However, *V. minor* inhibited both bacterial strains, which might be explained by the complicated chemical makeup of the plant extract. According to studies, entire extracts can be more harmful to bacteria than pure alkaloid or polyphenol fractions (Mahmoudi *et al.*, 2016; Manosalva *et al.*, 2016; Shaheen *et al.*, 2019). Similar results were also reported by Grujic et al. (2015), who tested different types of *V. minor* extracts on Gram-negative and Gram-positive bacteria, with strong inhibitory effects against the latter (Grujić *et al.*, 2015).

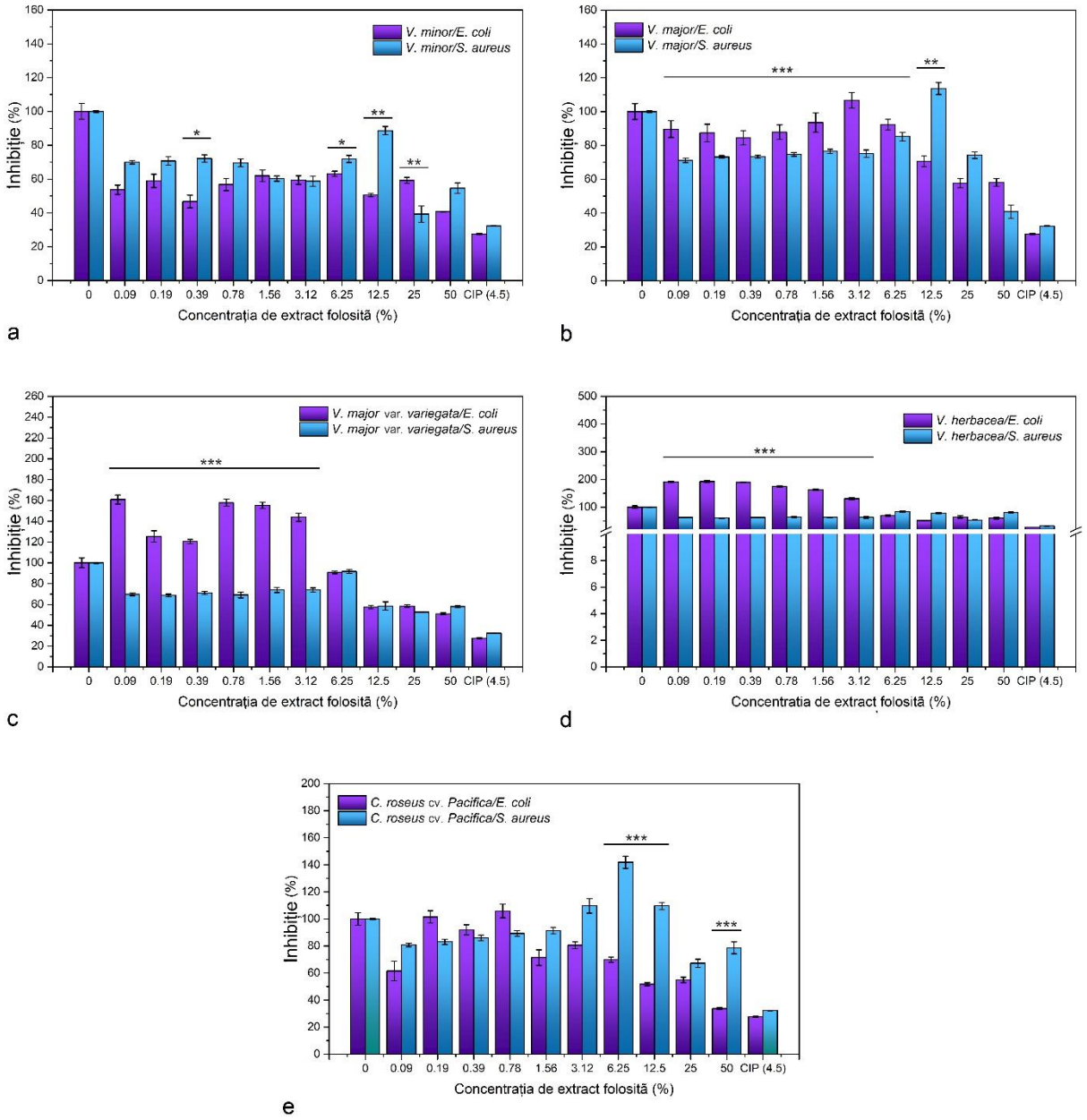

Figure 29. Antibacterial effect of *Vinca minor*, *V. major*, *V. major* var. *variegata*, *V. herbacea*, and *Catharanthus roseus* cv. Pacifica plant extracts, determined through the microdilution method against *E. coli* and *S. aureus*. The values represent the mean of minimum three replicates ± standard error of the mean (s.e.m.) **(a)** *V. minor*, **(b)** *V. major*, **(c)** *V. major* var. *variegata*, **(d)** *V. herbacea*, **(e)** *C. roseus* cv. Pacifica. *** $p < 0.0001$, ** $p < 0.001$, * $p < 0.05$ (Ciorîță *et al.*, 2021c).

3.4.3.3 Induced morphological alterations in the studied bacteria

SEM analysis of bacteria exposed to *Vinca* and *C. roseus* extracts was used to identify some induced morphological changes. The extremely noticeable glycocalyx was present on the surface of *E. coli* that had been exposed to a plant extract of *V. major* var. *variegata* (Fig. 30). This aspect may help to explain why the proliferative effect of this extract was noticed on the *E. coli* strain in accordance to the results of the microdilution test. Compared to untreated strains, bacteria treated with all extracts at a 25% concentration shrank in length (Fig. 31).

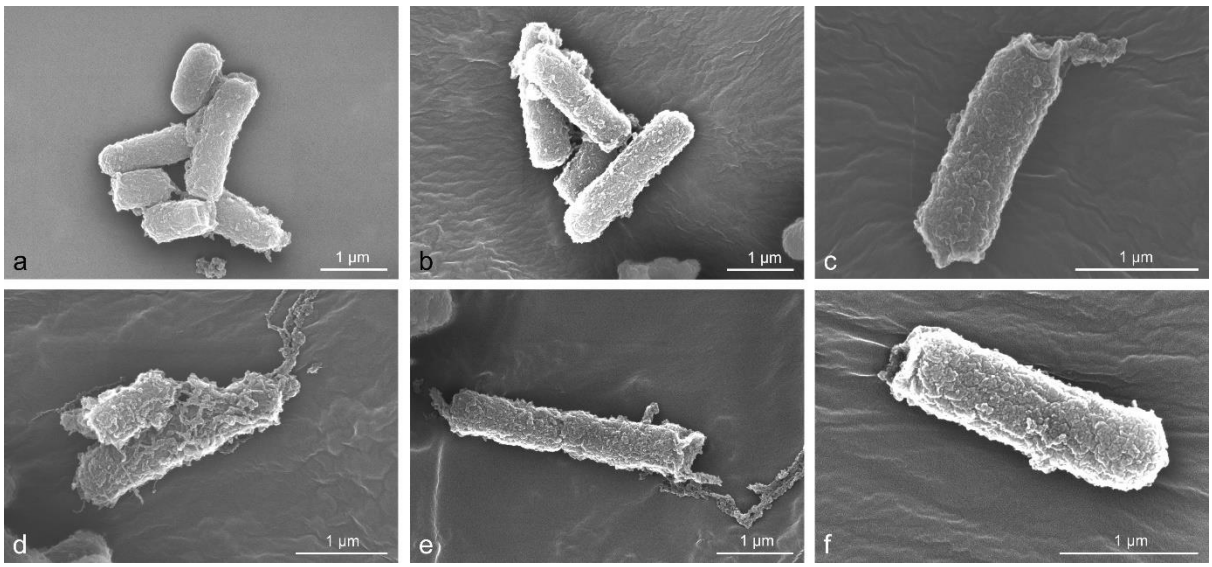

Figure 30. SEM micrographs of *E. coli* bacterial strain treated with *Vinca* and *C. roseus* plant extracts at the identified MIC values; **(a)** control *E. coli* (untreated), **(b)** 2% *V. minor*, **(c)** 15% *V. major*, **(d)** 10% *V. major* var. *variegata*, **(e)** 5% *V. herbacea*, and **(f)** 5% *C. roseus* cv. Pacifica.

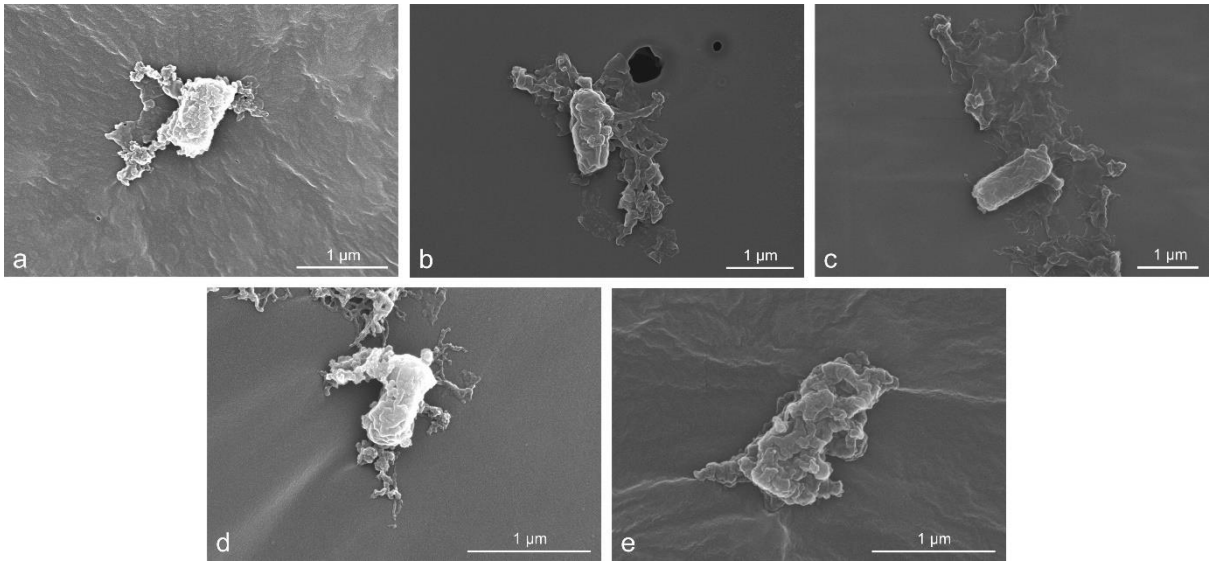

Figure 31. SEM micrographs of *E. coli* bacterial strain treated with 25% *Vinca* and *C. roseus* plant extracts; **(a)** control *E. coli* (untreated), **(b)** *V. minor*, **(c)** *V. major*, **(d)** *V. major* var. *variegata*, **(e)** *V. herbacea*, and **(f)** *C. roseus* cv. Pacifica.

As the extract of *V. minor* proved very effective against *E. coli* strains, the bacilli were measured using SEM images and a script developed in the MATLAB program. Thus, the size variations of the control strains, those treated with 3% extract and those treated with 25% extract were established (Fig. 32).

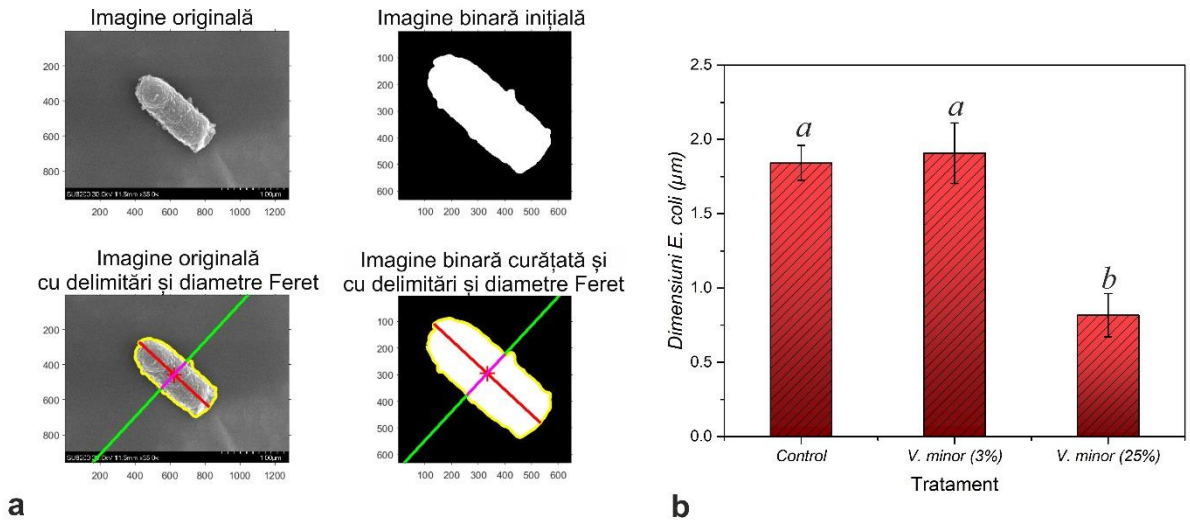

Figure 32. (a) Computational analysis of *E. coli* dimensions determined with the help of a MATLAB script and **(b)** size distribution of *E. coli*. The values marked with same letter are not statistically significant according to the Tukey test at $p < 0.05$ (Ciorîță *et al.*, 2021a).

It was observed that bacteria treated with 25% extract concentration were significantly ($p < 0.05$) smaller than those treated with 3% extract concentration and the untreated control. In comparison to untreated bacteria, bacteria treated with 3% extract showed a small but non-significant increase in size.

S. aureus behaved morphologically differently to the various extracts (Fig. 33). *S. aureus* did not significantly vary from the untreated control after being exposed to *V. minor* extract at a MIC of 5%, while bacteria exposed to *V. major* and *V. major* var. *variegata* exhibited a smoother surface (Fig. 33). The glycocalyx was more pronounced in *S. aureus* treated with extract of *V. herbacea* at a dosage of 2%, and bacteria treated with extract of *C. roseus* cv. Pacifica at a concentration of 25% had extensive extracellular matrix, similar to bacteria that form biofilms (Fig. 33f).

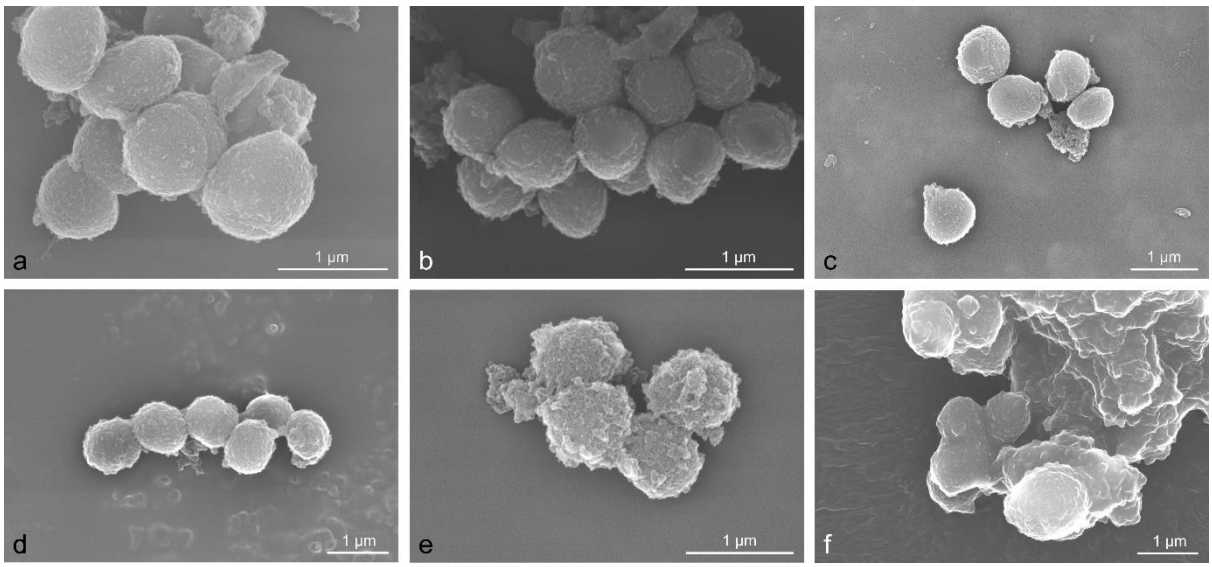

Figure 33. SEM micrographs of *S. aureus* treated with *Vinca* and *C. roseus* plant extracts; **(a)** control *S. aureus* (untreated), **(b)** 5% *V. minor*, **(c)** 2% *V. major*, **(d)** 2% *V. major* var. *variegata*, **(e)** 2% *V. herbacea*, **(f)** 25% *C. roseus* cv. Pacifica.

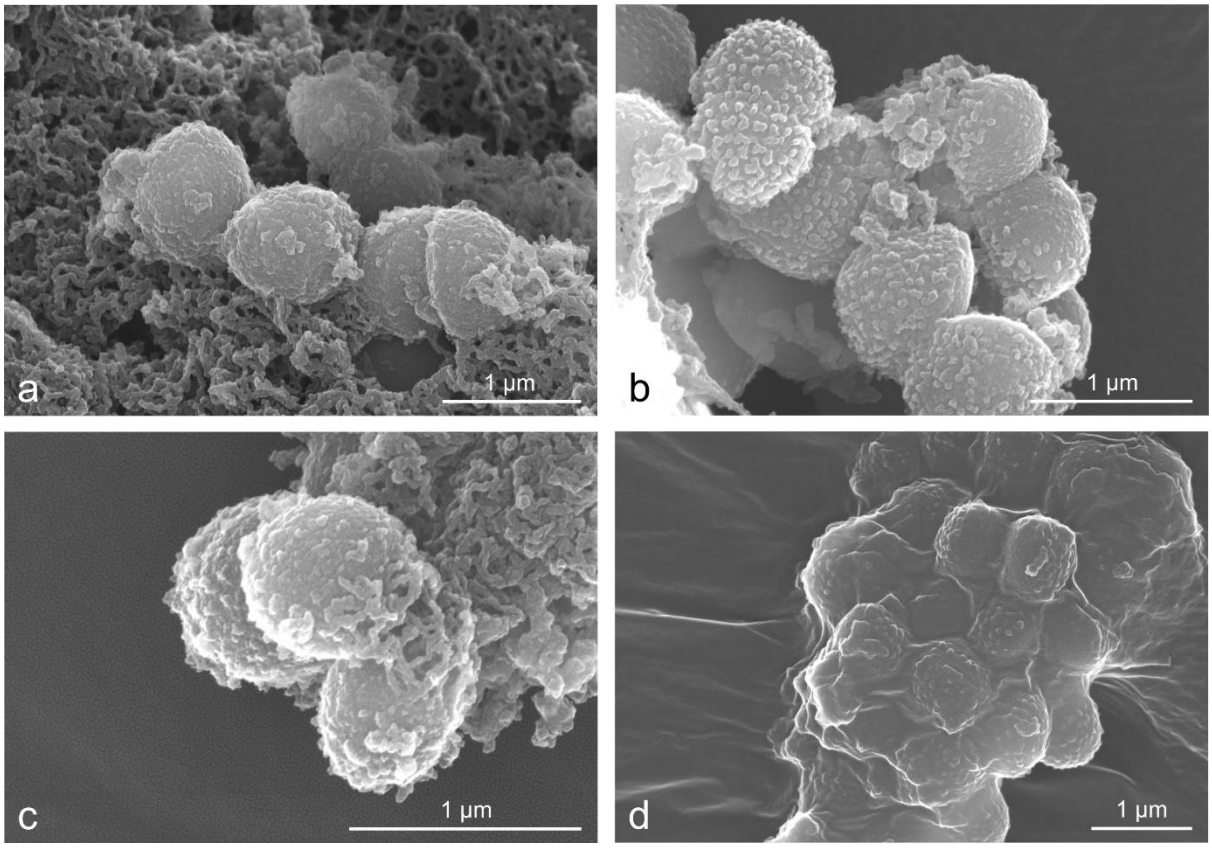

Figure 34. SEM micrographs of *S. aureus* treated with 25% *Vinca* and *C. roseus* plant extract concentration; **(a)** *V. minor*, **(b)** *V. major*, **(c)** *V. major* var. *variegata*, **(d)** *V. herbacea*, **(e)** *C. roseus* cv. Pacifica.

The results showed that the extract of *V. herbacea* at the concentration of 25% has the same effect as the extract of *C. roseus* on the morphology of *S. aureus* cocci (Fig. 34). *S. aureus* cocci treated with *V. major* had a rough

appearance, but those treated with *V. minor* and *V. major* var. *variegata* were almost completely disintegrated and only a few retained their shape (Fig. 34).

Spearman correlation statistical analysis showed that growth inhibition of *E. coli* strain is negatively correlated with TAC (ρ = -0.6), and this result indicates a decrease in the optical density generated by the bacteria while increasing the concentration of alkaloids in the plant extracts (Fig. 35). Considering that *V. minor* had the highest total alkaloid content and the best inhibitory effect against *E. coli* bacterial cells, this correlation is justified. Moreover, the positive correlation between TPC and bacterial inhibition by the microdilution method (ρ = 0.7) suggests that the proliferative effect of *V. herbacea* extract on *E. coli* may be generated by the high content of polyphenols in this extract (Fig. 35). Also, TPC was negatively correlated with the inhibitory effect on *S. aureus* bacterial cells (ρ = -0.6), explaining why the same extract (*V. herbacea*) had the strongest inhibitory effect on *S. aureus*.

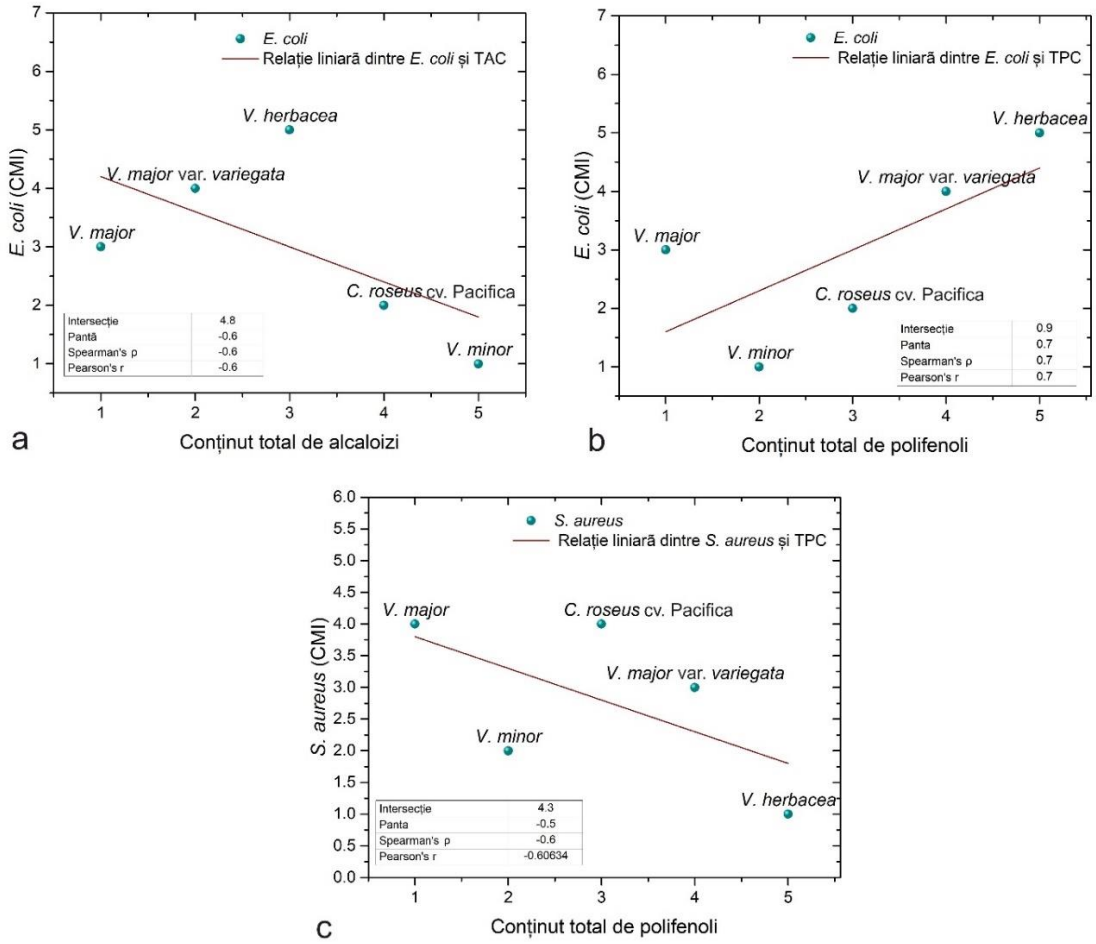

Figure 35. MIC, total polyphenol, and total alkaloid contents correlations of *Vinca minor*, *V. major*, *V. major* var. *variegata*, *V. herbacea*, and *Catharanthus roseus* cv. Pacifica plant extracts, determined against **(a-b)** *E. coli* and **(c)** *S. aureus*. MIC = minimal inhibitory concentraton, TAC = total alkaloid content, TPC = total poliphenol content.

These findings suggest a connection between plant extracts' chemical constituents and their impact on both Gram-positive and Gram-negative bacteria. As a result, alkaloids are powerful antibacterial agents against *E. coli*

but do not prevent the growth of the *S. aureus* strain, whereas polyphenols are effective against the growth of *S. aureus* and aid in the proliferation of *E. coli*. Similar findings were also reported in the specialized literature, where isolated polyphenol or alkaloid fractions exhibited the effects seen in the study (Adamczak *et al.*, 2020; Deepika *et al.*, 2019; Dubey *et al.*, 2013; Ganeshpurkar *et al.*, 2017).

The outcomes of morphological analysis on bacteria treated with *Vinca* and *C. roseus* plant extracts are in agreement with those previously described. The *V. major* var. *variegata* and *V. herbacea* extract-treated *E. coli* bacilli displayed the most pronounced extracellular matrix, and this characteristic is related to the proliferative effect shown in the case of both extracts as it shows a stronger pathogenicity (Aruldass *et al.*, 2013; Suwalak *et al.*, 2009). Additionally, the breakdown of *S. aureus* cocci produced by the plant extracts was comparable to the outcomes seen in other studies (Gupta *et al.*, 2015), although more research is required to fully comprehend how the chemicals in the plant extracts interact with the bacterium (Jhanji *et al.*, 2019).

3.4.4 Cytotoxicity determination

The cytotoxicity of *Vinca minor*, *V. major*, *V. major* var. *variegata*, *V. herbacea*, and *Catharanthus roseus* cv. Pacifica plant extracts was determined against human normal keratinocytes (HaCaT) and human melanoma (A375) cell lines, in vitro. *C. roseus* (also known as *V. rosea*) was chosen as means of comparison for its antitumor activity, based on the literature data. According to ISO 10993-5:2009(E) (ISO10993-5:2009(E), 2009), cell viability can be interpreted as following: weak cytotoxicity at 80-60%, moderate cytotoxicity at 60-40%, and highly cytotoxic at and under 40%.

MTT results showed that *Vinca* plant extracts have a proliferative effect against HaCaT cell lines at 48 h, for concentrations up to 1% (including 2% for *V. minor*), while they inhibited the development of A375 cell lines at 72 h (Fig. 36). LDH release indicates the integrity of the outer plasmatic membrane and depending on the formula used for concentration calculation, the inhibitory capacity or necrosis degrees could be determined (Macavei *et al.*, 2016). Therefore, for A375 cell lines, the plant extracts had a strong inhibitory capacity which could be associated with apoptosis or necrosis, with values above (*V. minor*, *V. herbacea*, *C. roseus* cv. Pacifica) or very close to (*V. major* and *V. major* var. *variegata*) those of the Tween 20 treated samples (Fig. 37). Positive values of LDH release were observed only on HaCaT cells treated with *C. roseus* cv. Pacifica plant extract, while the other plant extracts used indicate an obstruction of the plasmatic membrane, with values below those of the untreated control (Fig. 37b).

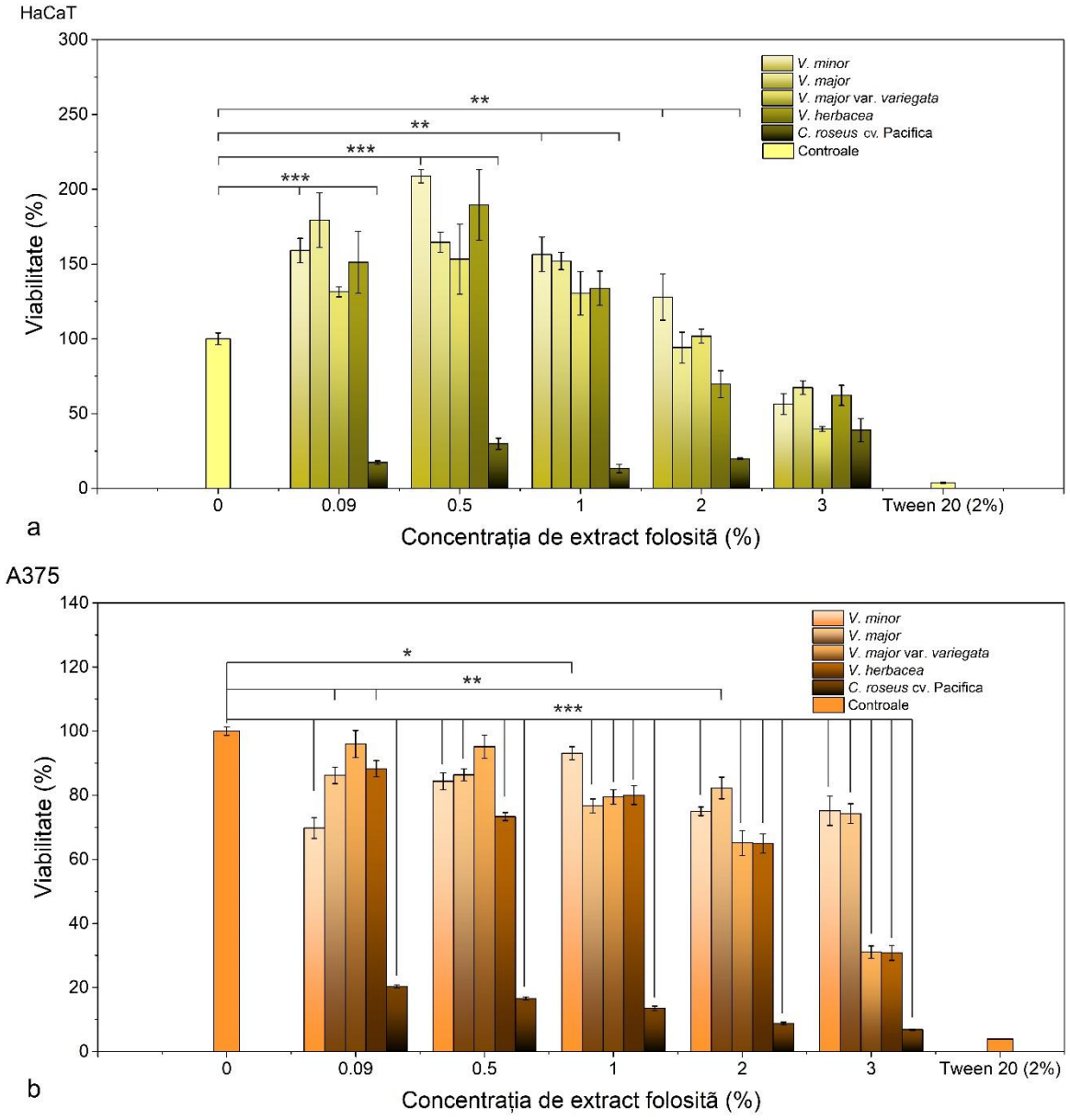

Figure 36. MTT cell viability assays of *Vinca minor*, *V. major*, *V. major* var. *variegata*, *V. herbacea*, and *Catharanthus roseus* cv. Pacifica plant extracts, against **(a)** HaCaT keratinocytes, **(b)** A375 melanoma; *** $p < 0.0001$, ** $p < 0.001$, * $p < 0.05$.

The minimum value at which 50% of the cells (IC50) are negatively affected was determined using the MTT assay. This value was different in the two types of cells treated with the same type of extract (Table 11). As a result, a higher dose of *V. minor* (9% compared to 4.25% for HaCaT) and *V. major* (7.04% compared to 3.89% for HaCaT) plant extract is required to inhibit A375 melanoma. However, the plant extracts of *V. major* var. *variegata* (2.37%) and *V. herbacea* (2.3%) proved very effective in inhibiting the development of A375 cells, the minimum values for this being below the minimum values reached by HaCaT cells (2.85% for *V. major* var. *variegata* and 2.89 % for *V. herbacea*), and this aspect indicates that a lower dose of plant extract is required to inhibit cancer cells and therefore normal cells will not be affected (Table 11). In Figure 38, you can see the effect of the extracts used on the concentration of NO in the culture medium where the treated cells were.

Table 11. The minimal concentration at which 50% of the cells (IC_{50}) are affected by the *Vinca* and *C. roseus* plant extracts

Cell line	IC_{50} (%)				
	V. minor	*V. major*	*V. major* var. *variegata*	*V. herbacea*	*C. roseus* cv. Pacifica
HaCaT	4.25	3.89	2.85	2.89	0.63
A375	9	7.04	2.37	2.3	<0.2

In comparison to HaCaT cells, the effects of the extracts were substantially more pronounced in A375 cells. Intense oxidative stress and the production of reactive oxygen species can cause cellular damage (Suman *et al.*, 2013). Nitric oxide (NO) in the culture medium can, however, be a sign of both pro- and anti-apoptotic effects. Low amounts can therefore prevent apoptosis from progressing while also preventing the growth of tumor cells through apoptosis (Levytskyy *et al.*, 2004). As a result, the analyses' findings must be compared to those of other biochemical studies in order to be considered definitive (MTT and LDH in the present case).

On both of the tested cell types, the extract of *C. roseus* cv. Pacifica displayed the most adverse effects. Two of the alkaloids generated by this plant, vinblastine and vincristine, are also utilized in chemotherapy in conjunction with other cytostatics (Amos, 2011; Emara *et al.*, 2000; Moudi *et al.*, 2013). Although this plant's HPLC examination revealed a high concentration of alkaloids, it also included other natural substances in significant amounts, which together with the alkaloids produced the effects that were observed. The remaining *Vinca* extracts tested exhibited a proliferative effect on keratinocytes and a dose-dependent inhibitory effect on melanoma. *Vinca* alkaloids interact with β-tubulin at the GDP+ end of microtubules, at a locus known as the "vinca domain" (Khattak *et al.*, 2016). The effects, however, are different depending on the concentration (Jordan *et al.*, 2007), and besides vincristine and vinblastine, there are other alkaloids that can bind to this domain (Zhou *et al.*, 2005). However, in the studied literature there is no evidence to attest the mode of action between other alkaloids isolated from *Vinca* species and microtubules, for which much more complex analyzes are needed.

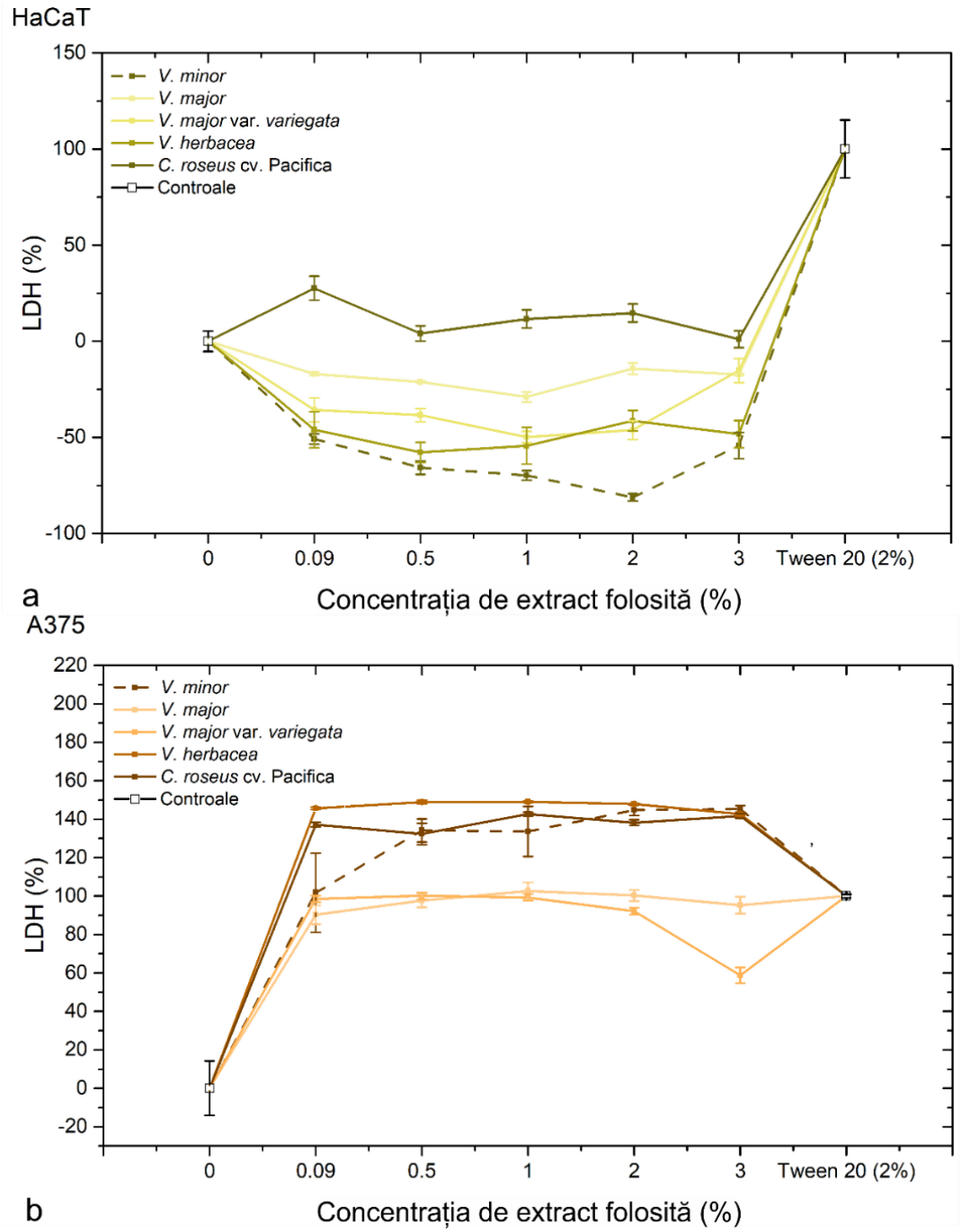

Figure 37. LDH release assay of the cells treated with *Vinca minor*, *V. major*, *V. major* var. *variegata*, *V. herbacea*, and *Catharanthus roseus* cv. Pacifica plant extracts. **(a)** HaCaT keratinocytes, **(b)** A375 melanoma.

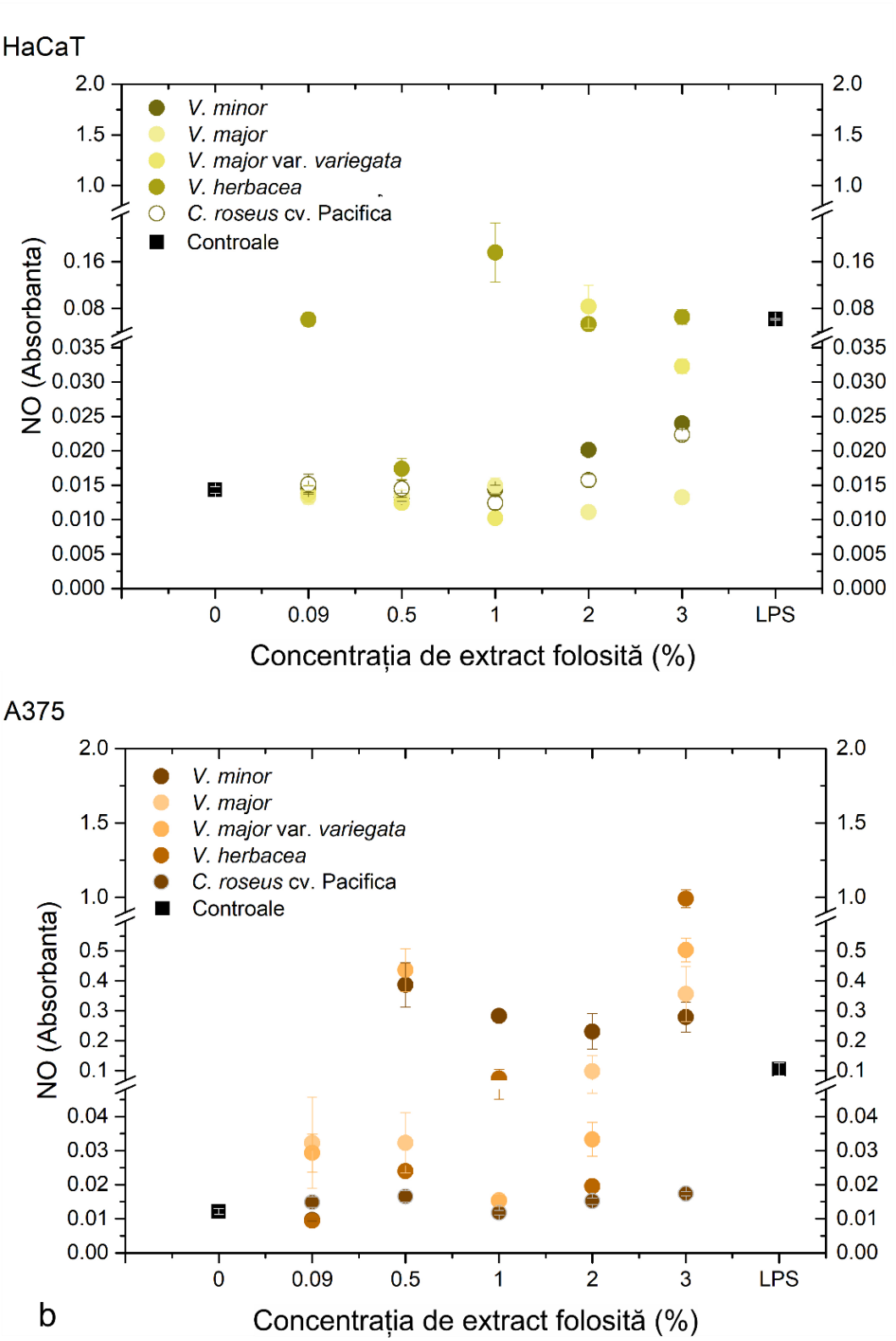

Figure 38. NO concentration of cells treated with *Vinca minor*, *V. major*, *V. major* var. *variegata*, *V. herbacea*, and *Catharanthus roseus* cv. Pacifica plant extracts. **(a)** HaCaT keratinocytes, **(b)** A375 melanoma; LPS = lypopolyzaharides.

A375 and HaCaT cell sections were analyzed by TEM to look for any potential ultrastructural alterations brought on by the plant extracts employed. All five of the utilized extracts had various effects on human melanoma (Fig.

39). The appearance of numerous vesicular structures in A375 cells treated with *V. minor* extract (Fig. 39b) set these cells apart, while numerous mitochondria were observed in cells treated with the other extracts.

The number of mitochondria present in the cytoplasm of HaCaT keratinocytes treated with *Vinca* extracts was high (Fig. 40), although the differences from untreated cells were negligible. Normal cells, on the other hand, were significantly too damaged after being exposed to *C. roseus* extract to be fixed and analyzed by TEM.

The MTT assay's viability results, which showed proliferative effects on HaCaT cells, appear to be related to the abundance of mitochondrial particles detected by TEM examination. The polyphenol concentration of plant extracts may be related to this proliferation (Zhu *et al.*, 2008). On the other hand, the *V. minor* extract had a significant negative impact on the ultrastructural appearance of A375 cells. Lysosomes are a sign of necrosis when they are present in significant numbers (Arunkumar *et al.*, 2020), and other investigations have produced comparable findings (Danciu *et al.*, 2018).

Although the findings of this study indicate that *Vinca* leaf extracts have pharmacological efficacy that is as promising as that obtained from *C. roseus*, additional research will be required to ascertain the mode of action at the subcellular level, but this aspect presents a potential area of future study.

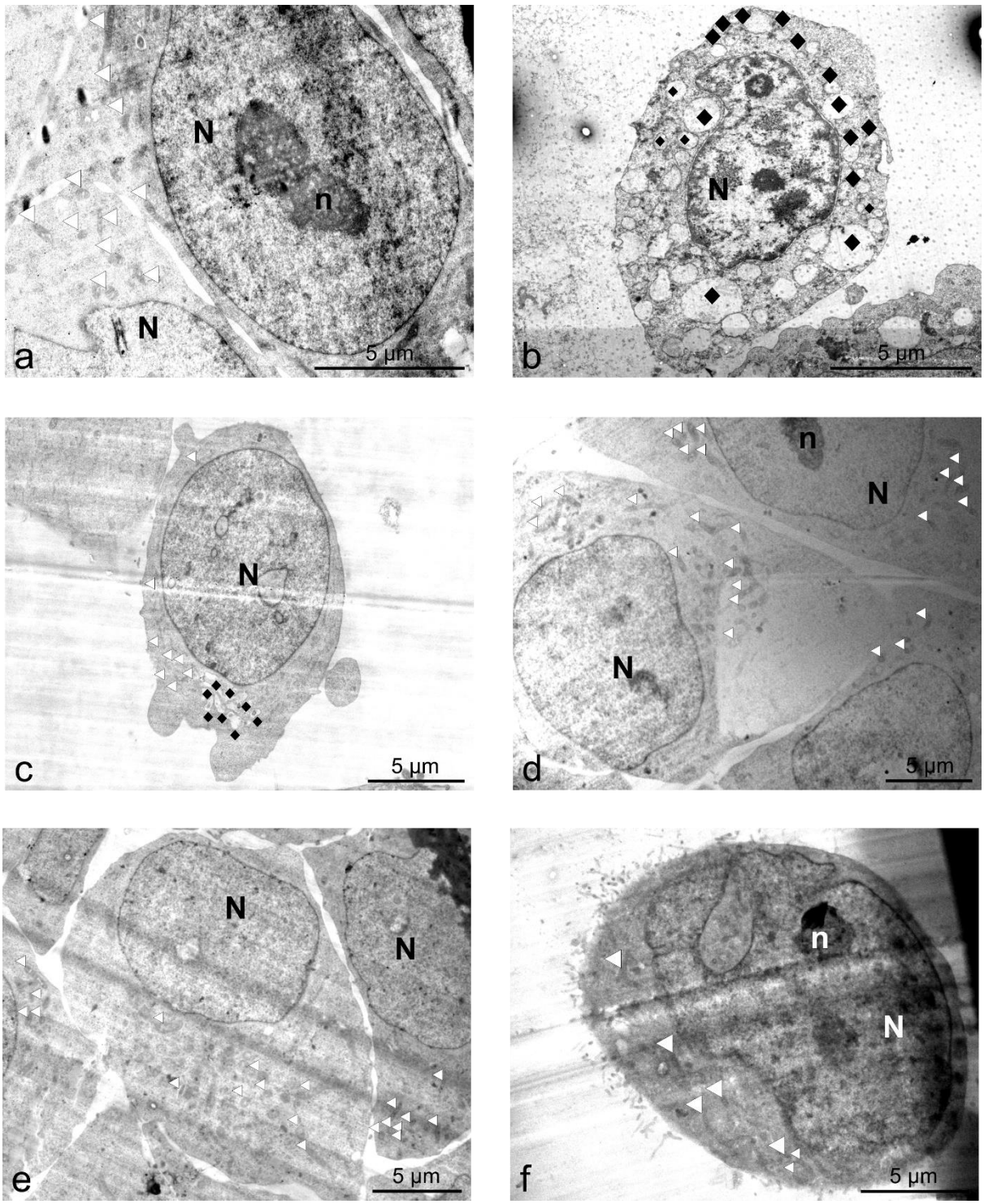

Figure 39. TEM micrographs of A375 cells treated with *Vinca* and *C. roseus* plant extracts at IC_{50} values; **(a)** untreated control, **(b)** *V. minor*, **(c)** *V. major*, **(d)** *V. major* var. *variegata*, **(e)** *V. herbacea*, **(f)** *C. roseus*; white triangles = mitochondria, black rhombs = vesicular bodies; N = nucleus, n = nucleolus.

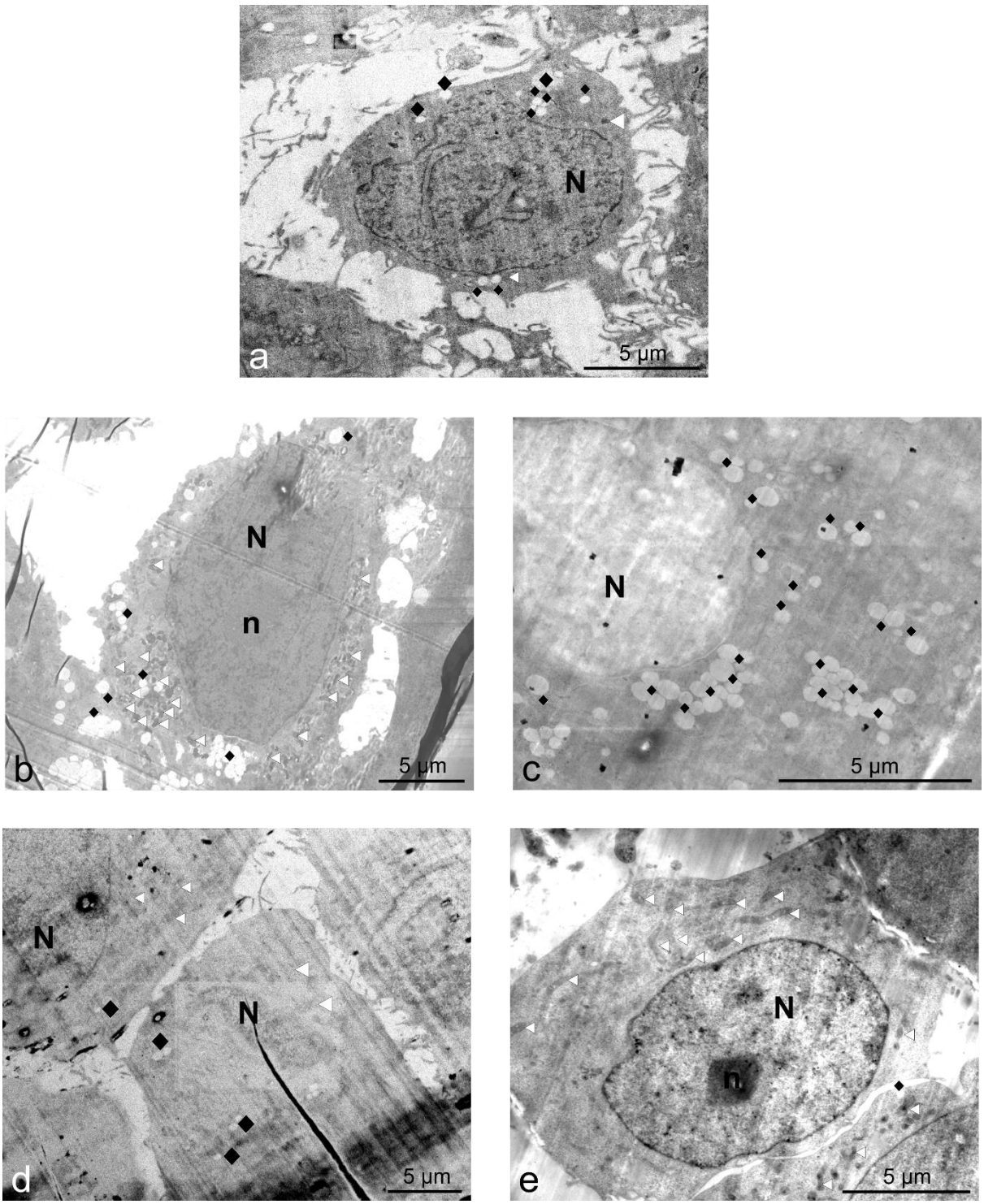

Figure 40. TEM micrographs of HaCaT cells treated with *Vinca* plant extracts at IC_{50} value; **(a)** untreated control, **(b)** *V. minor*, **(c)** *V. major*, **(d)** *V. major* var. *variegata*, **(e)** *V. herbacea*; white triangles = mitochondria, black rhombs = vesicular bodies; N = nucleus, n = nucleolus.

3.5 Green synthesis of Ag-MnO_2 nanoparticles using *Chelidonium majus* or *Vinca minor* plant extracts

Based on the findings of the cytotoxicity and antibacterial activity tests, the plant extract of *V. minor* was chosen for this study, and the extract of *C. majus* was used as a reference because the literature claimed that it was successful in producing metal nanoparticles. In a prior work (Pârvu *et al.*, 2013), phytochemical analysis of *C.*

majus extract was conducted. Three different types of nanoparticles (NPs) with varying shapes and sizes between 9 and 30 nm were produced using the extracts alone and in a 1:1 combination.

3.5.1 Ag-MnO_2 nanoparticle characterization

Ag-MnO_2 nanoparticles were obtained with *Chelidonium majus* or *Vinca minor* and were physically characterized and tested for antimicrobial potential and effect on normal human cell lines (HaCaT) and human cancer cell lines (A375).

3.5.1.1 Physical characterization of Ag-MnO_2 nanoparticles

C. majus nanoparticles (CmNPs) were the largest, with an average size of 32.47 nm ±0.73 nm, and those obtained with *V. minor* extract (VmNPs) with an average size of 10.09 nm ±0.14 nm. The NPs obtained with a mix of *C. majus* and *V. minor* (MNPs) had an average size of 9.36 nm ±0.19 (Fig. 41).

EDX analysis revealed a „core-shell" type of NPs with MnO_2 in the inside and Ag on the outside. Moreover, the outer layer was covered with a thin hallow that is most probably from the natural compounds of the plant extracts (Fig. 42).

NPs' crystallinity was assessed through XRD (Fig. 43). Four distinct diffraction peaks were seen at 2θ corresponding to (111), (200), (220), and (311) refraction planes, characteristic of the face centered cubic of silver; and (110), (101), and (211) characteristic of MnO_2. These results demonstrate that all three types of nanoparticles had crystalline structure and the Ag-MnO_2 complex was successfully formed.

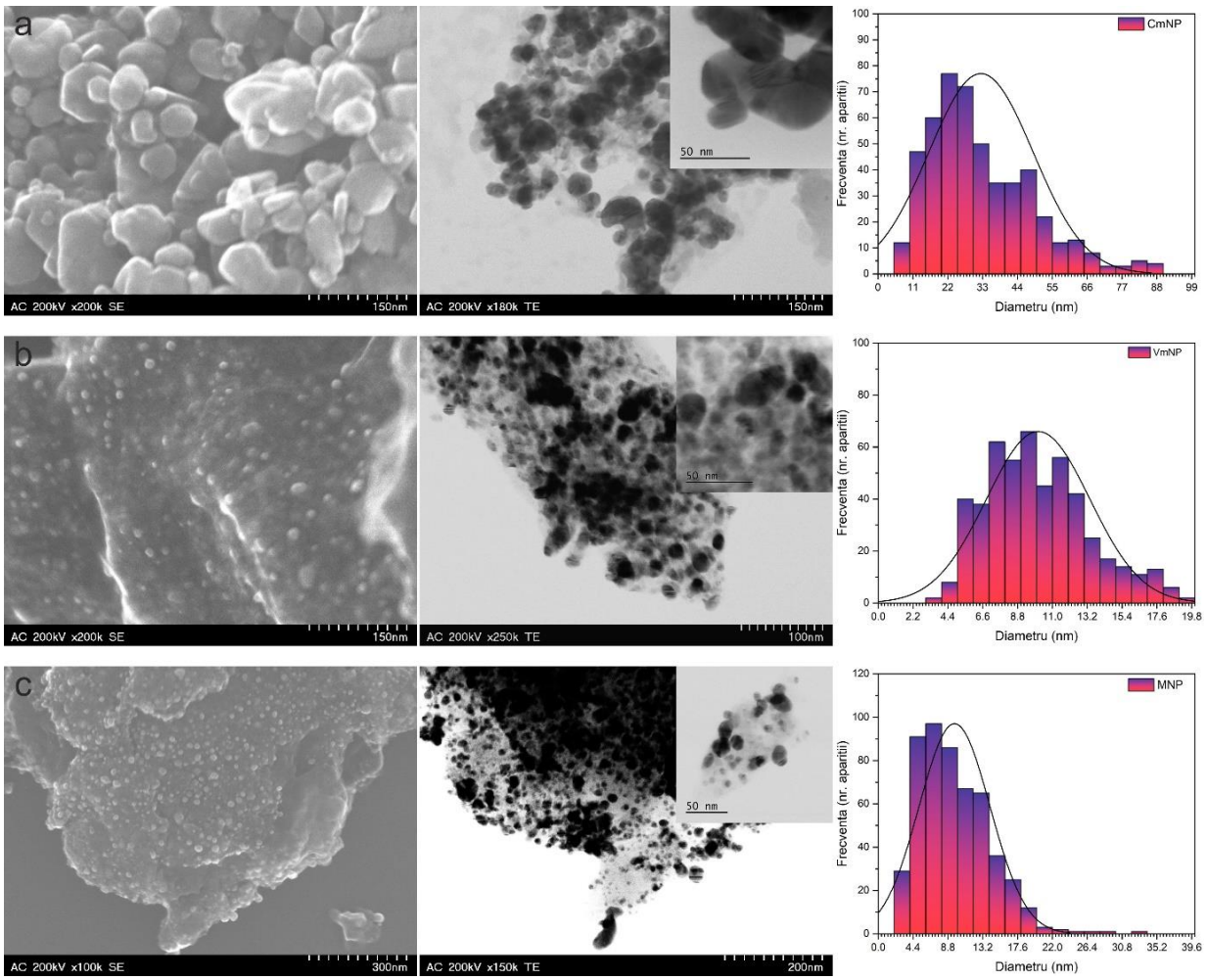

Figure 41. STEM micrographs of Ag-MnO_2 nanoparticles synthesized with *C. majus* and *V. minor* plant extracts and their size distribution. **(a)** CmNPs, **(b)** VmNPs, **(c)** MNPs.

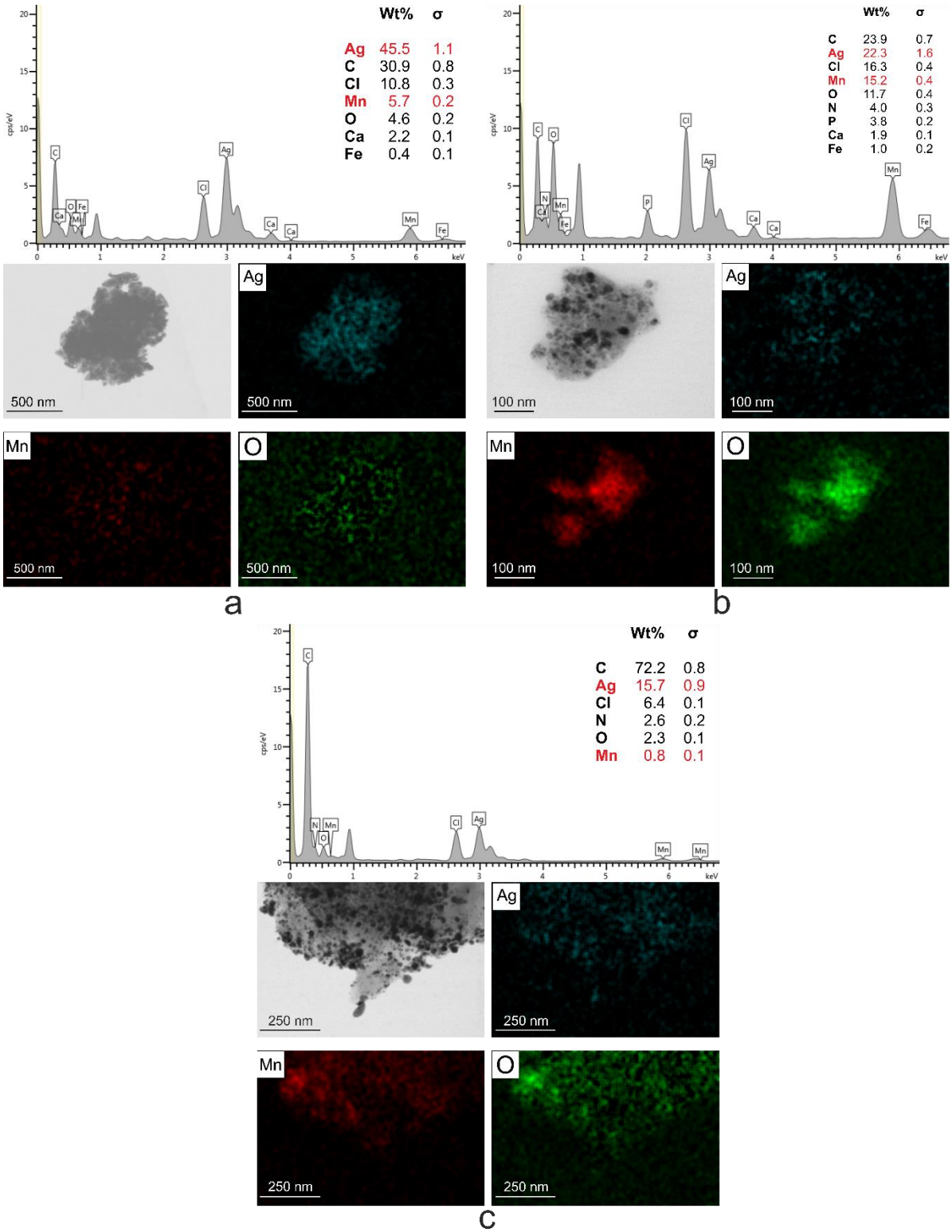

Figure 42. EDX spectra of the obtained Ag-MnO_2 nanoparticles; **(a)** CmNPs, **(b)** VmNPs, **(c)** MNPs; Wt% = weight procentage.

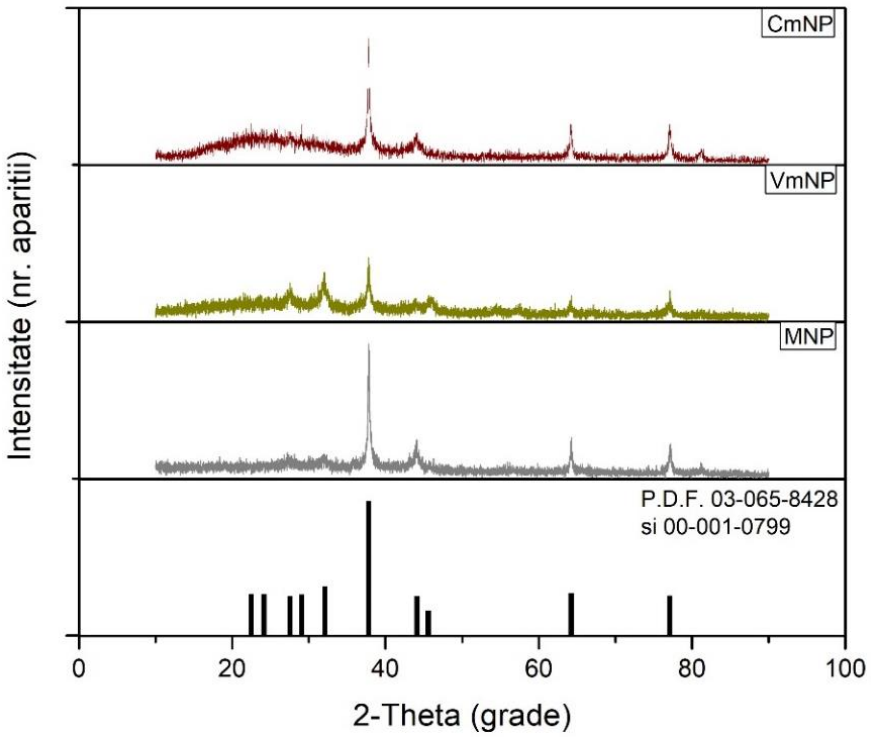

Figure 43. X-ray diffraction spectra of the obtained Ag-MnO_2 nanoparticles and compared to P.D.F. data base („powder diffraction file") of the X SmartLab diffractometer.

Similar results were also reported in the specialized literature, where plant extracts were used to obtain Ag, MnO_2 or Ag-MnO_2 nanoparticles (Alavi *et al.*, 2018; AlSalhi *et al.*, 2019; Anandan *et al.*, 2019; Dehghanizadea *et al.*, 2018; Kunkalekar *et al.*, 2012; Ramalingam *et al.*, 2017).

The specific metal-oxygen vibrations for the NPs as well as the absorption bands corresponding to the functional groups of the organic compounds in the natural extracts could be found using Fourier Transform IF spectroscopy (FTIR) analysis (Fig. 44). The findings of the phytochemical analyses conducted on the two extracts support the fact that the wide vibration bands are the cause of the complicated chemical makeup of the used extracts (section 3.4 and (Pârvu *et al.*, 2013)). The important FTIR spectral range is between 1750–500 cm^{-1}. 1750–1580 cm^{-1} spectral range where aldehydes, ketones (C=O), C=C and N-H (amino acids) groups all exhibited extinction vibrations. Another significant finding was that the extinction vibrations in the region where the alkaloids respond were extremely powerful in the case of VmNP:1742, 1458, 1074, and 745 cm^{-1}.

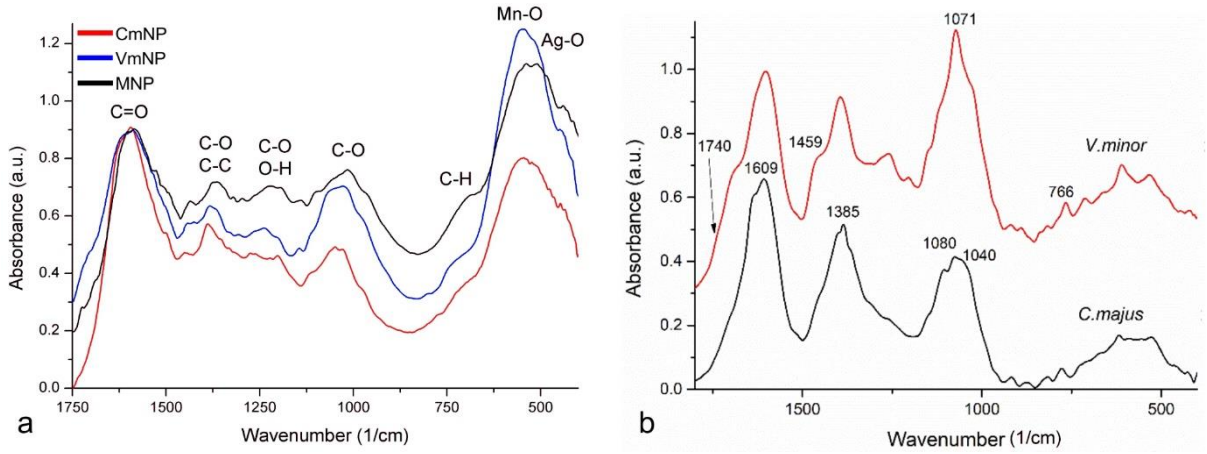

Figure 44. FTIR spectra of the obtained Ag-MnO_2 nanoparticles synthesized with *C. majus* and *V. minor* plant extracts **(a)** and of the plant extracts alone **(b)** (Ciorîță *et al.*, 2020).

The morphological results revealed the production of an outer layer as well, and the FTIR analysis verified its presence. This organic shell had the same structure as the extracts that had been independently studied. Despite being found, the distinctive vibrational bands for the O-H (3400 cm^{-1}) and C-H (2846 cm^{-1}), bonds are not important because they are unique to a variety of bioactive chemicals (Baciu *et al.*, 2013; Zavoi *et al.*, 2011). The significant vibration domains for the nanoparticles produced in this investigation were those that were recorded between 175 and 500 cm^{-1}. Aldehydes, ketones, and amino acids all exhibited the extinction vibrations of C=O groups in the range of 1750–1580 cm^{-1} as well as C=C and N-H (Baciu *et al.*, 2013; Dobrucka *et al.*, 2017; Farahanikia *et al.*, 2011).

In the case of CmNPs and VmNPs, the distinct vibrational bands of C-O and C-H bonds were found around 1450-1300 cm^{-1}, and for MNPs, the results were similar to those of prior studies at 1380 cm^{-1} and 1365 cm^{-1} (Dobrucka *et al.*, 2017). Specific vibrational bands for C-O, N-H, and O-H bonds are observed around 1270-1150 cm^{-1} (Poojary *et al.*, 2015). Between 600 and 450 cm^{-1}, the typical vibrations for Mn-O are widely distributed. (Gharibshahi *et al.*, 2017; Huang *et al.*, 2013; Jaganyi *et al.*, 2013). Ag-Ag metallic bonds could not be seen because they resonate below the wavelength of 400 cm^{-1} (Gharibshahi *et al.*, 2017). Instead, the vincamine-specific spectra at wavelengths of 1742, 1458, 1074, and 745 cm^{-1} were found (S.D.B.S.). These bands were found in the extract of *V. minor* and the VmNPs (at 1742 cm^{-1} and 1459 cm^{-1} and shouldered at 1071 cm^{-1} and 766 cm^{-1}).

The berbamine in *C. majus* extract exhibits significant aromatic vibrations at 1609 cm^{-1}, C-H bonds at 385 cm^{-1}, a particular band for ring deformation at 1080 cm^{-1}, and a shoulder-shaped OCO extinction of the dioxolane ring at 1040 cm^{-1} (Leona *et al.*, 2007). The spectrum of CmNPs also contained all of these bands, but significantly displaced or in the shape of shoulders. So, it is also possible to state that the generated nanoparticles had a covering consisting of plant extracts.

3.5.1.2 Antimicrobial activity of Ag-MnO_2 nanoparticles

The antimicrobial activity of the nanoparticles was tested by the diffusimetric method on two bacterial strains of *E. coli* and *S. aureus* and on a fungal strain of *C. albicans* (Fig. 45)

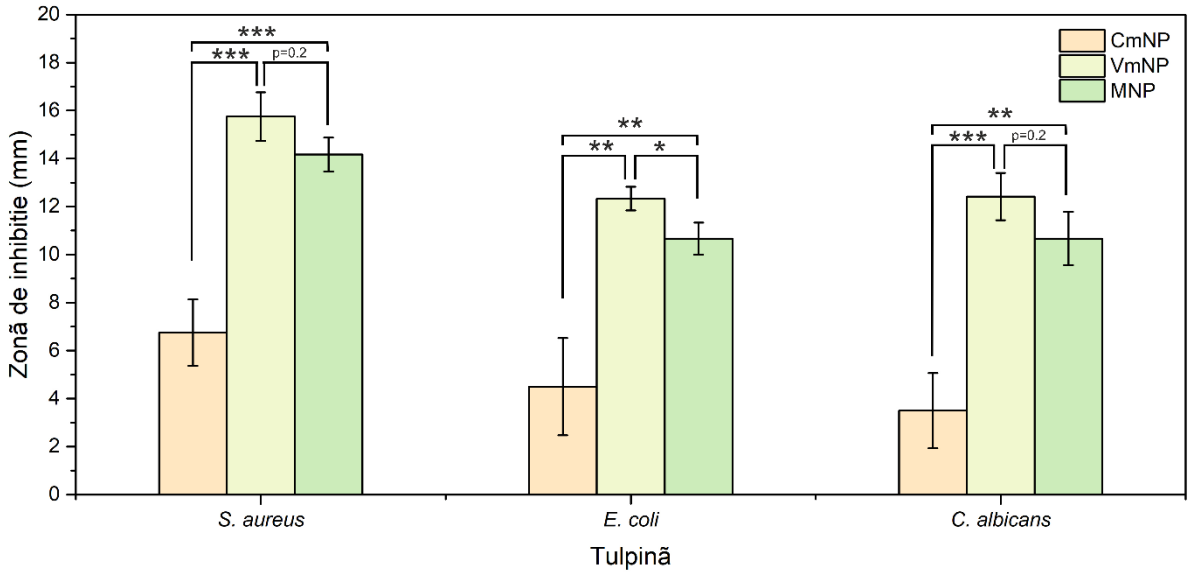

Figure 45. Antimicrobial effect of the obtained NPs assayed through the diffusimetric method against *E. coli*, *S. aureus*, and *C. albicans* (Ciorîță *et al.*, 2021a).

The results showed that nanoparticles obtained with *V. minor* extract were the most effective antimicrobial, followed by those prepared with a mixture of extracts, and those prepared only with *C. majus* extract had the weakest effect. The antimicrobial effects of silver are very well documented (Ahmed *et al.*, 2016; Kunkalekar *et al.*, 2014; Lü *et al.*, 2017; Naraginti *et al.*, 2017; Senthil *et al.*, 2017), and the Mn nanoparticles obtained in other studies they have been found to be equally effective in this regard (Hoseinpour *et al.*, 2018a; Hoseinpour *et al.*, 2018b). Therefore, it is possible that these two metals (Ag and Mn) as well as the extract, which remained as a coating layer on the surface of the nanoparticles and was effective against both bacterial strains when tested independently, are to blame for the inhibitory effect seen in the research (section 3.4.3).

3.5.1.3 Cytotoxicity of Ag-MnO_2 nanoparticles

Using the MTT, LDH, and NO methods, the cytotoxicity of NPs was examined on human normal cells (HaCaT) and human cancer cells (A375). Despite having the same basic component (Ag-MnO_2), the two types of cells responded differently to NP treatment, and their varied responses were either brought on by the extract employed or the physical characteristics of the NPs.

Accordingly, CmNPs had a proliferative effect on HaCaT cells (viability over 100%) at concentrations between 1 µg/mL and 250 µg/mL. Thereafter, the viability dropped as a function of concentration up to 89.07% at 1000 µg/mL. Nine out of the ten concentrations utilized in the case of A375 cells showed a proliferative effect (Fig. 46).

At concentrations above 250 µg/mL, VmNPs had a moderate cytotoxic effect on HaCaT cells. At the same concentrations, the effect on A375 cells was moderate (viability 47.25%) or high (viability 35.87%) (Fig. 46b). A375 cells were consequently noticeably more impacted than HaCaT cells (p 0.0001). At concentrations more than 500 µg/mL, MNPs had an adverse effect on both cell types (Fig. 46c).

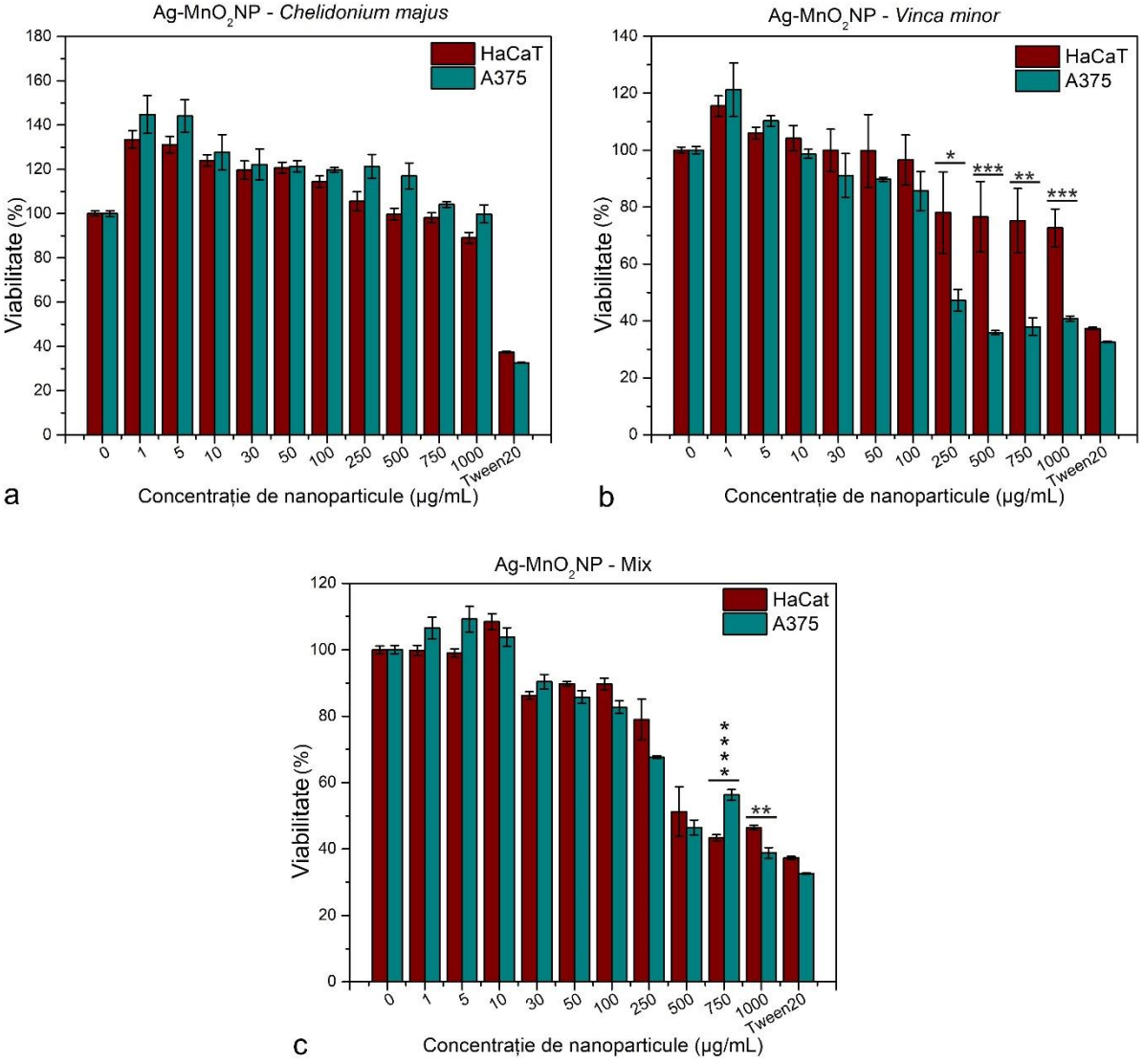

Figure 46. Cytotoxic effect of the obtained Ag-MnO_2 nanoparticles, on HaCaT keratinocytes and A375 melanoma. ****: p<0.0001, ***: p<0.005, **: p<0.05, *: p<0.1 (Ciorîță *et al.*, 2020).

Additionally, the two cell lines responded differentially to the NPs utilized in the LDH test. In contrast to untreated cells, CmNPs-treated HaCaT cells continuously released LDH (p = 1, SD = 0.03 according to χ^2 test). Contrarily, A375 cells showed a dose-dependent response, with LDH concentrations rising up to 16.43% between 1 and 100 µg/mL NP concentration in the culture medium and steadily falling down to -30% at high concentrations (Fig. 47).

When cells were exposed to VmNPs, a dose-dependent response was seen (Fig. 47b), with A375 cells being substantially more impacted than HaCaT cells (p 0.0001). The same results were seen with MNPs (Fig. 47c).

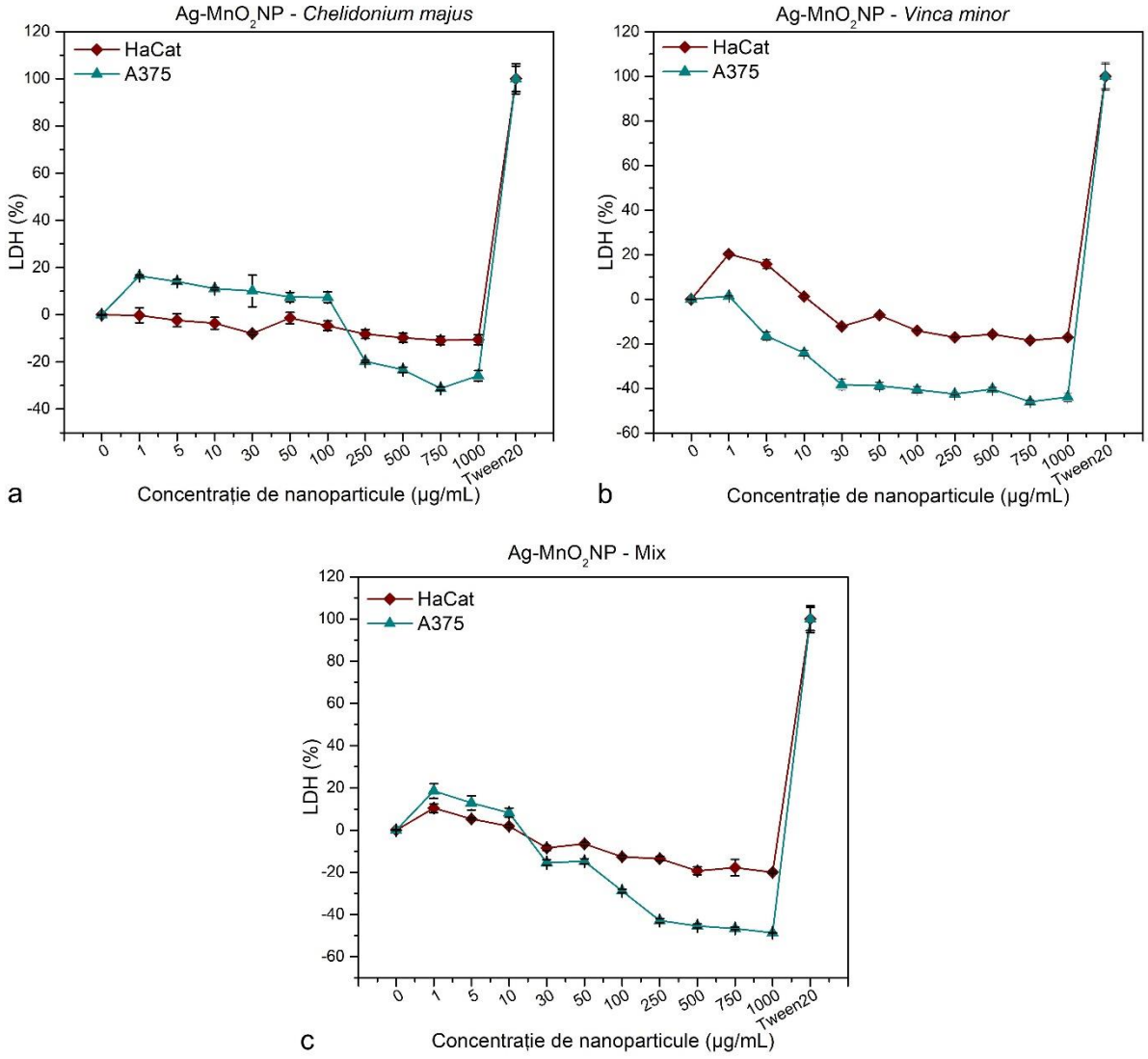

Figure 47. LDH release assay of the HaCaT and A375 cell lines treated with Ag-MnO_2 nanoparticles (Ciorîță *et al.*, 2020).

When compared to untreated cells, the NO concentration in the media of A375 cells treated with CmNPs was consistently low at all concentrations examined (p = 1, SD = 0.0008). At doses ranging from 1 to 250 µg/mL, HaCaT cells responded in a dose-dependent way, recording NO levels that were significantly higher than those of the untreated control (Fig. 48a).

A375 cells were substantially more impacted by VmNPs than HaCaT, with results that were much better as compared to untreated cells at doses above 100 µg/mL (Fig. 48b). MNPs treatment also produced a dose-dependent response, but the effects were not as good as the untreated controls for both cell types (Fig. 48c).

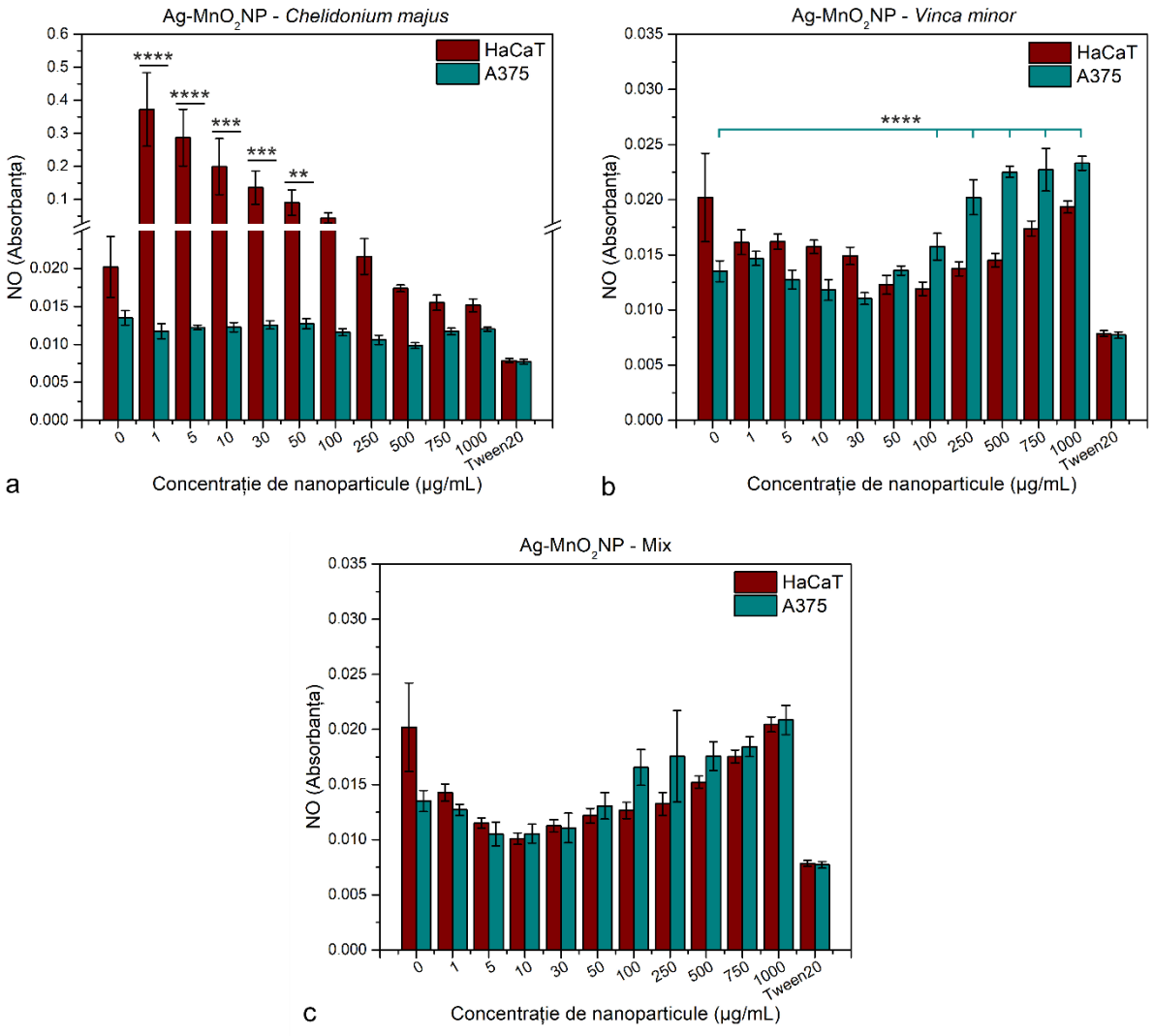

Figure 48. NO concentration of the HaCaT and A375 cell lines treated with Ag-MnO_2 nanoparticles (Ciorîță *et al.*, 2020).

Intense mitochondrial activity was observed in HaCaT cells treated with CmNPs at low doses, and these findings were consistent with those of the NO study of the media. We can infer that the nanoparticles had a proliferative effect on the keratinocytes because the release of LDH was consistent for the treated cells compared to the untreated ones. The inhibitory effect of CmNPs on cancer cells did not result in cytotoxicity (>80% viability), but melanoma was more sensitive to this treatment than normal cells, according to the results of LDH analyses. The cells responded to VmNPs treatment in a dose-dependent manner, but the adverse effects were more pronounced in melanoma. MNPs inhibited both cell lines and were associated with cell necrosis as a result.

The ability of the studied cells to uptake Ag-MnO_2 nanoparticles produced with *C. majus* and *V. minor* was examined by TEM. For this kind of analysis, MNPs and CmNPs were chosen since they represented the extremes of the mean size distribution.

MNPs and CmNPs both found electron-dense particles inside both types of cells (Fig. 49).

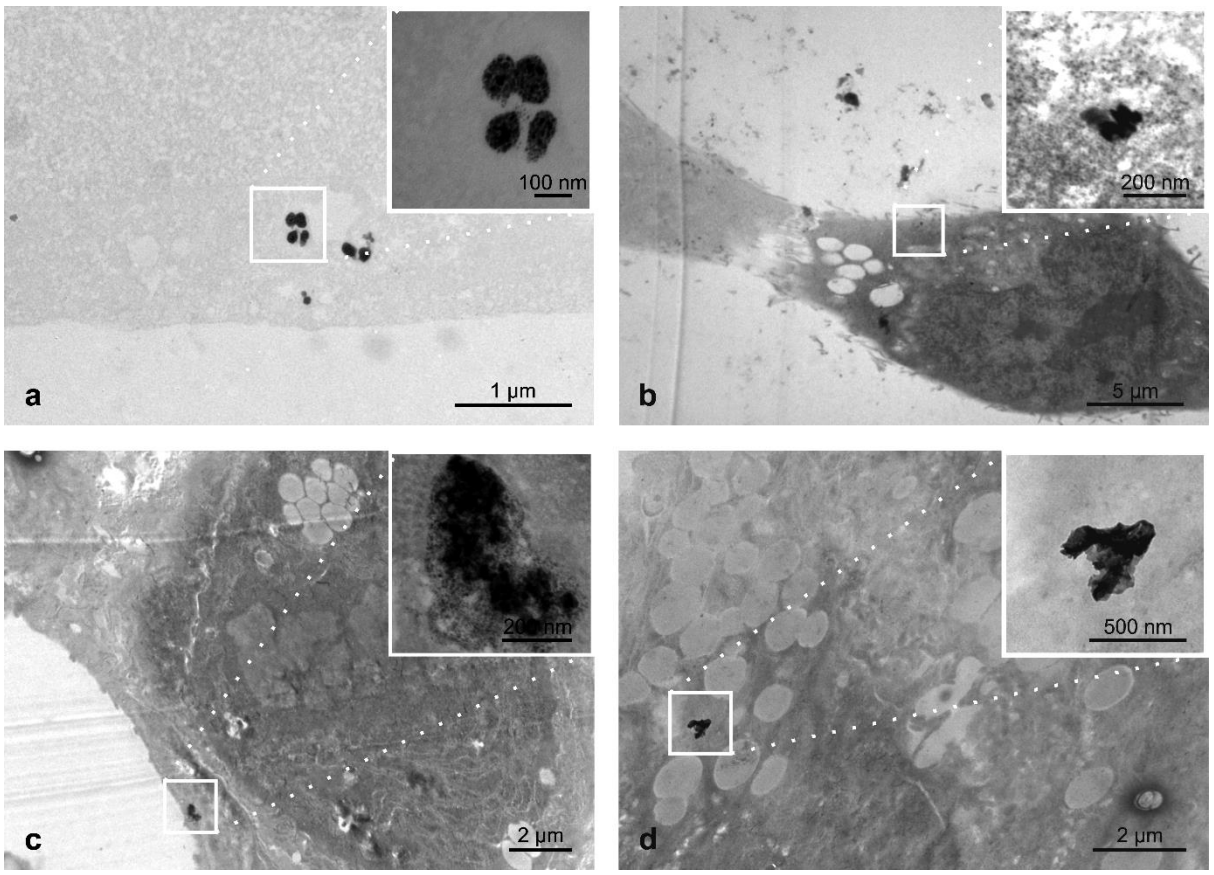

Figure 49. TEM micrographs of the cells treated with the obtained Ag-MnO_2 nanoparticles. The electron dense accumulations are most probably internalized nanoparticles. **(a)** A375 treated with MNPs, **(b)** A375 treated with CmNPs, **(c)** HaCaT treated with MNPs, **(d)** HaCaT treated with CmNPs (Ciorîță *et al.*, 2020).

An EDX study of the cells in the regions with such deposits was carried out to see if the observed electron-dense particles are in fact nanoparticles. Ag was therefore discovered to be a component of the electron-dense deposits in both types of cells (Fig. 50). MnO_2 cannot be detected by the EDX detector in the complex environment of human cells since it is present inside the NP in minute levels. Therefore, while the element Mn could be detected through physical analysis of nanoparticles suspended in water or an organic solvent, it could not be detected through physical analysis of nanoparticles that had been ingested by cells, where the element that surrounded the nanoparticles, specifically Ag, was visible.

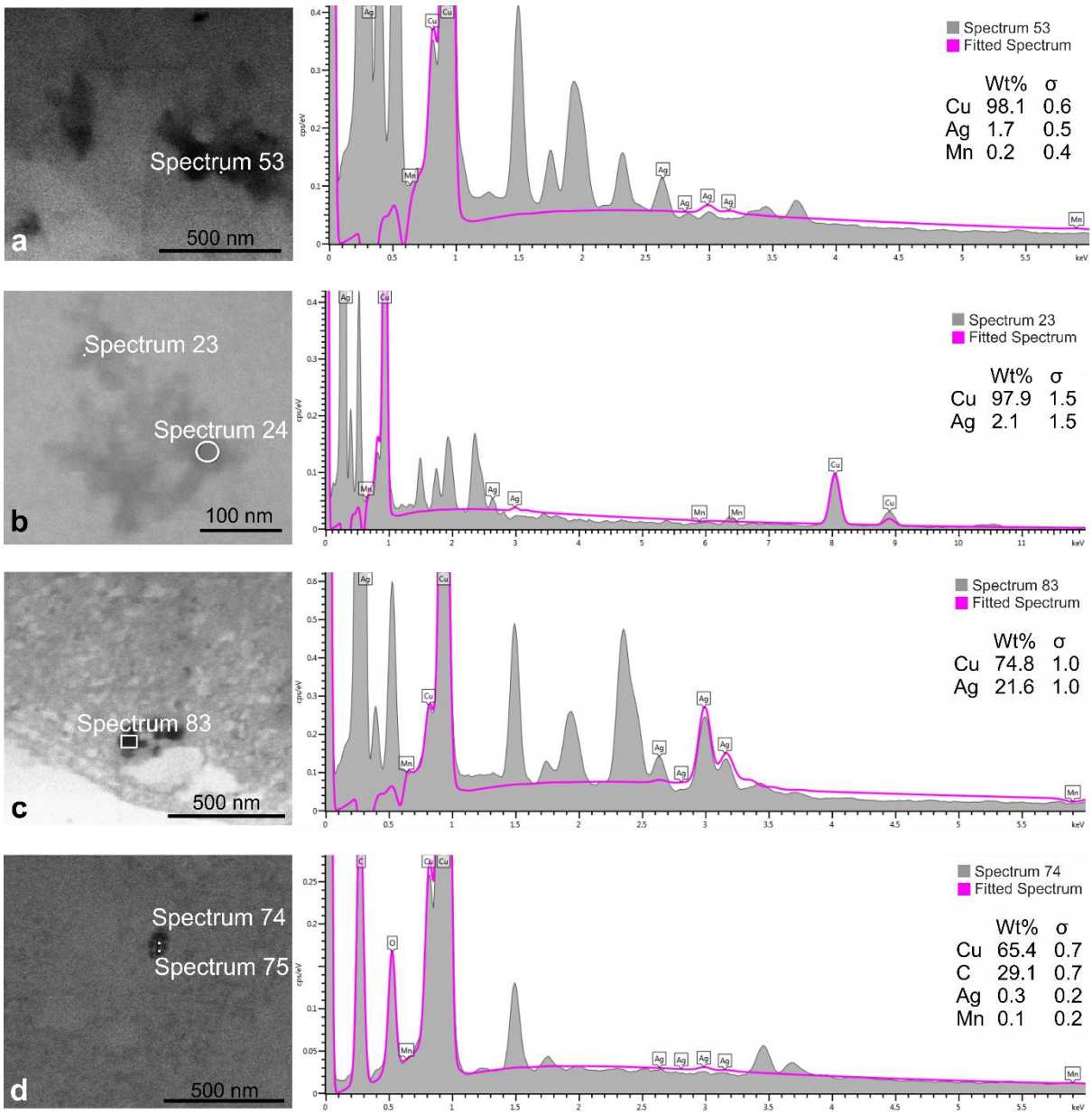

Figure 50. EDX analysis of the HaCaT and A375 cells treated with **Ag-MnO_2** nanoparticles; **(a)** HaCaT treated with MNPs, **(b)** HaCaT treated with CmNPs, **(c)** A375 treated with MNPs, **(d)** A375 treated with CmNPs. The purple fitting line is the ideal EDX spectra for Ag; Wt% – percentual weight units (Ciorîță *et al.*, 2020).

Small nanoparticles can be internalized by cells, according to the results of the TEM analyses, but the precise process by which this happens has not yet been thoroughly elucidated in the literature. The experimental paradigm that states that the same cells can react differently to the same type of nanoparticles is a factor in this study's analysis of in vitro experiments, which examine interactions between cells and nanoparticles (Jiang *et al.*, 2019). All these observed effects may have several explanations. Several theories claim that: (1) usually below 10 nm nanoparticles are toxic (Andersson *et al.*, 2011), but the electrical charge of their surface has an impact on the minimum size threshold at which a cell can have a toxic response; (2) endocytosis is dependent on nanoparticle size; and (3) passive assimilation is preferred over active internalization (Akter *et al.*, 2018; Fröhlich,

2012; Shang *et al.*, 2014). The mechanical resistance to cell deformation is a key goal in in vitro nanoparticle research (Hui *et al.*, 2019). As a result, cancer cells are often less rigid than the tumor tissues they form or normal cells (Coughlin *et al.*, 2013; Guo *et al.*, 2014). Strain resistance for HaCaT cells is 100 kPa (Graf *et al.*, 2018), while for A375 it ranges from 0.76 kPa to 3.9 kPa (Clark *et al.*, 2015; Lekka *et al.*, 2012; Pogoda *et al.*, 2012; Sobiepanek *et al.*, 2017). This factor has the potential to affect how quickly nanoparticles are assimilated. ilver nanoparticles have also been shown to negatively impact human cell lines (Arora *et al.*, 2015; Carrola *et al.*, 2016), yet the cytotoxicity of Ag ions is decreased when combined with MnO_2 (Krishnaraj *et al.*, 2016). The MNPs had an Ag-MnO_2 ratio that was skewed towards Ag, and when combined with the smaller dimensions and intricate chemical makeup of the extracts employed, the observed effects are concise.

4 Conclusions

This doctoral dissertation contrasts the pharmacological potential of hydroalcoholic leaf extracts from *Catharanthus* roseus and *Vinca* species. Different research techniques (electron microscopy, HPLC, computational analyses, X-ray diffraction, REAC, DPPH, etc.) were used through activities carried out in several specialized laboratories to study some morphological aspects of the leaves of the chosen species, the chemical composition of the leaf extracts, and their pharmacological effects. In addition, the extract of *V. minor* was chosen based on the results and combined with the extract of *Chelidonium majus* to create Ag-MnO_2 nanoparticles. Tests on bacteria, fungi, and human cell cultures were then used to evaluate the physical and biological properties of these nanoparticles. Consequently, based on information from the literature and the findings of the study, plant extracts (tinctures) of *Vinca minor, V. major, V. major* var. *variegata*, *V. herbacea,* and *Catharanthus roseus*, the following conclusions were drawn:

The anatomy and morphology of leaves from *Vinca* species and *C. roseus* species, the chemical composition of the obtained plant extracts, the in vitro antioxidant activity, the antibacterial activity and the cytotoxicity on normal and cancerous human cells were analyzed. Thus:

1. Leaf morphology and anatomy showed that there is a direct relationship between stomatal index, trichome density, epicuticular waxes, mesophyll intercellular spaces, cell walls and plant chemical composition, and this result constitutes a first element of novelty in the study carried out.
2. Chemical composition of extracts from representative species of *Vinca* and *C. roseus* cv. Pacifica was correlated with leaf morphology and the total contents of alkaloids, polyphenols and flavonoids were comparatively highlighted.
3. The antioxidant effect of the leaf extracts analyzed was studied in relation to the species and was correlated with their chemical composition, but the strong effect observed in the extract of *V. herbacea* could be associated with the rich content of rutin.
4. *V. herbacea* has a proliferative effect on *E. coli*, but inhibits the development of *S. aureus*. Similar effects were also observed for *V. major* var. *variegata* and *V. major*. The extract of *V. minor* inhibited both bacterial strains, and the extract of *C. roseus* cv. Pacifica had a proliferative effect on Gram-positive bacteria and an inhibitory effect on Gram-negative ones. Therefore, the high content of alkaloids/flavonoids influenced the action on different types of bacteria.
5. The morphology of the tested bacteria was affected by the extracts used, and the effect induced on the *E. coli* strain by the *V. minor* extract is dose-dependent.
6. When compared to healthy human cells (HaCaT), human cancer cells (A375) had decreased mitochondrial activity. *C. roseus* cv. Pacifica had a significant cytotoxic effect on both cell lines, while the other examined extracts suppressed proliferation in a dose-dependent way. The study of the cells' ultrastructure also supported these findings.

7. Although the cytotoxic effects on melanoma were moderate overall, the *V. minor* extract was considered for the next study, as the effects on keratinocytes were less harmful than the rest of the extracts used.

Therefore, three different types of Ag-MnO_2 nanoparticles were made using the extract of *V. minor* as well as a hydroalcoholic extract of *C. majus*. The elemental ratio and type of the chemical bonds produced were measured by EDX and FTIR, and the shape of these nanoparticles was examined by electron microscopy and X-ray diffraction. The nanoparticles are polygonal in shape and range in size from 9 to 30 nm on average. According to the results, we can conclude that:

1. Nanoparticles obtained with *V. minor* extract have a uniform (narrow) size distribution with an average of 10 nm and the best results against the bacteria *E. coli* and *S. aureus* and *C. albicans* fungus. The effects were also negative on human melanoma (A375), without affecting normal cells (HaCaT).
2. The nanoparticles obtained with *C. majus* extract had an average size of 30 nm, with the weakest results against the microorganisms tested, and on human cells the effects were proliferative.
3. The nanoparticles obtained with a 1:1 mixture of the two extracts had the smallest dimensions, with an average of 9 nm. Antimicrobial effects were moderate, but in the case of cells, negative effects were observed in both lines.

Through the published works, this study contributes significantly to the specialized literature. Based on the findings, it was decided that the extract of *V. minor* was the most effective due to its chemically rich composition and inhibitory/proliferative effects in vitro. As a result, it was further chosen to be tested for its ability to reduce the formation of nanoparticles. The doctoral thesis's bibliographic support was based on 352 titles, many of which were scientific papers from national and, especially, international literature. Various research techniques used to examine *Vinca* and *Catharanthus* plants provide valuable insights for multidisciplinary approaches involving various specialists.

5 Dissemination

(according to Appendix Order 6129_2016 minimal standards_CNATDCU, Biology and Biochemistry Committee)

Main author in ISI journals articles (* from the thesis):

1. * **Ciorîță, A.,** Zăgrean-Tuza, C., Moț, A. C., Carpa, R., Pârvu, M. (2021). The phytochemical analysis of *Vinca* L. species leaf extracts is correlated with the antioxidant, antibacterial, and antitumor effects. Molecules, *26*(10), 3040. https://doi.org/10.3390/molecules26103040; **FI:** 4.411; **AIS:** 0.6.
2. * **Ciorîță, A.,** Tripon, S.-C., Mircea, I.-G., Podar, D., Barbu-Tudoran, L., Mircea, C., Pârvu, M. (2021). The morphological and anatomical traits of the leaf in representative *Vinca* species observed on indoor-and outdoor-grown plants. Plants-Basel, *10*(4), 622. https://doi.org/10.3390/plants10040622; **FI:** 3.935.
3. * **Ciorîță, A.,** Suciu, M., Macavei, S., Kacso, I., Lung, I., Soran, M.-L., Pârvu, M. (2020). Green synthesis of Ag-MnO_2 nanoparticles using *Chelidonium majus* and *Vinca minor* extracts and their *in vitro* cytotoxicity. Molecules, *25*(4), 819. https://doi.org/10.3390/molecules25040819; **FI:** 4.411; **AIS**: 0.6.
4. Stefan-van Staden, R.-I., Negut, C. C., Gheorghe, S. S., **Ciorîță A.** (2021). 3D stochastic microsensors for molecular recognition and determination of heregulin-alpha in biological samples. Analytical and Bioanalytical Chemistry, Early Access. doi: 10.1007/s00216-021-03295-7; **FI:** 3.637; **AIS:** 0.8.
5. Surducan, V., Surducan, E., Neamțu, C., Moț, A.-C., **Ciorîță, A.** (2020). Effects of long-term exposure to low-power 915 mhz unmodulated radiation on *Phaseolus vulgaris* L. Bioelectromagnetics, *41*(3), 200-212. https://doi.org/10.1002/bem.22253; **FI:** 2.278; **AIS**: 0.5.

Contributing author in ISI journals articles (* from the thesis):

1. Opriș, O., Soran, M.-L., Lung, I., **Ciorîță, A.**, Copolovici, L. (2021). Biotransformation of non-steroidal anti-inflammatory drugs induces ultrastructural modifications in green leafy vegetables. Journal of Soil Science and Plant Nutrition. https://doi.org/10.1007/s42729-021-00449-5; **FI:** 2.156; **AIS**: 0.4.
2. Suciu, M., Ionescu, C.-M., **Ciorita, A.**, Tripon, S.-C., Nica, D., Al-Salami, H., Barbu-Tudoran, L. (2020). Applications of superparamagnetic iron oxide nanoparticles in drug and therapeutic delivery, and biotechnological advancements. Beilstein Journal of Nanotechnology, *11*(1), 1092-1109. https://doi.org/10.3762/bjnano.11.94; **FI:** 2.612; **AIS**: 0.8.
3. Opriș, O., Lung, I., Soran, M.-L., **Ciorîță, A.**, Copolovici, L. (2020). Investigating the effects of non-steroidal anti-inflammatory drugs (NSAIDs) on the composition and ultrastructure of green leafy vegetables with important nutritional values. Plant Physiology and Biochemistry, *151*, 342-351. https://doi.org/10.1016/j.plaphy.2020.03.046. **FI:** 3.72; **AIS**: 0.8.

4. Opriș, O., **Ciorîță, A.**, Soran, M.-L., Lung, I., Copolovici, D., Copolovici, L. (2019). Evaluation of the photosynthetic parameters, emission of volatile organic compounds and ultrastructure of common green leafy vegetables after exposure to non-steroidal anti-inflammatory drugs (NSAIDs). Ecotoxicology, *28*(6), 631-642. https://doi.org/10.1007/s10646-019-02059-5. **FI:** 2.535; **AIS:** 0.8.

Main author in BDI journals articles (* from the thesis):

1. Sitar, C., **Ciorîță**, **A.** (2019). Ultrastructural aspects of *Eriogaster catax* and *Eriogaster lanestris* (Lepidoptera: Lasiocampidae). Studia Universitatis Babes-Bolyai, Biologia, *64*(2), 67-82.

Contributing author in BDI journals articles (* from the thesis):

1. Hirian, R., Palade, P., **Ciorîță, A.,** Macavei, S., Pop, V. (2021). Investigation of possible uniaxial anisotropy in $Co_{11}Zr_2$ magnetic phase. Studia Universitatis Babes-Bolyai, Physica, *65*, 11-17.

Member in research projects:

1. "TiO_2 nanotubes/ graphene-based nanomaterials to address the emerging contaminants pollution", RO-NO-2019-0616, 01.09.2020 – 31.08.2023, National Institute for Research and Development of Isotopic and Molecular Technologies (INCDTIM), https://www.itim-cj.ro/PNCDI/graftid/.
2. "Emerging technologies for industrial verification of 2D structures (graphene and nongraphic)", PN-III-P1-1.2-PCCDI-2017-0387, 2018-2021; INCDTIM, https://icechim-rezultate.ro/proiect.php?id=49&lang=ro.
3. "Partnership for transfer of innovative technologies and advanced materials in visual arts (production, conservation, restoration)", UBB-TeMATIC-Art, 2019-2022, Universitatea Babeș-Bolyai, http://tematicart.granturi.ubbcluj.ro/.

Member in community projects:

1. POCU 380/6/13/123886 – Antreprenoriat pentru inovare prin cercetare doctorală și postdoctorală, 2019-2022, Universitatea Babeș-Bolyai, https://fondurieuropene.centre.ubbcluj.ro/pocu-123886-antreprenoriat-pentru-inovare-prin-cercetare-doctorala-si-postdoctorala/.

Conferences

A. National

1. **Ciorîță, A.,** Suciu, M., Macavei, S., Kacso, I., Lung, I., Soran, M.-L., Pârvu, M. 3rd Edition of the National Conference for Ph.D. students; Online, 2020, România, https://conferinte.doctoranzi.geo.unibuc.ro/.

2. **Ciorîță, A.**, Zăgrean-Tuza, C., Moț, A.-C., Suciu, M., Karpa, R., Barbu-Tudoran, L., Pârvu, M. 2nd Edition of the National Conference for Ph.D. students; 2020, România, https://scoaladoctorala.geo.unibuc.ro/wp-content/uploads/2019/09/CNSD_editia-a-II-a.pdf.

3. **Ciorîță, A.**, Surducan, V., Surducan, E. Ediția a XVIII-a a Salonului Cercetării Științifice, Inovării și Inventicii, PROINVENT 2020, România, https://proinvent.utcluj.ro/salon_virtual.html.

4. **Ciorîță, A.**, Tripon, S.-C., Barbu-Tudoran, L., Pârvu, M. Ediția V-a a Simpozionului BIOTA: Biodiversitate-Tradiții și actualitate, 2018, România.

B. International

1. **Ciorîță, A.**, Surducan, V., Surducan, E. 12th International Conference „Processes in Isotopes and Molecules''; Poster: *Automated photographic device for real-time monitoring of in vitro biological samples*, 2019, România, http://pim.itim-cj.ro/2019/.

2. **Ciorîță, A.**, Tripon, S.-C., Podar, D., Barbu-Tudoran, L., Pârvu, M. 18th International Balkan Workshop on Applied Physics and Materials Science; Poster: *Light and electron microscopy analysis of the leaves of Vinca species*, 2018, România, http://ibwap.ro/.

3. **Ciorîță, A.,** Bugiel, M., Schaeffer, E., Jannasch, A. Microtubules: From Atoms to Complex Systems – Virtual; Poster: *Single kinesin-8, Kip3, stabilizes microtubules*, 2020, Germania, https://www.embo-embl-symposia.org/symposia/2020/EES20-05/index.html.

Professional training

1. Research internship at ZMBP-Cellular Nanoscience, Tübingen University, Germany, during March-June/2019, through Erasmus+ program. During the three months stay, I studied the *in vitro* behavior of kinesins using total internal reflection microscope (TIRF-M).

Awards

1. First place at the National Conference for PhD students, 2020, Romania; https://conferinte.doctoranzi.geo.unibuc.ro/.

2. First place for the Business plan competition organized by: *Antreprenoriat pentru Inovare și Managementul Inovării*, POCU: 380/6/13/123886; https://fondurieuropene.centre.ubbcluj.ro/pocu-123886-antreprenoriat-pentru-inovare-prin-cercetare-doctorala-si-postdoctorala/.

3. Second place at the „De la cercetare la Start-up" Competition organized by: *Antreprenoriat pentru Inovare și Managementul Inovării*, POCU: 380/6/13/123886; https://fondurieuropene.centre.ubbcluj.ro/pocu-123886-antreprenoriat-pentru-inovare-prin-cercetare-doctorala-si-postdoctorala/.

4. Gold medal at PROINVENT 2020 Saloon for "Dispozitiv fotografic pentru observarea în timp real a evoluției materialului biologic macroscopic *in vitro*"; https://proinvent.utcluj.ro/salon.html.

Other

1. Patent request: **Ciorîță, A.,** Surducan, V., Surducan, E. (2019) "Dispozitiv fotografic pentru observarea în timp real a evoluției materialului biologic macroscopic *in vitro*" request no. RO133721A0·2019-11-29.

REFERENCES

1. Abouzeid, S., Beutling, U., & Selmar, D. (2019a). Stress-induced modification of indole alkaloids:Phytomodificines as a new category of specialized metabolites. *Phytochemistry, 159*, 102-107. doi:https://doi.org/10.1016/j.phytochem.2018.12.015

2. Abouzeid, S., Hijazin, T., Lewerenz, L., Hansch, R., & Selmar, D. (2019b). The genuine localization of indole alkaloids in *Vinca minor* and *Catharanthus roseus*. *Phytochemistry, 168*, 112110. doi:10.1016/j.phytochem.2019.112110

3. Adamczak, A., Ożarowski, M., & Karpiński, T. M. (2020). Antibacterial activity of some flavonoids and organic acids widely distributed in plants. *Journal of Clinical Medicine, 9*(1). doi:10.3390/jcm9010109

4. Ahmad, A., Mukherjee, P., Senapati, S., Mandal, D., Khan, M. I., Kumar, R., & Sastry, M. (2003). Extracellular biosynthesis of silver nanoparticles using the fungus *Fusarium oxysporum*. *Colloids and Surfaces B: Biointerfaces, 28*, 313-318.

5. Ahmad, A., Wei, Y., Syed, F., Tahir, K., Rehman, A. U., Khan, A., Ullah, S., & Yuan, Q. (2017). The effects of bacteria-nanoparticles interface on the antibacterial activity of green synthesized silver nanoparticles. *Microbial Pathogenesis, 102*, 133-142. doi:10.1016/j.micpath.2016.11.030

6. Ahmed, S., Ahmad, M., Swami, B. L., & Ikram, S. (2016). A review on plants extract mediated synthesis of silver nanoparticles for antimicrobial applications: A green expertise. *Journal of Advanced Research, 7*, 17–28. doi:10.1016/j.jare.2015.02.007

7. Ainsworth, E. A., & Gillespie, K. M. (2007). Estimation of total phenolic content and other oxidation substrates in plant tissues using Folin–Ciocâlteu reagent. *Nature Protocols, 2*(4), 875-877. doi:10.1038/nprot.2007.102

8. Akar, Z., & Burnaz, N. A. (2019). A new colorimetric method for CUPRAC assay with using of TLC plate. *LWT - Food Science and Technology, 112*. doi:10.1016/j.lwt.2019.05.110

9. Akter, M., Sikder, M. T., Rahman, M. M., Ullah, A. K. M. A., Hossain, K. F. B., Banik, S., Hosokawa, T., Saito, T., & Kurasaki, M. (2018). A systematic review on silver nanoparticles-induced cytotoxicity: Physicochemical properties and perspectives. *Journal of Advanced Research, 9*, 1–16. doi:10.1016/j.jare.2017.10.008

10. Alam, B., Majumder, R., Akter, S., & Lee, S.-H. (2015). *Piper betle* extracts exhibit antitumor activity by augmenting antioxidant potential. *Oncology Letters, 9*, 863-868. doi:10.3892/ol.2014.2738

11. Alam, M. N., Bristi, N. J., & Rafiquzzaman, M. (2013). Review on *in vivo* and *in vitro* methods evaluation of antioxidant activity. *Saudi Pharmaceutical Journal, 21*, 143–152. doi:10.1016/j.jsps.2012.05.002

12. Alavi, M., & Karimi, N. (2018). Characterization, antibacterial, total antioxidant, scavenging, reducing power and ion chelating activities of green synthesized silver, copper and titanium dioxide nanoparticles using

Artemisia haussknechtii leaf extract. *Artificial Cells, Nanomedicine, and Biotechnology*, *46*(8), 2066–2081. doi:10.1080/21691401.2017.1408121

13. Alishah, H., Seyedi, S. P., Ebrahimipour, S. Y., & Esmaeili-Mahani, S. (2016). A green approach for the synthesis of silver nanoparticles using root extract of *Chelidonium majus*: characterization and antibacterial evaluation. *Journal of Cluster Science, 27*, 421-429. doi:10.1007/s10876-016-0968-0

14. Almagro, L., Fernández-Pérez, F., & Pedreño, M. A. (2015). Indole alkaloids from *Catharanthus roseus*: Bioproduction and their effect on human health. *Molecules, 20*(2), 2973-3000. doi:10.3390/molecules20022973

15. Almosnid, N. M., Zhou, X., Jiang, L., Ridings, A., Knott, D., Wang, S., Wei, F., Yuan, J., Altman, E., Gao, Y., & Miao, J. (2018). Evaluation of extracts prepared from 16 plants used in Yao ethnomedicine as potential anticancer agents. *Journal of Ethnopharmacology, 211*, 224–234. doi:10.1016/j.jep.2017.09.032

16. AlSalhi, M. S., Elangovan, K., Ranjitsingh, A. J. A., Murali, P., & Devanesan, S. (2019). Synthesis of silver nanoparticles using plant derived 4-N-methyl benzoic acid and evaluation of antimicrobial, antioxidant and antitumor activity. *Saudi Journal of Biological Sciences, 26*, 970–978. doi:10.1016/j.sjbs.2019.04.001

17. Amooaghaie, R., Saeri, M. R., & Azizi, M. (2015). Synthesis, characterization and biocompatibility of silver nanoparticles synthesized from *Nigella sativa* leaf extract in comparison with chemical silver nanoparticles. *Ecotoxicology and Environmental Safety, 120*, 400–408. doi:10.1016/j.ecoenv.2015.06.025

18. Amos, L. A. (2011). What tubulin drugs tell us about microtubule structure and dynamics. *Seminars in Cell & Developmental Biology, 22*, 916– 926. doi:10.1016/j.semcdb.2011.09.014

19. Anandan, M., Poorani, G., Boomi, P., Varunkumar, K., Anand, K., Chuturgoon, A. A., Saravanan, M., & Prabu, H. G. (2019). Green synthesis of anisotropic silver nanoparticles from the aqueous leaf extract of *Dodonaea viscosa* with their antibacterial and anticancer activities. *Process Biochemistry, 80*, 80–88. doi:10.1016/j.procbio.2019.02.014

20. Andersson, P. O., Lejon, C., Ekstrand-Hammarström, B., Akfur, C., Ahlinder, L., Bucht, A., & Österlund, L. (2011). Polymorph- and size-dependent uptake and toxicity of TiO_2 nanoparticles in living lung epithelial cells. *Toxicology, 7*(4), 514–523. doi:10.1002/smll.201001832

21. Andrade, E. A., Folquitto, D. G., Luz, L. E. C., Paludo, K. S., Farago, P. V., & Budel, J. M. (2017). Anatomy and histochemistry of leaves and stems of *Sapium glandulosum*. *Revista Brasileira de Farmacognosia, 27*, 282–289. doi:10.1016/j.bjp.2017.01.001

22. Andreicut, A.-D., Pârvu, A. E., Mot, A. C., Pârvu, M., Fischer Fodor, E., Cătoi, A. F., Feldrihan, V., Cecan, M., & Irimie, A. (2018). Phytochemical analysis of anti-inflammatory and antioxidant effects of *Mahonia aquifolium* flower and fruit extracts. *Oxidative Medicine and Cellular Longevity, 2018*. doi:10.1155/2018/2879793

23. Anzabi, Y. (2018). Biosynthesis of ZnO nanoparticles using barberry (*Berberis vulgaris*) extract and assessment of their physico-chemical properties and antibacterial activities. *Green Process Synth, 7*, 114–121. doi:10.1515/gps-2017-0014

24. Araruna, M. K., Brito, S. A., Morais-Braga, M. F., Santos, K. K., Souza, T. M., Leite, T. R., Costa, J. G., & Coutinho, H. D. (2012). Evaluation of antibiotic & antibiotic modifying activity of pilocarpine & rutin. *The Indian journal of medical research, 135*(2), 252–254.

25. Arima, H., Ashida, H., & Danno, G.-I. (2002). Rutin-enhanced Antibacterial Activities of Flavonoids against *Bacillus cereus* and *Salmonella enteritidis*. *Bioscience, Biotechnology, and Biochemistry, 66*(5), 1009-1014. doi:10.1271/bbb.66.1009

26. Arora, S., Tyagi, N., Bhardwaj, A., Rusu, L., Palanki, R., Vig, K., Singh, S. R., Singh, A. P., Palanki, S., Miller, M. E., Carter, J. E., & Singh, S. (2015). Silver nanoparticles protect human keratinocytes against UVB radiation-induced DNA damage and apoptosis: potential for prevention of skin carcinogenesis. *Nanomedicine: Nanotechnology, Biology, and Medicine, 11*, 1265–1275. doi:10.1016/j.nano.2015.02.024

27. Aruldass, C. A., Marimuthu, M. M., Ramanathan, S., Mansor, S. M., & Murugaiyah, V. (2013). Effects of *Mesua ferrea* Leaf and Fruit Extracts on Growth and Morphology of *Staphylococcus aureus*. *Microscopy and Microanalysis, 19*, 254–260. doi:10.1017/S1431927612013785

28. Arunkumar, R., Abraham, A. N., Shukla, R., Drummond, C. J., & Greaves, T. L. (2020). Cytotoxicity of protic ionic liquids towards the HaCat cell line derived from human skin. *Journal of Molecular Liquids, 314*, 113602. doi:https://doi.org/10.1016/j.molliq.2020.113602

29. Asaikkutti, A., Bhavan, P. S., Vimala, K., Karthik, M., & Cheruparambath, P. (2016). Dietary supplementation of green synthesized manganese-oxide nanoparticles and its effect on growth performance, muscle composition and digestive enzyme activities of the giant freshwater prawn *Macrobrachium rosenbergii*. *Journal of Trace Elements in Medicine and Biology*, *35*, 7–17. doi:10.1016/j.jtemb.2016.01.005

30. Aslam, J., Khan, S. H., Siddiqui, Z. H., Fatima, Z., Maqsood, M., Bhat, M. A., Nasim, S. A., Ilah, A., Ahmad, I. Z., Khan, S. A., Mujib, A., & Sharma, M. P. (2010). *Catharanthus roseus* (L.) G. Don. An Important Drug: It's Applications and Production. *International Journal of Comprehensive Pharmacy, 1*(4).

31. Azmir, J., Zaidul, I. S. M., Rahman, M. M., Sharif, K. M., Mohamed, A., Sahena, F., Jahurul, M. H. A., Ghafoor, K., Norulaini, N. A. N., & Omar, A. K. M. (2013). Techniques for extraction of bioactive compounds from plant materials: A review. *Journal of Food Engineering, 117*, 426–436. doi:10.1016/j.jfoodeng.2013.01.014

32. Baciu, A., Ranga, F., Fetea, F., Zavoi, S., & Socaciu, C. (2013). Fingerprinting food supplements and their botanical ingredients by coupled UV/Vis/FTIR spectrometry. *Bulletin UASVM Food Science and Technology, 70*(1), 8-15.

33. Bahadori, F., Topçu, G., Boğa, M., Türkekul, A., Kolak, U., & Kartal, M. (2012). Indole alkaloids from *Vinca major* and *V. minor* growing in Turkey. *Natural Product Communications, 7*(6), 731-734. doi:10.1177/1934578X1200700610

34. Bai, B., Qiao, Q., Arandiyan, H., Li, J., & Hao, J. (2016). Three-dimensional ordered mesoporous MnO_2 supported Ag nanoparticles for catalytic removal of formaldehyde. *Environmental Science and Technology, 50*, 2635−2640. doi:10.1021/acs.est.5b03342

35. Barabadi, H., Honary, S., Ebrahimi, P., A, M. M., Alizadeh, A., & Naghibi, F. (2014). Microbial mediated preparation, characterization and optimization of gold nanoparticles. *Brazilian Journal of Microbiology, 45*, 1493-1501.

36. Barrales-Cureño, H. J., Reyes, C. R., García, I. V., Valdez, L. G. L., De Jesús, A. G., Cortés Ruíz, J. A., Sánchez Herrera, L. M., Calderón Caballero, M. C., Magallón, J. A. S., Espinoza Perez, J., & Montiel Montoya, J. (2019). Alkaloids of pharmacological importance in *Catharanthus roseus*. In J. Kurek (Ed.), *Alkaloids - Their importance in Nature and Human Life* (Vol. 1, pp. 18). London, UK: Intech Open Ltd.

37. Basavaraja, S., Balaji, S. D., Lagashetty, A., Rajasab, A. H., & Venkataraman, A. (2008). Extracellular biosynthesis of silver nanoparticles using the fungus *Fusarium semitectum Materials Research Bulletin, 43*, 1164-1170. doi:10.1016/j.materresbull.2007.06.020

38. Behravan, M., Panahi, A., Naghizadeh, A., Ziaee, M., Mahdavi, R., & Mirzapour, A. (2019). Facile green synthesis of silver nanoparticles using *Berberis vulgaris* leaf and root aqueous extract and its antibacterial activity. *International Journal of Biological Macromolecules, 124*, 148–154. doi:10.1016/j.ijbiomac.2018.11.101

39. Belean, B., Gutt, R., Costea, C., & Balacescu, O. (2020). Microarray Image Analysis: From Image Processing Methods to Gene Expression Levels Estimation. *IEEE Access, 8*, 159196-159205. doi:10.1109/ACCESS.2020.3019844

40. Bertolino, L. T., Caine, R. S., & Gray, J. E. (2019). Impact of Stomatal Density and Morphology on Water-Use Efficiency in a Changing World. *Frontiers in Plant Science, 10*, 225. doi:10.3389/fpls.2019.00225

41. Bhadra, R., & Shanks, J. V. (1977). Transient Studies of Nutrient Uptake, Growth, and Indole Alkaloid Accumulation in Heterotrophic Cultures of Hairy Roots of *Catharanthus roseus*. *Biotechnology and Bioengineering*, *55*(3), 527–534.

42. Bhagwat, M. K., & Datar, A. G. (2014). Antibacterial activity of herbal extracts against five plant pathogenic bacteria. *Archives of Phytopathology and Plant Protection, 47*(7), 892–899. doi:10.1080/03235408.2013.870703

43. Bhainsa, K. C., & D'Souza, S. F. (2006). Extracellular biosynthesis of silver nanoparticles using the fungus *Aspergillus fumigatus*. *Colloids and Surfaces B: Biointerfaces, 47*, 160–164. doi:10.1016/j.colsurfb.2005.11.026

44. Bharathi, D., & Bhuvaneshwari, V. (2018). Synthesis of zinc oxide nanoparticles (ZnO NPs) using pure bioflavonoid rutin and their biomedical applications: antibacterial, antioxidant and cytotoxic activities. *Research on Chemical Intermediates*. doi:10.1007/s11164-018-03717-9

45. Bharde, A. A., Parikh, R. Y., Baidakova, M., Jouen, S., Hannoyer, B., Enoki, T., Prasad, B. L. V., Shouche, Y. S., Ogale, S., & Sastry, M. (2008). Bacteria-Mediated Precursor-Dependent Biosynthesis of Superparamagnetic Iron Oxide and Iron Sulfide Nanoparticles. *Langmuir, 24*, 5787-5794. doi:10.1021/la704019p

46. Bianco, A., Guiso, M., Nicoletti, M., Foddai, S., Piccin, A., Serafini , M., Ballero, M., & Poli, F. (2005). A comparative chemotaxonomic study on *Vinca sardoa* stearn and *Vinca difformis* Pourret. *Natural Product Research, 19*(6), 615–617. doi:10.1080/14786410512331330602

47. Binder, B. Y. K., Peebles, C. A. M., Shanks, J. V., & San, K.-Y. (2009). The Effects of UV-B Stress on the Production of Terpenoid Indole Alkaloids in *Catharanthus roseus* Hairy Roots. *Biotechnology Progress, 25*(3), 861–865.

48. Birla, S. S., Tiwari, V. V., Gade, A. K., Ingle, A. P., Yadav, A. P., & Rai, M. K. (2008). Fabrication of silver nanoparticles by *Phoma glomerata* and its combined effect against *Escherichia coli*, *Pseudomonas aeruginosa* and *Staphylococcus aureus Letters in Applied Microbiology, 48*, 173-179. doi:10.1111/j.1472-765x.2008.02510.x

49. Blainski, A., Lopes, G. C., & de Mello, J. C. P. (2013). Application and analysis of the Folin Ciocâlteu method for the determination of the total phenolic content from *Limonium brasiliense* L. *Molecules, 18*, 6852-6865. doi:10.3390/molecules18066852

50. Boga, M., Kolak, U., Topcu, G., Bahadori, F., Kartal, M., & Farnsworth, N. R. (2011). Two new indole alkaloids from *Vinca herbacea* L. *Phytochemistry Letters, 4*, 399–403. doi:10.1016/j.phytol.2011.07.008

51. Boyadzhiev, L., & Yordanov, B. (2004). Pertraction of indole alkaloids from *Vinca minor* L. *Separation Science and Technology, 39*(6), 1321-1329. doi:10.1081/SS-120030485

52. Braakhuis, H. M., Kloet, S. K., Kezic, S., Kuper, F., Park, M. V. D. Z., Bellmann, S., van der Zande, M., Le Gac, S., Krystek, P., Peters, R. J. B., Rietjens, I. M. C. M., & Bouwmeester, H. (2015). Progress and future of *in vitro* models to study translocation of nanoparticles. *Archives of Toxology, 89*, 1469-1495. doi:10.1007/s00204-015-1518-5

53. Bryan, N. S., & Grisham, M. B. (2007). Methods to detect nitric oxide and its metabolites in biological samples. *Free Radic. Biol. Med., 43*(5), 645–657.

54. Buege, J. A., & Aust, S. D. (1978). Microsomal lipid peroxidation. doi:10.1016/s0076-6879(78)52032-6

55. Butler, K. S., Peeler, D. J., Casey, B. J., Dair, B. J., & Elespuru, R. K. (2015). Silver nanoparticles: correlating nanoparticle size and cellular uptake with genotoxicity. *Mutagenesis, 30*, 577–591. doi:10.1093/mutage/gev020

56. Cao, Y.-N., Zheng, L.-L., Wang, D., Liang, X.-X., Gao, F., & Zhou, X.-L. (2018). Recent advances in microtubule-stabilizing agents. *European Journal of Medicinal Chemistry, 143*, 806-828. doi:10.1016/j.ejmech.2017.11.062

57. Carpa, R., Dragan-Bularda, M., & Muntean, V. (2014). General Microbiology. Practical Guide. In (pp. 58-61). Cluj-Napoca. Romania: Presa Universitara Clujeana.

58. Carriquí, M., Cabrera, H. M., Conesa, M. À., Coopman, R. E., Douthe, C., Gago, J., Gallé, A., Galmés, J., Ribas-Carbo, M., Tomás, M., & Flexas, J. (2015). Diffusional limitations explain the lower photosynthetic capacity of ferns as compared with angiosperms in a common garden study. *Plant, Cell and Environment, 38*, 448–460. doi:10.1111/pce.12402

59. Carrola, J., Bastos, V., Jarak, I., Oliveira-Silva, R., Malheiro, E., Daniel-da-Silva, A. L., Oliveira, H., Santos, C., Gil, A. M., & Duarte, I. F. (2016). Metabolomics of silver nanoparticles toxicity in HaCaT cells: Structure-activity relationships and role of ionic silver and oxidative stress. *Nanotoxicology*. doi:10.1080/17435390.2016.1177744

60. Carvalho, C. O., Chagas, A. C. S., Cotinguiba, F., Furlan, M., Brito, L. G., Chaves, F. C. M., Stephan, M. P., Bizzo, H. R., & Amarante, A. F. T. (2012). The anthelmintic effect of plant extracts on *Haemonchus contortus* and *Strongyloides venezuelensis*. *Veterinary Parasitology, 183*, 260– 268. doi:10.1016/j.vetpar.2011.07.051

61. Cauerhff, A., & Castro, G. R. (2013). Bionanoparticles, a green nanochemistry approach. *Electronic Journal of Biotechnology*. doi:10.2225/vol16-issue3-fulltext-3

62. Cepkova, P. H., Karlík, P., Viehmannova, I., Müllerova, V., Smejda, L., & Hejcman, M. (2016). Genetic and leaf-trait variability of *Vinca minor* at ancient and recent localities in Central Europe. *Biochemical Systematics and Ecology, 64*, 22-30. doi:10.1016/j.bse.2015.11.005

63. Ceresoli, G. L., & Zucali, P. A. (2015). Vinca alkaloids in the therapeutic management of malignant pleural mesothelioma. *Cancer Treatment Reviews, 41*(10), 853-858. doi:10.1016/j.ctrv.2015.10.006

64. Chagas, C. M., & Alisaraie, L. (2019). Metabolites of *Vinca* alkaloid vinblastine: tubulin binding and activation of nausea-associated receptors. *ACS Omega, 4*, 9784−9799. doi:10.1021/acsomega.9b00652

65. Chatterjee, A., Banerji, A., & Chakrabary, M. (1975). Monoterpenoid alkaloid from *Vinca major*. *Planta Medica, 28*, 109-111.

66. Chaudhary, S., Negi, A., & Dahiya, V. (2010). The study of *in vitro* antimicrobial activity and phytochemical analysis of some medicinal plants in Chamoli Garhwal Region. *PHCOG J, 2*(12), 481-485. doi:10.1016/S0975-3575(10)80035-5

67. Checchi, P. M., Nettles, J. H., Jun, Z., Snyder, J. P., & Joshi, H. C. (2003). Microtubule-interacting drugs for cancer treatment. *Trends In Pharmacological Sciences, 24*(7), 361-365. doi:10.1016/S0165-6147(03)00161-5

68. Chen, Q., Lu, X., Guo, X., Guo, Q., & Li, D. (2017). Metabolomics characterization of two apocynaceae plants, *Catharanthus roseus* and *Vinca minor*, using GC-MS and LC-MS methods in combination. *Molecules, 22*. doi:10.3390/molecules22060997

69. Cheng, G.-G., Zhao, H.-Y., Liu, L., Zhao, Y.-L., Song, C.-W., Gu, J., Sun, W.-B., Liu, Y.-P., & Luo, X.-D. (2016). Non-alkaloid constituents of *Vinca major*. *Chinese Journal of Natural Medicines, 14*(1), 56-60. doi:10.3724/SP.J.1009.2016.00056

70. Cheng, G.-G., Zhao, Y.-L., Zhang, Y., Lunga, P.-K., Hu, D.-B., Li, Y., Gu, J., Song, C.-W., Sun, W.-B., Liu, Y.-P., & Luo, X.-D. (2014). Indole alkaloids from cultivated *Vinca major*. *Tetrahedron, 70*, 8723-8729. doi:10.1016/j.tet.2014.09.026

71. Chiu, L. Y., Hsin, I. L., Yang, T. Y., Sung, W. W., Chi, J. Y., Chang, J. T., Ko, J. L., & Sheu, G. T. (2017). The ERK-ZEB1 pathway mediates epithelial-mesenchymal transition in pemetrexed resistant lung cancer cells with suppression by vinca alkaloids. *Oncogene, 36*(2), 242-253. doi:10.1038/onc.2016.195

72. Chiu, W. H., Luo, S. J., Chen, C. L., Cheng, J. H., Hsieh, C. Y., Wang, C. Y., Huang, W. C., Su, W. C., & Lin, C. F. (2012). *Vinca* alkaloids cause aberrant ROS-mediated JNK activation, Mcl-1 downregulation, DNA damage, mitochondrial dysfunction, and apoptosis in lung adenocarcinoma cells. *Biochem Pharmacol, 83*(9), 1159-1171. doi:10.1016/j.bcp.2012.01.016

73. Choi, Y. H., Tapias, E. C., Kim, H. K., Lefeber, A. W. M., Erkelens, C., Verhoeven, J. T. J., Brzin, J., Zel, J., & Verpoorte, R. (2004). Metabolic discrimination of *Catharanthus roseus* leaves infected by *Phytoplasma* using 1H-NMR spectroscopy and multivariate data analysis. *Plant Physiology, 135*(4), 2398-2410. doi:10.1104/pp.104.041012

74. Ciorîță, A., Gutt, R., Lung, I., Soran, M.-L., & Pârvu, M. (2021a). Green-synthesized Ag-MnO_2 nanoparticles as plausible non-invasive antimicrobial treatment of cultural heritage. *GeoPatterns, 6*, 6-10. doi:https://doi.org/10.5719/GeoP.6/1

75. Ciorîță, A., Suciu, M., Macavei, S., Kacso, I., Lung, I., Soran, M.-L., & Pârvu, M. (2020). Green synthesis of Ag-MnO_2 nanoparticles using *Chelidonium majus* and *Vinca minor* extracts and their *in vitro* cytotoxicity. *Molecules, 25*(4), 819. doi:10.3390/molecules25040819

76. Ciorîță, A., Tripon, S. C., Mircea, I. G., Podar, D., Barbu-Tudoran, L., Mircea, C., & Pârvu, M. (2021b). The Morphological and Anatomical Traits of the Leaf in Representative *Vinca* Species Observed on Indoor- and Outdoor-Grown Plants. *Plants, 10*(4), 622. doi:https://doi.org/10.3390/plants10040622;

77. Ciorîță, A., Zăgrean-Tuza, C., Moț, A., Carpa, R., & Pârvu, M. (2021c). The phytochemical analysis of *Vinca* L. species leaf extracts is correlated with the antioxidant, antibacterial, and antitumor effects *Molecules, 26*(10). doi:https://doi.org/10.3390/molecules26103040

78. Clark, A. G., & Vignjevic, D. M. (2015). Modes of cancer cell invasion and the role of the microenvironment. *Current Opinion in Cell Biology, 36*, 13–22. doi:10.1016/j.ceb.2015.06.004

79. Coughlin, M. F., Bielenberg, D. R., Lenormand, G., Marinkovic, M., Waghorne, C. G., Zetter, B. R., & Fredberg, J. J. (2013). Cytoskeletal stiffness, friction, and fluidity of cancer cell lines with different metastatic potential. *Clin Exp Metastasis, 30*, 237–250. doi:10.1007/s10585-012-9531-z

80. Crăciun, F., Bojor, O., & Alexan, M. (1977). *Farmacia Naturii* (Vol. 2). București: Editura Ceres.

81. Csiky, J., & Purger, D. (2013). Herbaceous periwinkle, *Vinca herbacea* Waldst. et Kit. 1799 (Apocynaceae), a new species of the Croatian flora. *Acta Bot. Croat., 72*(2), 399–406. doi:10.2478/botcro

82. Cvjetko, P., Milošić, A., Domijan, A.-M., Vrček, I. V., Tolić, S., Štefanić, P. P., Letofsky-Papst, I., Tkalec, M., & Balen, B. (2017). Toxicity of silver ions and differently coated silver nanoparticles in *Allium cepa* roots. *Ecotoxicology and Environmental Safety, 137*, 18–28. doi:10.1016/j.ecoenv.2016.11.009

83. D'Costa, V. M., King, C. E., Kalan, L., Morar, M., Sung, W. W. L., Schwarz, C., Froese, D., Zazula, G., Calmels, F., Debruyne, R., Golding, G. B., Poinar, H. N., & Wright, G. D. (2011). Antibiotic resistance is ancient. *Nature, 477*, 457-461. doi:10.1038/nature10388

84. Danciu, C., Zupko, I., Bor, A., Schwiebs, A., Radeke, H., Hancianu, M., Cioanca, O., Alexa, E., Oprean, C., Bojin, F., Soica, C., Paunescu, V., & Dehelean, C. A. (2018). Botanical Therapeutics: Phytochemical Screening and Biological Assessment of Chamomile, Parsley and Celery Extracts against A375 Human Melanoma and Dendritic Cells. *International Journal of Molecular Sciences, 19*(11). doi:10.3390/ijms19113624

85. Dar, M. A., Ingle, A., & Rai, M. (2013). Enhanced antimicrobial activity of silver nanoparticles synthesized by *Cryphonectria* sp. evaluated singly and in combination with antibiotics. *Nanomedicine: Nanotechnology, Biology, and Medicine, 9*, 105-110. doi:10.1016/j.nano.2012.04.00

86. Deepika, M. S., Thangam, R., Vijayakumar, T. S., Sasirekha, R., Vimala, R. T. V., Sivasubramanian, S., Arun, S., Babu, M. D., & Thirumurugan, R. (2019). Antibacterial synergy between rutin and florfenicol enhances therapeutic spectrum against drug resistant *Aeromonas hydrophila*. *Microbial Pathogenesis, 135*. doi:10.1016/j.micpath.2019.103612

87. Dehghanizadea, S., Arasteha, J., & Mirzaie, A. (2018). Green synthesis of silver nanoparticles using *Anthemis atropatana* extract: characterization and *in vitro* biological activities. *Artificial Cells, Nanomedicine, and Biotechnology, 46*(1), 160–168. doi:10.1080/21691401.2017.1304402

88. Dobrucka, R., Dlugaszewska, J., & Kaczmarek, M. (2017). Cytotoxic and antimicrobial effects of biosynthesized ZnO nanoparticles using of *Chelidonium majus* extract. *Biomed Microdevices, 20*(5). doi:10.1007/s10544-017-0233-9

89. Dong, M. W. (2006). *Modern HPLC for practicing scientists*: John Wiley and Sons.

90. Douillard, J.-Y., Laport, S., Fossella, F., Georgoulias, V., Pujol, J.-L., Kubota, K., Monnier, A., Kudo, S., Rubio, J. E., & Cucherat, M. (2007). Comparison of Docetaxel- and *Vinca* Alkaloid–Based Chemotherapy in the First-line Treatment of Advanced Non-small Cell Lung Cancer: A Meta-analysis of Seven Randomized Clinical Trials. *Journal of Thoracic Oncology, 2*(10), 939–946.

91. Du, J., Tang, J., Xu, S., Ge, J., Dong, Y., Li, H., & Jin, M. (2018). A review on silver nanoparticles-induced ecotoxicity and the underlying toxicity mechanisms. *Regulatory Toxicology and Pharmacology, 98*, 231–239. doi:10.1016/j.yrtph.2018.08.003

92. Du, T., Yang, L., Xu, X., Shi, X., Xu, X., Lu, J., Lv, J., Huang, X., Chen, J., Wang, H., Ye, J., Hu, L., & Shen, X. (2019). Vincamine as a GPR40 agonist improves glucose homeostasis in type 2 diabetic mice. *Journal of Endocrinology, 240*, 195–214. doi:10.1530/JOE-18-0432

93. Dubey, S., Ganeshpurkar, A., Bansal, D., & Dubey, N. (2013). Experimental studies on bioactive potential of rutin. *Chronicles of Young Scientists, 4*(2), 153-157. doi:10.4103/2229-5186.115556

94. Durán, N., Marcato, P. D., Alves, O. L., De Souza, G. I. H., & Esposito, E. (2005). Mechanistic aspects of biosynthesis of silver nanoparticles by several *Fusarium oxysporum* strains. *Journal of Nanobiotechnology, 3*(8). doi:10.1186/1477-3155-3-8

95. E.E.A. European Environment Agency. Retrieved from https://eunis.eea.europa.eu;

https://eunis.eea.europa.eu/references/1780/species

https://eunis.eea.europa.eu/species-taxonomic-browser.jsp?expand=47,254824,255217,2851,2854&genus=Vinca#level_Vinca

https://eunis.eea.europa.eu/species/152524

https://eunis.eea.europa.eu/species/152525

https://eunis.eea.europa.eu/species/152530

https://eunis.eea.europa.eu/species/152533

https://eunis.eea.europa.eu/species/152536

https://eunis.eea.europa.eu/species/152528

https://eunis.eea.europa.eu/species/152529

96. Egorova, E. M., Kubatiev, A. A., & Schvets, V. I. (2016). *Biological effects of metal nanoparticles*: Springer International Publishing Switzerland.

97. El-Fiki, M. A., El-Taher, A. M., EL-Gendy, A. G., & Lila, M. I. (2019). Morphological and anatomical studies on some taxa of family Apocynaceae. *Al-Azhar Journal of Agricultural Research, 44*(1), 136-147.

98. Emara, L. H., El-Menshawi, B. S., & Estefan, M. Y. (2000). *In vitro–in vivo* correlation and comparative bioavailablity of vincamine in prolonged-release preparations. *Drug Development and Industrial Pharmacy, 26*(3), 243–251

99. Erlandsen, S. L., Kristich, C. J., Dunny, G. M., & Wells, C. L. (2004). High-resolution visualization of the microbial glycocalyx with low-voltage scanning electron microscopy: dependence on cationic dyes. *The journal of histochemistry and cytochemistry : official journal of the Histochemistry Society, 52*(11), 1427-1435. doi:10.1369/jhc.4A6428.2004

100. Eswaraiah, G., Peele, K. A., Krupanidhi, S., Indira, M., Kumar, R. B., & Venkateswarulu, T. C. (2020). GC–MS analysis for compound identification in leaf extract of *Lumnitzera racemosa* and evaluation of its *in*

vitro anticancer effect against MCF7 and HeLa cell lines. *Journal of King Saud University – Science, 32*, 780–783. doi:10.1016/j.jksus.2019.01.014

101. Ethiraj, A. S., Jayanthi, S., Ramalingam, C., & Banerjee, C. (2016). Control of size and antimicrobial activity of green synthesized silver nanoparticles. *Materials Letters, 185*, 526–529. doi:10.1016/j.matlet.2016.07.114

102. Ettebong, E., Nwafor, P., & Okokon, J. (2012). *In vivo* antiplasmodial activities of ethanolic exract and fractions of *Eleucine indica*. *Asian Pacific Journal of Tropical Medicine, 2012*, 673-676. doi:10.1016/S1995-7645(12)60105-9

103. EUCAST. (2020a). *Antimicrobial susceptibility testing*: European Committee on Antimicrobial Susceptibility Testing.

104. EUCAST. (2020b). Breakpoint tables for interpretation of MICs and zone diameters Version 10.0, valid from 2020-01-01. Retrieved from http://www.eucast.org

105. EUCAST. (2020c). *EUCAST reading guide for broth microdilution*: European Committee on Antimicrobial Susceptibility Testing.

106. European Commission. Retrieved from https://ec.europa.eu

107. European Commission Decision C. (2019). Horizon 2020 Work-Programme 2018-2020. In (pp. 94). http://ec.europa.eu/research/eic/index.cfm.

108. European Committee on Antimicrobial Susceptibility Testing. (2020). Retrieved from https://www.eucast.org/

109. Everette, J. D., Bryant, Q. M., Green, A. M., Abbey, Y. A., Wangila, G. W., & Walker, R. B. (2010). Thorough study of reactivity of various compound classes toward the Folin-Ciocâlteu reagent. *Journal of Agricultural and Food Chemistry, 58*, 8139–8144. doi:10.1021/jf1005935

110. Fan, J., Yu, L., & Xu, C. (2019). Dual role for autophagy in lipid metabolism in *Arabidopsis*. *The Plant Cell, 31*, 1598–1613. doi:10.1105/tpc.19.00170

111. Fandy, T. E., Abdallah, I., Khayat, M., Colby, D. A., & Hassan, H. E. (2016). *In vitro* characterization of transport and metabolism of the alkaloids: vincamine, vinpocetine and eburnamonine. *Cancer Chemotherapy and Pharmacology, 77*, 259–267. doi:10.1007/s00280-015-2924-3

112. Farahanikia, B., Akbarzadeh, T., Jahangirzadeh, A., Yassa, N., Ardekani, M. R. S., Mirnezami, T., Hadjiakhoondi, A., & Khanavi, M. (2011). Phytochemical investigation of *Vinca minor* cultivated in Iran. *Iranian Journal of Pharmaceutical Research, 10*(4), 777-785.

113. Farcaș, A. D., Moț, A. C., Zăgrean-Tuza, C., Toma, V., Cimpoiu, C., Hosu, A., Pârvu, M., Roman, I., & Silaghi-Dumitrescu, R. (2018). Chemo-mapping and biochemicalmodulatory and antioxidant/prooxidant effect of *Galium verum* extract during acute restraint and dark stress in female rats. *PloS One, 13*(7). doi:10.1371/journal.pone.0200022

114. Farnsworth, N. R., Svoboda, G. H., & Blomster, R. N. (1968). Antiviral Activity of Selected *Cutharanthas* Alkaloids. *Journal of Pharmaceutical Sciences, 57*(12), 2174-2175. doi:10.1002/jps.2600571235

115. Fayaz, A. M., Balaji, K., Girilal, M., Yadav, R., Kalaichelvan, P. T., & Venketesan, R. (2010). Biogenic synthesis of silver nanoparticles and their synergistic effect with antibiotics: a study against Gram-positive and Gram-negative bacteria. *Nanomedicine: Nanotechnology, Biology, and Medicine, 6,* 103–109. doi:10.1016/j.nano.2009.04.006

116. Fernández-Pérez, F., Almagro, L., Pedreño, M. A., & Gómez Ros, L. V. (2010). Synergistic and cytotoxic action of indole alkaloids produced from elicited cell cultures of *Catharanthus roseus*. *Pharmaceutical Biology, 51*(3), 304-310. doi:10.3109/13880209.2012.722646

117. Fernandez, V., Guzman-Delgado, P., Graca, J., Santos, S., & Gil, L. (2016). Cuticle Structure in Relation to Chemical Composition: Re-assessing the Prevailing Model. *Frontiers in Plant Science, 7*, 427. doi:10.3389/fpls.2016.00427

118. Ferreres, F., Pereira, D. M., Valenta, P., Andrade, P. B., Seabra, R. M., & Sottomayor, M. (2008). New phenolic compounds and antioxidant potential of *Catharanthus roseus*. *J Agric. Food Chem., 56*, 9967–9974.

119. Fleming, T. (2000). *PDR for herbal medicines*: Medical Economics Company.

120. Foddai, M., Maldini, M., Addis, R., Petretto, G. L., Chessa, M., & Pintore, G. (2017). Profiling of the bioactive compounds in flowers, leaves and roots of *Vinca sardoa*. *Natural Product Communications, 12*(6), 933 - 936. doi:10.1177/1934578X1701200625

121. Fröhlich, E. (2012). The role of surface charge in cellular uptake and cytotoxicity of medical nanoparticles. *International Journal of Nanomedicine, 7*, 5577–5591. doi:10.2147/IJN.S36111

122. Fumoleau, P., & Guiu, S. (2012). New *Vinca* Alkaloids in Clinical Development. *Current Breast Cancer Reports, 5*(1), 69-72. doi:10.1007/s12609-012-0096-2

123. Gagua, N., Mchedlidze, K., Vachnadze, V., & Bakuridze, A. (2012). Structural peculiarities of the vegetative organs of the species of *Vinca*. *PHCOG J, 4*(28), 49-55. doi:10.5530/pj.2012.28.10

124. Ganesh, D., Fuehrer, H.-P., Starzengrüber, P., Swoboda, P., Khan, W. A., Reismann, J. A. B., Mueller, M. S. K., Chiba, P., & Noedl, H. (2012). Antiplasmodial activity of flavonol quercetin and its analogues in *Plasmodium falciparum*: evidence from clinical isolates in Bangladesh and standardized parasite clones. *Parasitology Research, 110*, 2289–2295.

125. Ganeshpurkar, A., & Saluja, A. K. (2017). The pharmacological potential of rutin. *Saudi Pharmaceutical Journal, 25*, 149–164. doi:10.1016/j.jsps.2016.04.025

126. Ganguly, R., Singh, A. K., Kumar, R., Gupta, A., Pandey, A. K., & Pandey, A. K. (2019). Nanoparticles as modulators of oxidative stress. *Nanotechnology in Modern Animal Biotechnology*, 29-35. doi:10.1016/B978-0-12-818823-1.00003-X

127. Garcia-Lazaro, R. S., Lamdan, H., Caligiuri, L. G., Lorenzo, N., Berengeno, A. L., Ortega, H. H., Alonso, D. F., & Farina, H. G. (2020). *In vitro* and *in vivo* antitumor activity of Yerba Mate extract in colon cancer models. *Journal of Food Science*. doi:10.1111/1750-3841.15169

128. Gascoigne, K. E., & Taylor, S. S. (2009). How do anti-mitotic drugs kill cancer cells? *Journal of Cell Science, 122*(15), 2579-2585. doi:10.1242/jcs.039719

129. Gharibshahi, L., Saion, E., Gharibshahi, E., Shaari, A. H., & Matori, K. A. (2017). Structural and optical properties of Ag nanoparticles synthesized by thermal treatment method. *Materials, 10*. doi:10.3390/ma10040402

130. Ghédira, K., & Goetz, P. (2017). Petite pervenche *Vinca minor* L. (Apocynaceae). *Phytothérapie, 15*, 169-172. doi:10.1007/s10298-017-1136-x

131. Goklany, S., Loring, R. H., Glick, J., & Lee-Parsons, C. W. T. (2009). Assessing the Limitations to Terpenoid Indole Alkaloid Biosynthesis in *Catharanthus roseus* Hairy Root Cultures Through Gene Expression Profiling and Precursor Feeding. *Biotechnology Progress, 25*(5), 1289–1296.

132. Gomaa, E. Z. (2017). Antimicrobial, antioxidant and antitumor activities of silver nanoparticles synthesized by *Allium cepa* extract: A green approach. *Journal of Genetic Engineering and Biotechnology, 15*, 49–57. doi:10.1016/j.jgeb.2016.12.002

133. Gopinath, V., Priyadarshini, S., Loke, M. F., Arunkumar, J., Marsili, E., MubarakAli, D., Velusamy, P., & Vadivelu, J. (2017). Biogenic synthesis, characterization of antibacterial silver nanoparticles and its cell cytotoxicity. *Arabian Journal of Chemistry, 10*, 1107–1117. doi:10.1016/j.arabjc.2015.11.011

134. Gotoh, E., Suetsugu, N., Higa, T., Matsushita, T., Tsukaya, H., & Wada, M. (2018). Palisade cell shape affects the light-induced chloroplast movements and leaf photosynthesis. *Scientific Reports, 8*(1), 1472. doi:10.1038/s41598-018-19896-9

135. Goyal, P., Khanna, A., Chauhan, A., Chauhan, G., & Kaushik, P. (2008). *In vitro* evaluation of crude extracts of *Catharanthus roseus* for potential antibacterial activity. *International Journal of Green Pharmacy, 2*(3), 176-181.

136. Graf, C., Nordmeyer, D., Sengstock, C., Ahlberg, S., Diendorf, J. r., Raabe, J. r., Epple, M., Köller, M., Lademann, J. r., Vogt, A., Rancan, F., & Rühl, E. (2018). Shape-dependent dissolution and cellular uptake of silver nanoparticles. *Langmuir, 34*, 1506−1519. doi:10.1021/acs.langmuir.7b03126

137. Grellier, P., Sinou, V., Garreau-de Loubresse, N., Bylen, E., Boulard, Y., & Schrevel, J. (1999). Selective and reversible effects of *Vinca* alkaloids on *Trypanosoma cruzi* epimastigote forms: Blockage of cytokinesis without inhibition of the organelle duplication. *Cell Motility and the Cytoskeleton, 42*, 36–47.

138. Grewal, D. S. (2019). Funding nanotechnology-a comparative study of global and national funding. *Journal of Nanomedicine, Nanoscience and Technology*. doi:Tech: JNNT-105.

139. Grimmett, G. (1999). What is percolation? *Springer, 10*, 1-31. doi:10.1007/978-3-662-03981-6-1

140. Grujić, S. M., Radojevic, I. D., Vasic, S. M., Comic, L. R., & Topuzovic, M. D. (2015). Antimicrobial and antibiofilm activities of secondary metabolites from *Vinca minor* L. *Applied Biochemistry and Microbiology, 51*(5), 572–578. doi:10.1134/S0003683815050087

141. Grujić, S. M., Radojević, I. D., Vasić, S. M., Čomić, L. R., & Topuzović, M. D. (2014). Antimicrobial activity and some phytochemical analysis of two extracts *Vinca minor* L. *Kragujevac Journal of Science, 3*, 145-154.

142. Guan, Y., Guo, Z., Che, H., Mu, J., Zhang, X., Zhang, Z., Wang, G., Bai, Y., & Xie, H. (2018). Core/shell nanorods of MnO_2/carbon embedded with Ag nanoparticles as high-performance electrode materials for supercapacitors. *Chemical Engineering Journal, 331*, 23–30. doi:10.1016/j.cej.2017.08.107

143. Gubin, S. P. (2008). *Magnetic Nanoparticles*. Germany: Wiley-VCH

144. Gülçin, I., Beydemir, Ş., Topal, F., Gagua, N., Bakuridze, A., Bayram, R., & Gepdiremen, A. (2012). Apoptotic, antioxidant and antiradical effects of majdine and isomajdine from *Vinca herbacea* Waldst. and Kit. *Journal of Enzyme Inhibition and Medicinal Chemistry, 27*(4), 587–594. doi:10.3109/14756366.2011.604318

145. Gunalan, S., Sivaraj, R., & Venckatesh, R. (2012). *Aloe barbadensis Miller* mediated green synthesis of mono-disperse copper oxide nanoparticles: Optical properties. *Spectrochimica Acta Part A: Molecular and Biomolecular Spectroscopy, 97*, 1140–1144. doi:10.1016/j.saa.2012.07.096

146. Güneş, H., Alper, M., & Çelikoğlu, N. (2019). Anticancer effect of the fruit and seed extracts of *Momordica charantia* L. (Cucurbitaceae) on human cancer cell lines. *Tropical Journal of Pharmaceutical Research, 18*(10), 2057-2065. doi:10.4314/tjpr.v18i10.9

147. Guo, X., Bonin, K., Scarpinato, K., & Guthold, M. (2014). The effect of neighboring cells on the stiffness of cancerous and non-cancerous human mammary epithelial cells. *New Journal of Physics, 16*. doi:10.1088/1367-2630/16/10/105002

148. Gupta, A., Mahajan, S., & Sharma, R. (2015). Evaluation of antimicrobial activity of Curcuma longa rhizome extract against Staphylococcus aureus. *Biotechnology Reports, 6*, 51-55. doi:https://doi.org/10.1016/j.btre.2015.02.001

149. Gurău, M. (2007). *Botanică sistematică*. Bacău: Alma Mater.

150. Guzman, P., Fernandez, V., Garcia, M. L., Khayet, M., Fernandez, A., & Gil, L. (2014). Localization of polysaccharides in isolated and intact cuticles of eucalypt, poplar and pear leaves by enzyme-gold labelling. *Plant Physiology and Biochemistry, 76*, 1-6. doi:10.1016/j.plaphy.2013.12.023

151. Han, X., Gelein, R., Corson, N., Wade-Mercer, P., Jiang, J., Biswas, P., Finkelstein, Jacob N.,, Elder, A., & Oberdörster, G. (2011). Validation of an LDH assay for assessing nanoparticle toxicity. *Toxicology, 287*, 99–104. doi:10.1016/j.tox.2011.06.011

152. Hanafy, M. S., Matter, M. A., Asker, M. S., & Rady, M. R. (2016). Production of indole alkaloids in hairy root cultures of *Catharanthus roseus* L. and their antimicrobial activity. *South African Journal of Botany, 105*, 9–18. doi:10.1016/j.sajb.2016.01.004

153. Hanan, N. A., Chiu, H. I., Ramachandran, M. R., Tung, W. H., Zain, N. N. M., Yahaya, N., & Lim, V. (2018). Cytotoxicity of plant-mediated synthesis of metallic nanoparticles: A systematic review. *International Journal of Molecular Sciences, 19*. doi:10.3390/ijms19061725

154. Handa, S. S., Khanuja, S. P. S., Longo, G., & Rakesh, D. D. (2008). Extraction technologies for medicinal an aromatic plants. *International Centre for Science and High Technologies*, 75-80.

155. Hasa, D., Perissutti, B., Cepek, C., Bhardwaj, S., Carlino, E., Grassi, M., Invernizzi, S., & Voinovich, D. (2013a). Drug salt formation via mechanochemistry: The case study of vincamine. *Molecular Pharmaceutics, 10*, 211−224. doi:10.1021/mp300371f

156. Hasa, D., Perissutti, B., Dall'Acqua, S., Chierotti, M. R., Gobetto, R., Grabnar, I., Cepek, C., & Voinovich, D. (2013b). Rationale of using *Vinca minor* Linne dry extract phytocomplex as a vincamine's oral bioavailability enhancer. *European Journal of Pharmaceutics and Biopharmaceutics*. doi:10.1016/j.ejpb.2012.11.025

157. Hezarjaribi, H. Z., Elmi, T., Dayer, M. S., Gholami, S., Fakhar, M., Akbariqomi, M., & Ghaffarifar, F. (2015). A systematic review of the effects of Iranian pharmaceutical plant extracts on *Giardia lamblia*. *Asian Pacific Journal of Tropical Disease, 5*(12), 925-929. doi:10.1016/S2222-1808(15)60959-8

158. Hong, T., Lin, H., & He, D. (2018). Characteristics and correlations of leaf stomata in different *Aleurites montana* provenances. *PloS One, 13*(12), e0208899. doi:10.1371/journal.pone.0208899

159. Hoseinpour, V., & Ghaemi, N. (2018a). Green synthesis of manganese nanoparticles: Applications and future perspective–A review. *Journal of Photochemistry & Photobiology, B: Biology, 189*, 234–243. doi:10.1016/j.jphotobiol.2018.10.022

160. Hoseinpour, V., Souri, M., & Ghaemi, N. (2018b). Green synthesis, characterisation, and photocatalytic activity of manganese dioxide nanoparticles. *Micro & Nano Letters, 13*(11), 1560–1563. doi:10.1049/mnl.2018.5008

161. Hua Shu, C. C. (1995). *Catharanthus* G. Don, Gen. Hist. 4: 95. 1837. In *Flora of China* (Vol. 16, pp. 156–157).

162. Huang, W., Ratkowsky, D., Hui, C., Wang, P., Su, J., & Shi, P. (2019). Leaf Fresh Weight Versus Dry Weight: Which is Better for Describing the Scaling Relationship between Leaf Biomass and Leaf Area for Broad-Leaved Plants? *Forests, 10*(3). doi:10.3390/f10030256

163. Huang, Y.-J., & Li, W.-S. (2013). Preparation of manganese dioxide for oxygen reduction in zinc air battery by hydro thermal method. *Journal of Inorganic Materials, 28*(3), 341-346. doi:10.3724/SP.J.1077.2012.12474

164. Hui, Y., Yi, X., Hou, F., Wibowo, D., Zhang, F., Zhao, D., Gao, H., & Zhao, C.-X. (2019). Role of nanoparticle mechanical properties in cancer drug delivery. *ACS Nano, 13*, 7410−7424. doi:10.1021/acsnano.9b03924

165. Hurtada, J. M. U. P. A., Divina, B. P., & Ducusin, R. J. T. (2012). Anthelmintic Efficacy of Jackfruit (*Artocarpus heterophyllus* L.) and Tamarind (*Tamarindus indica* L.) Leaves Decoction Against Gastrointestinal Nematodes of Goats. *Philippine Journal of Veterinary and Animal Science, 38*(2), 157-166.

166. I.P.N.I. International Plant Name Index. Retrieved from https://www.ipni.org/

167. Ingle, A., Gade, A., Pierrat, S., Sönnichsen, C., & Rai, M. (2008). Mycosynthesis of silver nanoparticles using the fungus *Fusarium acuminatum* and its activity against some human pathogenic bacteria. *Current Nanoscience, 4*, 141-144.

168. Ishikura, N., & Minekishi, K. (1978). New delphinidin glycosides isolated from *Vinca major* flowers. *Botanical Magazine Tokyo, 91*, 181-186.

169. Islam, B., Lustberg, M., Staff, N. P., Kolb, N., Alberti, P., & Argyriou, A. A. (2019). *Vinca* alkaloids, thalidomide and eribulin-induced peripheral neurotoxicity: From pathogenesis to treatment. *Journal of Peripheral Nerve Society, 24(Suppl. 2)*, S63–S73. doi:10.1111/jns.12334

170. ISO10993-5:2009(E). (2009). International Organization for Standardization. In *Biological evaluation of medical devices - Part 5: Tests for in vitro cytotoxicity* (3rd ed.).

171. Jaganyi, D., Altaf, M., & Wekesa, I. (2013). Synthesis and characterization of whisker-shaped MnO_2 nanostructure at room temperature. *Appl Nanosci, 3*, 329–333. doi:10.1007/s13204-012-0135-3

172. Jaleel, A. C., Gopi, R., Manivannan, P., Gomathinayagam, M., Sridharan, R., & Panneerselvam, R. (2008). Antioxidant potential and indole alkaloid profile variations with water deficits along different parts of two varieties of *Catharanthus roseus*. *Colloids and Surfaces B: Biointerfaces, 62*, 312–318. doi:10.1016/j.colsurfb.2007.10.013

173. Jaleel, C. A., Gopi, R., Azooz, M. M., & Panneerselvam, R. (2009). Leaf anatomical modifications in *Catharanthus roseus* as affected by plant growth promoters and retardants. *Global Journal of Molecular Sciences, 4*(1), 1-5.

174. Jayaseelan, C., Rahuman, A. A., Kirthi, A. V., Marimuthu, S., Santhoshkumar, T., Bagavan, A., Gaurav, K., Karthik, L., & Rao, K. V. B. (2012). Novel microbial route to synthesize ZnO nanoparticles using *Aeromonas hydrophila* and their activity against pathogenic bacteria and fungi. *Spectrochimica Acta Part A: Molecular and Biomolecular Spectroscopy, 90*, 78– 84. doi:10.1016/j.saa.2012.01.006

175. Jhanji, R., Bhati, V., Singh, A., & Kumar, A. (2019). Phytomolecules against bacterial biofilm and efflux pump: An *in silico* and *in vitro* study. *Journal of Biomolecular Structure and Dynamics*. doi:10.1080/07391102.2019.1704884

176. Jiang, Z., Shan, K., Song, J., Liu, J., Rajendran, S., Pugazhendhi, A., Jacob, J. A., & Chen, B. (2019). Toxic effects of magnetic nanoparticles on normal cells and organs. *Life Sciences, 220*, 156–161. doi:10.1016/j.lfs.2019.01.056

177. Johnson, I. S., Armstrong, J. G., Gorman, M., & Burnett, J. P. (1963). The *Vinca* Alkaloids : A New Class of Oncolytic Agents. *Cancer Research, 23*, 1390-1427.

178. Jones, W. P., & Kinghorn, A. D. (2006). *Chapter 13. Extraction of plant secondary metabolites* (S. D. Sarker, Z. Latif, & A. I. Gray Eds. 2 ed. Vol. 20): Humana Press.

179. Jordan, M. A., & Kamath, K. (2007). How do microtubule-targeted drugs work? An overview. *Current Cancer Drug Targets, 7*, 730-742.

180. Jordan, M. A., Thrower, D., & Wilson, L. (1991). Mechanism of inhibition of cell proliferation by *Vinca* alkaloids. *Cancer Research, 51*, 2212-2222.

181. Jyoti, K., Baunthiyal, M., & Singh, A. (2018). Characterization of silver nanoparticles synthesized using *Urtica dioica* Linn. leaves and their synergistic effects with antibiotics. *Journal of Radiation Research and Applied Sciences, 9*, 217-227. doi:10.1016/j.jrras.2015.10.002

182. Kabesh, K., Senthilkumar, P., Ragunathan, R., & Raj Kumar, R. (2015). Phytochemical Analysis of *Catharanthus roseus* Plant Extract and its Antimicrobial Activity. *International Journal of Pure & Applied Bioscience, 3*(2), 162-172.

183. Kadzinski, M., Cinelli, M., Ciomek, K., Coles, S. R., Nadagouda, M. N., Varma, R. S., & Kirwan, K. (2016). Co-constructive development of a green chemestry-based model for the assessment of nanoparticles synthesis;. *European Journal of Operational Research, 264*(2), 427-490. doi:10.1016/j.ejor.2016.10.019

184. Kathiresan, K., Manivannan, S., Nabeel, M. A., & Dhivya, B. (2009). Studies on silver nanoparticles synthesized by marine fungus, *Penicillium fellutanum* isolated from coastal mangrove sediment. *Colloids and Surfaces B: Biointerfaces, 71*, 133–137. doi:10.1016/j.colsurfb.2009.01.016

185. Kedare, S. B., & Singh, R. P. (2011). Genesis and development of DPPH method of antioxidant assay. *J Food Sci Technol, 48*(4), 412–422. doi:10.1007/s13197-011-0251-1

186. Khan, A., El-Toni, A. M., Alsalhi, M., Aldwayyan, A. S., & Alhoshan, M. (2012). Preparation of magnetic polyacrylonitrile core–shell nanospheres by the miniemulsion polymerization method. *Materials Letters, 76*, 141–143. doi:10.1016/j.matlet.2012.02.089

187. Khan, Z. U. H., Khan, A., Shah, A., Wan, P., Chen, Y., Khan, A. U., Tahir, K., Muhammad, N., & Khan, H. U. (2016). Enhanced photocatalytic and electrocatalytic applications of green synthesized silver nanoparticles. *Journal of Molecular Liquids, 220*, 248–257. doi:10.1016/j.molliq.2016.04.082

188. Khanavi, M., Pourmoslemi, S., Farahanikia, B., Hadjiakhoondi, A., & Ostad, S. N. (2010). Cytotoxicity of *Vinca minor*. *Pharmaceutical Biology, 48*(1), 96–100. doi:10.3109/13880200903046187

189. Kharissova, O. V., Dias, H. V. R., Kharisov, B. I., Perez, B. O., & Perez, V. M. J. (2013). The greener synthesis of nanoparticles. *Trends in Biotechnology, 31*(4), 240-248. doi:10.1016/j.tibtech.2013.01.003

190. Khattak, S., & Khan, H. (2016). Anti-cancer potential of phyto-alkaloids: A prospective review. *Current Cancer Therapy Reviews, 12*, 66-75. doi:10.2174/1573394712666160617081

191. Kidner, C. A., & Umbreen, S. (2010). Why is Leaf Shape so Variable? *International Journal of Plant Developmental Biology, 4*(1), 64-75.

192. Koyuncu, M. (2012). A new species of *Vinca* (Apocynaceae) from eastern Anatolia, Turkey. *Turkish Journal of Botany*, *36*, 247-251. doi:10.3906/bot-1103-19

193. Krishnaraj, C., Ji, B.-J., Harper, S. L., & Yun, S.-I. (2016). Plant extract-mediated biogenic synthesis of silver, manganese dioxide, silver-doped manganese dioxide nanoparticles and their antibacterial activity against food- and water-borne pathogens. *Bioprocess Biosyst Eng*, *39*, 759–772. doi:10.1007/s00449-016-1556-2

194. Kulwa, F., Li, C., Zhao, X., Cai, B., Xu, N., Qi, S., Chen, S., & Teng, Y. (2019). A State-of-the-art Survey for Microorganism Image Segmentation Methods and Future Potential *IEEE Access*, *7*, 100243-100269. doi:10.1109/ACCESS.2019.2930111

195. Kunkalekar, R. K., Naik, M. M., Dubey, S. K., & Salker, A. V. (2012). Antibacterial activity of silver-doped manganese dioxide nanoparticles on multidrug-resistant bacteria. *Journal of Chemical Technology & Biotechnology*. doi:10.1002/jctb.3915

196. Kunkalekar, R. K., Prabhu, M. S., Naik, M. M., & Salker, A. V. (2014). Silver-doped manganese dioxide and trioxide nanoparticles inhibit both Gram-positive and Gram-negative pathogenic bacteria. *Colloids and Surfaces B: Biointerfaces*, *113*, 429– 434. doi:10.1016/j.colsurfb.2013.09.036

197. Leclercq, R., Canton, R., Brown, D. F. J., Giske, C. G., Heisig, P., MacGowan, A. P., Mouton, J. W., Nordmann, P., Rodloff, A. C., Rossolini, G. M., Soussy, C.-J., Steinbakk, M., Winstanley, T. G., & Kahlmeter, G. (2013). EUCAST expert rules in antimicrobial susceptibility testing. *Clinical Microbiology and Infection*, *19*(2), 141–160.

198. Lekka, M., Pogoda, K., Gostek, J., Klymenko, O., Prauzner-Bechcicki, S., Wiltowska-Zuber, J., Jaczewska, J., Lekki, J., & Stachura, Z. (2012). Cancer cell recognition – Mechanical phenotype. *Micron*, *43*, 1259–1266. doi:10.1016/j.micron.2012.01.019

199. Leona, M., & Lombardi, J. R. (2007). Identification of berberine in ancient and historical textiles by surfaceenhanced Raman scattering. *Journal of Raman Spectroscopy*, *38*, 853–858.

200. Levytskyy, R. M., Filyak, Y. Z., & Stoika, R. S. (2004). Correlation between generation of nitric oxide and cell viability in human peripheral blood mononuclear cells and leukemic jurkat T-cell line. *Experimental Oncology*, *26*(3), 217-220.

201. Li, C., Xu, C., Gui, C., & Fox, M. D. (2010). Distance Regularized Level Set Evolution and Its Application to Image Segmentation. *IEEE Transactions on Image Processing*, *19*(12), 3243-3254. doi:10.1109/TIP.2010.2069690

202. Liao, F.-Y., Xie, Y., & Jiang, H. (2013). The effect of water stress on the physiology of *Vinca major* 'variegata'. *Applied Mechanics and Materials*, *409-410*, 782-787. doi:10.4028/www.scientific.net/AMM.409-410.782

203. Liu, C., Li, Y., Xu, L., Chen, Z., & He, N. (2019). Variation in leaf morphological, stomatal, and anatomical traits and their relationships in temperate and subtropical forests. *Scientific Reports*, *9*. doi:10.1038/s41598-019-42335-2

204. Liu, J., Liu, Y., Pan, Y.-j., Zu, Y.-G., & Tang, Z.-H. (2015). Determination of alkaloids in *Catharanthus roseus* and *Vinca minor* by high-performance liquid chromatography – tandem mass spectrometry. *Analytical Letters*. doi:10.1080/00032719.2015.1094664

205. Lobert, S., Vulevic, B., & Correia, J. J. (1996). Interaction of *Vinca* Alkaloids with Tubulin: A Comparison of Vinblastine, Vincristine, and Vinorelbine. *Biochemistry, 35*, 6806-6814.

206. Lü, S., Wu, Y., & Liu, H. (2017). Silver nanoparticles synthesized using *Eucommia ulmoides* bark and their antibacterial efficacy. *Materials Letters*, *196*, 217–220. doi:10.1016/j.matlet.2017.03.068

207. Lundgren, M. R., Mathers, A., Baillie, A. L., Dunn, J., Wilson, M. J., Hunt, L., Pajor, R., Fradera-Soler, M., Rolfe, S., Osborne, C. P., Sturrock, C. J., Gray, J. E., Mooney, S. J., & Fleming, A. J. (2019). Mesophyll porosity is modulated by the presence of functional stomata. *Nature Communications*, *10*(1), 2825. doi:10.1038/s41467-019-10826-5

208. Macavei, S. G., Suciu, M., Craciunescu, I., Barbu-Tudoran, L., Tripon, S. C., & Balan, R. (2016). Hyperthermia effects on normal and tumor skin cells. *Annals of R.S.C.B., 21*(1), 11-21.

209. Magge, R. S., & DeAngelis, L. M. (2015). The double-edged sword: Neurotoxicity of chemotherapy. *Blood Rev, 29*(2), 93-100. doi:10.1016/j.blre.2014.09.012

210. Mahmoudi, S., Khali, M., Benkhaled, A., Benamirouche, K., & Baiti, I. (2016). Phenolic and flavonoid contents, antioxidant and antimicrobial activities of leaf extracts from ten Algerian *Ficus carica* L. varieties. *Asian Pacific Journal of Tropical Biomedicine, 6*(3), 239–245. doi:10.1016/j.apjtb.2015.12.010

211. Mahmoudvand, H., Sharififar, F., Sharifi, I., Ezatpour, B., Harandi, M. F., Makki, M. S., Zia-Ali, N., & Jahanbakhsh, S. (2014). *In Vitro* Inhibitory Effect of *Berberis vulgaris* (Berberidaceae) and Its Main Component, Berberine against Different *Leishmania* Species. *Iranian Journal of Parasitology, 9*(1), 28-36.

212. Maincent, P., Devissaguet, J. P., Leverge, R., Sado, P. A., & Couvreur, P. (1984). Preparation and *in vivo* studies of a new drug delivery system. *Applied Biochemistry and Biotechnology*, *10*, 263-265. doi:10.1007/bf02783760

213. Manosalva, L., Mutis, A., Urzúa, A., Fajardo, V., & Quiroz, A. (2016). Antibacterial activity of alkaloid fractions from *Berberis microphylla* G. Forst and study of synergism with ampicillin and cephalothin. *Molecules*, *21*(76). doi:10.3390/molecules21010076

214. Mardani-Nejad, S. (2017). Rapid screening of antioxidant activity, fracture rate and scavenging of free radicals by hairy root of Periwinkle (*Catharanthus roseus* L. G. Don). *Journal of Herbal Drugs, 7*(4), 257-267.

215. Martino, E., Casamassima, G., Castiglione, S., Cellupica, E., Pantalone, S., Papagni, F., Rui, M., Siciliano, A. M., & Collina, S. (2018). *Vinca* alkaloids and analogues as anti-cancer agents: Looking back, peering ahead. *Bioorganic & Medicinal Chemistry Letters, 28*(17), 2816-2826. doi:10.1016/j.bmcl.2018.06.044

216. Matuschek, E., Brown, D. F. J., & Kahlmeter, G. (2014). Development of the EUCAST disk diffusion antimicrobial susceptibility testing method and its implementation in routine microbiology laboratories. *Clinical Microbiology and Infection, 20*(4), O255–O266. doi:10.1111/1469-0691.12373

217. McCoy, E., & O'Connor, S. E. (2008). Natural products from plant cell cultures. *Progress in Drug Research, 65*(329), 331-370.

218. Mierziak, J., Kostyn, K., & Kulma, A. (2014). Flavonoids as important molecules of plant interactions with the environment. *Molecules, 19*, 16240-16265. doi:10.3390/molecules191016240

219. Minaee, S., Boykov, Y., Porikli, F., Plaza, A., Kehtarnavaz, N., & Terzopoulos, D. (2020). Image Segmentation Using Deep Learning: A Survey. doi:arXiv:2001.05566

220. Moeller, S., Wöhrmann, T., Huettel, B., & Weising, K. (2015). Development of 18 polymorphic microsatellite markers for *Vinca minor* (Apocynaceae) via 454 pyrosequencing. *Applications in Plant Sciences, 3*(5). doi:10.3732/apps.1500015

221. Mohammadi, B., & Salouti, M. (2015). Extracelullar biosynthesis of silver nanoparticles by *Penicillium chrysogenum* and *Penicillium expansum*. *Synthesis and Reactivity in Inorganic, Metal-Organic, and Nano-Metal Chemistry, 45*, 844-847. doi:10.1080/15533174.2013.862640

222. Mokry, J., Kompis, I., Dubravkova, L., & Sefcovic, P. (1962). Alkaloids of *Vinca minor* L. The structure of vincadine and vincaminoreine. *Tetrahedron Letters, 25*, 1185-1188.

223. Moon, S. A., Salunke, B. K., Alkotaini, B., Sathiyamoorthi, E., & Kim, B. S. (2014). Biological synthesis of manganese dioxide nanoparticles by *Kalopanax pictus* plant extract. *Nanobiotechnology, 9*(4), 220–225. doi:10.1049/iet-nbt.2014.0051

224. Moon, S. H., Pandurangan, M., Kim, D. H., Venkatesh, J., Patel, R. V., & Mistry, B. M. (2018). A rich source of potential bioactive compounds with anticancer activities by *Catharanthus roseus* cambium meristematic stem cell cultures. *Journal of Ethnopharmacology, 217*(107–117). doi:10.1016/j.jep.2018.02.021

225. Moț, A. C., Bischin, C., Mureșan, B., Pârvu, M., Damian, G., Vlase, L., & Silaghi-Dumitrescu, R. (2016). Antioxidant activity evaluation by physiologically relevant assays based on haemoglobin peroxidase activity and cytochrome c-induced oxidation of liposomes. *Natural Product Research, 30*(11), 1315-1319. doi:10.1080/14786419.2015.1054824

226. Moudi, M., Go, R., Seok Yien, C. Y., & Nazre, M. (2013). *Vinca* alkaloids. *International Journal of Preventive Medicine, 41*(11), 1231-1235.

227. Mousavi, B., Tafvizi, F., & Bostanabad, S. Z. (2018). Green synthesis of silver nanoparticles using *Artemisia turcomanica* leaf extract and the study of anti-cancer effect and apoptosis induction on gastric cancer cell line (AGS). *Artificial Cells, Nanomedicine, and Biotechnology*. doi:10.1080/21691401.2018.1430697

228. Mukunthan, K., Elumalai, E., Trupti, N. P., & Ramachandra Murty, V. (2011). *Catharanthus roseus*: a natural source for the synthesis of silver nanoparticles. *Asian Pacific Journal of Tropical Biomedicine, 1*(4), 270-274. doi:10.1016/S2221-1691(11)60041-5

229. Müller, L., Fröhlich, K., & Böhm, V. (2011). Comparative antioxidant activities of carotenoids measured by ferric reducing antioxidant power (FRAP), ABTS bleaching assay (aTEAC), DPPH assay and peroxyl radical scavenging assay. *Food Chemistry, 129*, 139–148. doi:10.1016/j.foodchem.2011.04.045

230. Muntean, L. S., Tămaș, M., Muntean, S., Muntean, L., Duda, M. M., Vârban, D. I., & Florian, S. (2007). *Tratat de plante medicinale cultivate și spontane*. Cluj-Napoca: Editura Rizoprint.

231. Murata, J., Roepke, J., Gordon, H., & De Luca, V. (2008). The leaf epidermome of *Catharanthus roseus* reveals its biochemical specialization. *The Plant Cell, 20*(3), 524-542. doi:10.1105/tpc.107.056630

232. Naaz, F., Haider, M. R., Shafi, S., & Yar, M. S. (2019). Anti-tubulin agents of natural origin: Targeting taxol, vinca, and colchicine binding domains. *Eur J Med Chem, 171*, 310-331. doi:10.1016/j.ejmech.2019.03.025

233. Nair Sreekala, G., Abdullakutty, F., & Beena, B. (2019). Green synthesis, characterization and photo catalytic degradation efficiency of Trimanganese Tetroxide nanoparticle. *International Journal of Nano Dimension, 10*(4), 400-409.

234. Nakawaga, T., Gonda, K., Kamei, T., Cong, L., Hamada, Y., Kitamura, N., Tada, H., Ishida, T., Aimiya, T., Furusawa, N., Nakano, Y., & Ohuchi, N. (2016). X-ray computed tomography imaging of a tumor with high sensitivity using gold nanoparticles conjugated to a cancer-specific antibody via polyethylene glycol chains on their surface. *Science and Technology of Advanced Materials, 17*(1), 387-397. doi:10.1080/14686996.2016.1194167

235. Naraginti, S., Kumari, P. L., Das, R. K., Sivakumar, A., Patil, S. H., & Andhalkar, V. V. (2016). Amelioration of excision wounds by topical application of green synthesized, formulated silver and gold nanoparticles in albino Wistar rats. *Materials Science and Engineering C, 62*, 293–300. doi:10.1016/j.msec.2016.01.069

236. Naraginti, S., & Li, Y. (2017). Preliminary investigation of catalytic, antioxidant, anticancer and bactericidal activity of green synthesized silver and gold nanoparticles using *Actinidia deliciosa*. *Journal of Photochemistry & Photobiology, B: Biology, 170*, 225–234. doi:10.1016/j.jphotobiol.2017.03.023

237. Naraginti, S., & Sivakumar, A. (2014). Eco-friendly synthesis of silver and gold nanoparticles with enhanced bactericidal activity and study of silver catalyzed reduction of 4-nitrophenol. *Spectrochimica Acta Part A: Molecular and Biomolecular Spectroscopy, 128*, 357–362. doi:10.1016/j.saa.2014.02.083

238. Nasrollahzadeh, M., Maham, M., Rostami-Vartooni, A., Bagherzadeh, M., & Sajadi, S. M. (2015). Berberry fruit extract assisted in situ green synthesis of Cu nanoparticles supported on a reduced graphene oxide-Fe_3O_4 nanocomposite as a magnetically separable and reusable catalyst for the O-arylation of phenols with aryl halides under ligand-free conditions. *Royal Society of Chemistry, 5*, 64769-64780. doi:10.1039/c5ra10037b

239. Nasrollahzadeh, M., Sajjadi, M., & Sajadi, S. M. (2018). Biosynthesis of copper nanoparticles supported on manganese dioxide nanoparticles using *Centella asiatica* L. leaf extract for the efficient catalytic reduction of organic dyes and nitroarenes. *Chinese Journal of Catalysis, 39*, 109–117. doi:10.1016/S1872-2067(17)62915-2

240. National Nanotechnology Initiative. Retrieved from https://www.nano.gov

241. . National Research Council of the National Academies. (2012). In *A Research Strategy for Environmental, Health, and Safety Aspects of Engineered Nanomaterials* (pp. 24). Washington, D.C.: The National Academies Press.

242. Negahdary, M., Arefian, Z., Dastjerdi, H. A., & Ajdary, M. (2019). Toxic effects of Mn_2O_3 nanoparticles on rat testis and sex hormone. *Journal of Natural Science, Biology and Medicine, 6*(2), 335-339. doi:10.4103/0976-9668.159998

243. Nenadis, N., Wang, L.-F., Tsimidou, M., & Zhang, H.-Y. (2011). Estimation of Scavenging Activity of Phenolic Compounds Using the ABTS•+ Assay. *Journal of Agricultural and Food Chemistry, 52*, 4669−4674.

244. Newman, D. J. (2008). Natural products as leads to potential drugs: An old process or the new hope for drug discovery? *Journal of Medicinal Chemistry, 51*(9), 2589–2599. doi:10.1021/jm0704090

245. Noghabi, M. P., Parizadeh, M. R., Ghayour-Mobarhan, M., Taherzadeh, D., Hosseini, H. A., & Darroudi, M. (2017). Green synthesis of silver nanoparticles and investigation of their colorimetric sensing and cytotoxicity effects. *Journal of Molecular Structure, 1146,* 499-503. doi:10.1016/j.molstruc.2017.05.145

246. Nouri, F., Nourollahi-Fard, S. R., Foroodi, H. R., & Sharifi, H. (2016). In vitro anthelmintic effect of Tobacco (*Nicotiana tabacum*) extract on parasitic nematode, *Marshallagia marshalli*. *Journal of Parasitic Diseases, 40*(3), 643–647. doi:10.1007/s12639-014-0550-3

247. O'Connor, S. E. (2008). Alkaloid biosynthesis. *Wiley Encyclopedia of Chemical Biology, 1,* 17-33. doi:10.1002/9780470048672

248. O'Connor, S. E., & Maresh, J. J. (2006). Chemistry and biology of monoterpene indole alkaloid biosynthesis. *Natural Product Reports, 23*, 532–547. doi:10.1039/b512615k

249. Ochirova, K. S., Ovanova, E. A., & Dordzhieva, V. I. (2018). *Vinca minor* L. leaf anatomical structure. *Journal of Pharmaceutical Sciences and Research, 10*(10), 2528-2530.

250. Ognyanov, I. (1965). Die struktur des herbalins - eines oxindol-alkaloids aus *Vinca herbacea* W. K. [The structure of herbalin - an oxidol-alkaloid from *Vinca herbacea* W. K.]. *European Journal of Inorganic Chemistry, 99*, 2052-2056. doi:10.1002/cber.19660990636

251. Ogunyemi, S. O., Zhang, F., Abdallah, Y., Zhang, M., Wang, Y., Sun, G., Qiu, W., & Li, B. (2019). Biosynthesis and characterization of magnesium oxide and manganese dioxide nanoparticles using *Matricaria chamomilla* L. extract and its inhibitory effect on *Acidovorax oryzae* strain RS-2. *Artificial Cells, Nanomedicine, and Biotechnology, 47*(1), 2230–2239. doi:10.1080/21691401.2019.1622552

252. Okouneva, T., Hill, B. T., Wilson, L., & Jordan, M. A. (2003). The Effects of Vinflunine, Vinorelbine, and Vinblastine on Centromere Dynamics. *Molecular Cancer Therapeutics, 2*, 427–436.

253. Opriş, O., Ciorîţă, A., Soran, M.-L., Lung, I., Copolovici, D., & Copolovici, L. (2019). Evaluation of the photosynthetic parameters, emission of volatile organic compounds and ultrastructure of common green leafy vegetables after exposure to non-steroidal anti-inflammatory drugs (NSAIDs). *Ecotoxicology, 28*, 631–642. doi:10.1007/s10646-019-02059-5

254. Özçelik, B., Kartal, M., & Orhan, I. (2011). Cytotoxicity, antiviral and antimicrobial activities of alkaloids, flavonoids, and phenolic acids. *Pharmaceutical Biology, 49*(4), 396-402. doi:10.3109/13880209.2010.519390

255. Ozyurek, M., Guclu, K., Tutem, E., Basxkan, K. S., Erca, E., Celik, S. E., Baki, S., Yıldız, L., Karaman, S., & Apak, R. (2011). A comprehensive review of CUPRAC methodology. *Analytical Methods, 3*. doi:10.1039/C1AY05320E

256. P.O.W. Plants of the World Online. Retrieved from http://powo.science.kew.org/;

http://www.plantsoftheworldonline.org/taxon/urn:lsid:ipni.org:names:2619-1;

http://www.plantsoftheworldonline.org/taxon/urn:lsid:ipni.org:names:82683-1

http://www.plantsoftheworldonline.org/taxon/urn:lsid:ipni.org:names:82686-1

http://www.plantsoftheworldonline.org/taxon/urn:lsid:ipni.org:names:82691-1

http://www.plantsoftheworldonline.org/taxon/urn:lsid:ipni.org:names:77174889-1

http://www.plantsoftheworldonline.org/taxon/urn:lsid:ipni.org:names:82697-1

http://www.plantsoftheworldonline.org/taxon/urn:lsid:ipni.org:names:82701-1

http://www.plantsoftheworldonline.org/taxon/urn:lsid:ipni.org:names:77119119-1

http://www.plantsoftheworldonline.org/taxon/urn:lsid:ipni.org:names:2251-1

http://www.plantsoftheworldonline.org/taxon/urn:lsid:ipni.org:names:77880-1

http://www.plantsoftheworldonline.org/taxon/urn:lsid:ipni.org:names:77879-1

http://www.plantsoftheworldonline.org/taxon/urn:lsid:ipni.org:names:77875-1

http://www.plantsoftheworldonline.org/taxon/urn:lsid:ipni.org:names:77878-1

http://www.plantsoftheworldonline.org/taxon/urn:lsid:ipni.org:names:77877-1

http://www.plantsoftheworldonline.org/taxon/urn:lsid:ipni.org:names:77881-1

http://www.plantsoftheworldonline.org/taxon/urn:lsid:ipni.org:names:77882-1

http://www.plantsoftheworldonline.org/taxon/urn:lsid:ipni.org:names:77876-1

http://www.plantsoftheworldonline.org/taxon/urn:lsid:ipni.org:names:77153515-1

257. Pandey-Rai, S., Mallavarapu, G. R., Naqvi, A. A., Yadav, A., Rai, S. K., Srivastava, S., Singh, D., Mishra, R., & Kumar, S. (2006). Volatile components of leaves and flowers of periwinkle *Catharanthus roseus* (L.) G. Don from New Delhi. *Flavour and Fragrance Journal, 21*, 427–430. doi:10.1002/ffj.1606

258. Pârvu, M., & Pârvu, A. E. (2011a). Antifungal plant extracts. *Science against microbial pathogens: communicating current research and technological advances*.

259. Pârvu, M., & Pârvu, A. E. (2011b). Antifungal plant extracts.

260. Pârvu, M., Pârvu, A. E., Crăciun, C., Barbu-Tudoran, L., & Tamaș, M. (2008). Antifungal activities of *Chelidonium majus* extract on *Botrytis cinerea in vitro* and ultrastructural changes in its conidia. *J. Phytopathology, 156*, 550–552. doi:10.1111/j.1439-0434.2008.01410.x

261. Pârvu, M., Vlase, L., Fodorpataki, L., Pârvu, O., Bartha, C., Roșca-Casian, O., Barbu-Tudoran, L., & Pârvu, A. E. (2013). Chemical composition of celandine (*Chelidonium majus* L.) extract and its effects on *Botrytis tulipae* (Lib.) lind fungus and the tulip. *Notulae Botanicae Horti Agrobotanici*, *41*(2), 414-426.

262. Patil, P. J., & Ghosh, J. S. (2010). Antimicrobial Activity of *Catharanthus roseus* – A Detailed Study. *British Journal of Pharmacology and Toxicology, 1*(1), 40-44.

263. Păun, E., Mihalea, A., Dumitrescu, A., Verzea, M., & Coșocariu, O. (1988). *Tratat de plante medicinale și aromatice cultivate* (Vol. 2). București: Editura Academiei Republicii Socialiste România.

264. Pękal, A., & Pyrzynska, K. (2014). Evaluation of aluminium complexation reaction for flavonoid content assay. *Food Analytical Methods, 7*(9), 1776–1782. doi:10.1007/s12161-014-9814-x

265. Petra, S. A., Georgescu, M. I., Manescu, C. R., Toma, F., Badea, M. L., Dobrescu, E., & Popa, V. I. (2020). Leaves anatomical and physiological adaptations of *Vinca major* 'Variegata' and *Hedera helix* L. to specific roof garden conditions. *Notulae Botanicae Horti Agrobotanici, 47*(4), 318-328. doi:10.15835/nbha48111784

266. PLANTS. United States Department of Agriculture. PLANTS Database. Retrieved from https://plants.sc.egov.usda.gov;

https://plants.sc.egov.usda.gov/java/

https://plants.sc.egov.usda.gov/java/ClassificationServlet?source=display&classid=VINCA

https://plants.usda.gov/core/profile?symbol=VINCA;

https://plants.usda.gov/core/profile?symbol=VIMI2

https://plants.usda.gov/core/profile?symbol=VIMA

https://plants.usda.gov/core/profile?symbol=VIHE3

https://plants.sc.egov.usda.gov/java/nameSearch?keywordquery=catharanthus&mode=Scientific%20Name&sort=1

https://plants.usda.gov/core/profile?symbol=CARO14

267. Pogoda, K., Jaczewska, J., Wiltowska-Zuber, J., Klymenko, O., Zuber, K., Fornal, M., & Lekka, M. (2012). Depth-sensing analysis of cytoskeleton organization based on AFM data. *Eur Biophys J, 41*, 79–87. doi:10.1007/s00249-011-0761-9

268. Poojary, M. M., Vishnumurthy, K. A., & Adhikari, A. V. (2015). Extraction, characterization and biological studies of phytochemicals from *Mammea suriga*. *Journal of Pharmaceutical Analysis, 5*(3), 182–189. doi:10.1016/j.jpha.2015.01.002

269. Pyuskyulev, B., Ognyanov, I., & Panov, P. (1967). Alkaloide aus *Vinca herbacea* W. K. II Norfluorocurarin. [Alkaloids from *Vinca herbacea* W. K. II norfluorocurarin]. *Tetrahedron Letters, 46*, 4559-4562. doi:10.1016/s0040-4039(01)-89555-1

270. Rabbani-Chadegani, A., Paydar, P., Amirshenava, M., & Aramvash, A. (2015). An in vitro study on the effect of vinca alkaloid, vinorelbine, on chromatin histone, HMGB proteins and induction of apoptosis in mice non-adherent bone marrow cells. *Drug and Chemical Toxicology, 38*(2), 220-226. doi:10.3109/01480545.2014.933347

271. Rajput, M. S., Nair, V., Chauhan, A., Jawanjal, H., & Dange, V. (2011). Evaluation of antidiarrheal activity of aerial parts of *Vinca major* in experimental animals. *Middle-East Journal of Scientific Research, 7*(5), 784-788.

272. Ramalingam, J. R., Vaali-Mohammed, M.-A., Al-Lohedan, H. A., & Appaturi, J. N. (2017). Synthesis and bio-physical characterization of silver nanoparticle and Ag-mesoporous MnO_2 nanocomposite for anti-microbial and anti-cancer activity. *Journal ofMolecular Liquids, 243*, 348–357. doi:10.1016/j.molliq.2017.08.037

273. Re, R., Pellegrini, N., Proteggente, A., Pannala, A., Yang, M., & Rice-Evans, C. (1999). Antioxidant activity applying an improved ABTS radical cation decolorization assay. *Free Radical Biology & Medicine, 26*(9/10), 1231–1237.

274. Redda, Y. T., Kebede, E., Cruz, C., Gugsa, G., Awol, N., & Mengeste, B. (2014). Potential antibacterial activity of crude extracts from *Aloe vera*, *Zingiber officinale* and *Vinca major* medicinal plants. *International Journal of Microbiological Research, 5*(3), 202-207. doi:10.5829/idosi.ijmr.2014.5.3.86177

275. Rischer, H., Oresic, M., Seppanen-Laakso, T., Katajamaa, M., Lammertyn, F., Ardiles-Diaz, W., Van Montagu, M. C. E., Inze, D., Oksman-Caldentey, K.-M., & Goossens, A. (2006). Gene-to-metabolite networks for terpenoid indole alkaloid biosynthesis in *Catharanthus roseus* cells. *PNAS, 103*(14), 5614–5619. doi:10.1073/pnas.0601027103

276. Risinger, A. L., Giles, F. J., & Mooberry, S. L. (2009). Microtubule dynamics as a target in oncology. *Cancer Treatment Reviews, 35*(3), 255-261. doi:10.1016/j.ctrv.2008.11.001

277. Roepke, J., Salim, V., Wu, M., Thamm, A. M., Murata, J., Ploss, K., Boland, W., & De Luca, V. (2010). *Vinca* drug components accumulate exclusively in leaf exudates of Madagascar periwinkle. *Proc Natl Acad Sci U S A, 107*(34), 15287-15292. doi:10.1073/pnas.0911451107

278. Rongai, D., Milano, F., & Scio, E. (2012). Inhibitory effect of plant extracts on conidial germination of the phytopathogenic fungus *Fusarium oxysporum*. *American Journal of Plant Sciences, 3*, 1693-1698. doi:http://dx.doi.org/10.4236/ajps.2012.312207

279. Rouhani, S., Salehi, N., Kamalinejad, M., & Zayeri, F. (2013). Efficacy of *Berberis vulgaris* Aqueous Extract on Viability of *Echinococcus granulosus* Protoscolices. *Journal of Investigative Surgery, 1-5*. doi:10.3109/08941939.2013.818746

280. Royer, D. L. (2001). Stomatal density and stomatal index as indicators of paleoatmospheric CO_2 concentration. *Review of Palaeobotany and Palynology, 114*, 1-28. doi:https://doi.org/10.1016/S0034-6667(00)00074-9

281. Ruan, Y. L. (2012). Signaling role of sucrose metabolism in development. *Mol Plant, 5*(4), 763-765. doi:10.1093/mp/sss046

282. S.D.B.S. Spectral Database for Organic Compounds. Retrieved from [https://sdbs.db.aist.go.jp/sdbs/cgi-bin/direct_frame_disp.cgi?sdbsno=10560&

283. Saifuddin, N., Wong, C. W., & Nur Yasumira, A. A. (2009). Rapid Biosynthesis of Silver Nanoparticles Using Culture Supernatant of Bacteria with Microwave Irradiation. *E-Journal of Chemistry, 6*(1), 61-70.

284. Salaheldin, T. A., El-Chaghaby, G. A., & El-Sherbiny, M. A. (2019). Green synthesis of silver nanoparticles using *Portulacaria afra* plant extract: characterization and evaluation of its antibacterial, anticancer activities. *Novel Research in Microbiology Journal, 3*(1), 215-222. doi:10.21608/nrmj.2019.28107

285. Samiyarsih, S., Nettyani, N., & Dian, P. (2019). Variability of *Catharanthus roseus* based on morphological and anatomical characters, and chlorophyll contents. *Biodiversitas Journal of Biological Diversity, 20*(10). doi:10.13057/biodiv/d201029

286. Sampathkumar, A., Krupinski, P., Wightman, R., Milani, P., Berquand, A., Boudaoud, A., Hamant, O., Jönsson, H., & Meyerowitz, E. M. (2014). Subcellular and supracellular mechanical stress prescribes cytoskeleton behavior in *Arabidopsis cotyledon* pavement cells. *eLife, 3*, e01967. doi:10.7554/eLife.01967.001

287. Sapala, A., Runions, A., Routier-Kierzkowska, A.-L., Gupta, M. D., Hong, L., Hofhuis, H., Verger, S., Mosca, G., Li, C.-B., Hay, A., Hamant, O., Roeder, A. H., Tsiantis, M., Prusinkiewicz, P., & Smith, R. S. (2018). Why plants make puzzle cells, and how their shape emerges. *eLife, 7*, e32794. doi:10.7554/eLife.32794

288. Sathyavathi, R., Krishna, M. B., Rao, S. V., Saritha, R., & Rao, D. N. (2010). Biosynthesis of Silver Nanoparticles Using *Coriandrum sativum* Leaf Extract and Their Application in Nonlinear Optics. *Advanced Science Letters, 3*(2), 1-6. doi:10.1166/asl.2010.1099

289. Scarlat, A. (2019). *Tratat de fitomedicină* (Vol. I, II). Ploiești: Editura Karta-Graphic.

290. Scheindlin, S., & Rubin, N. (1955). Isolation of an alkaloid from *Vinca minor*. *Journal Of The American Pharmaceutical Association, 44*(6), 330-332.

291. Schutz, F. A., Bellmunt, J., Rosenberg, J. E., & Choueiri, T. K. (2011). Vinflunine: drug safety evaluation of this novel synthetic vinca alkaloid. *Expert Opinion on Drug Safety, 10*(4), 645-653. doi:10.1517/14740338.2011.581660

292. Segev, R., Nannapaneni, R., Sindurakar, P., Kim, H., Read, H., & Lijek, S. (2015). The effect of the stomatal index on the net rate of photosynthesis in the leaves of *Spinacia oleracea*, *Vinca minor*, *Rhododendron* spp, *Epipremnum aureum*, and *Hedera* spp. *Journal of Emerging Investigators*.

293. Senthil, B., Devasena, T., Prakash, B., & Rajasekar, A. (2017). Non-cytotoxic effect of green synthesized silver nanoparticles and its antibacterial activity. *Journal of Photochemistry & Photobiology, B: Biology, 177*, 1–7. doi:10.1016/j.jphotobiol.2017.10.010

294. Shaheen, H. A., & Issa, M. Y. (2019). *In vitro* and *in vivo* activity of *Peganum harmala* L. alkaloids against phytopathogenic bacteria. *Scientia Horticulturae*. doi:10.1016/j.scienta.2019.108940

295. Shang, L., Nienhaus, K., & Nienhaus, G. U. (2014). Engineered nanoparticles interacting with cells: size matters. *Journal of Nanobiotechnology, 12*.

296. Sharma, B., Dhamija, I., Kumar, S., & Chaudhary, H. (2015). *In vitro* and *in vivo* evaluation of antitumor activity of methanolic extract of *Argyreia nervosa* leaves on Ehrlich ascites carcinoma. *A Journal of the Bangladesh Pharmacological Society, 10*, 399-408. doi:10.3329/bjp.v10i2.22334

297. Sharma, O. P., & Bhat, T. K. (2009). DPPH antioxidant assay revisited. *Food Chemistry, 113*, 1202–1205. doi:10.1016/j.foodchem.2008.08.008

298. Sharma, V. C., Gaherwar, S., & Thakur, M. (2014). Microwave-mediated green synthesis of silver nanoparticles by using *Vinca rosea* & its application in air pollution control. *Indian Journal of Scientific Research, 4*, 100-103.

299. Shi, P., Li, Y., Hui, C., Ratkowsky, D. A., Yu, X., & Niinemets, Ü. (2020). Does the law of diminishing returns in leaf scaling apply to vines? – Evidence from 12 species of climbing plants. *Global Ecology and Conservation, 21*. doi:10.1016/j.gecco.2019.e00830

300. Simoens, C., Vermorken, J. B., Korst, A. E., Pauwels, B., De Pooter, C. M., Pattyn, G. G., Lambrechts, H. A., Breillout, F., & Lardon, F. (2006). Cell cycle effects of vinflunine, the most recent promising *Vinca* alkaloid, and its interaction with radiation, *in vitro*. *Cancer Chemotherapy and Pharmacology, 58*(2), 210-218. doi:10.1007/s00280-005-0147-8

301. Şimşek Sezer, E. N., & Uysal, T. (2018). Volatile and phenolic compositions of the leaves of two *Vinca* L. species from Turkey. *Current Perspectives on Medicinal and Aromatic Plants, 1*(2), 103-110.

302. Singhal, G., Bhavesh, R., Kasariya, K., Sharma, A. R., & Singh, R. P. (2011). Biosynthesis of silver nanoparticles using *Ocimum sanctum* (Tulsi) leaf extract and screening its antimicrobial activity. *Journal of Nanoparticle Research, 13*, 2981–2988. doi:10.1007/s11051-010-0193-y

303. Sobiepanek, A., Milner-Krawczyk, M., Lekka, M., & Kobiela, T. (2017). AFM and QCM-D as tools for the distinction of melanoma cells with a different metastatic potential. *Biosensors and Bioelectronics, 93*, 274–281. doi:10.1016/j.bios.2016.08.088

304. Soejima, T., Nishizawa, K., & Isoda, R. (2018). Monodisperse manganese oxide nanoparticles: Synthesis, characterization, and chemical reactivity. *Journal of Colloid and Interface Science, 510*, 272–279. doi:10.1016/j.jcis.2017.09.082

305. Söhretoglu, D., Masullo, M., Piacente, S., & Kirmizibekmez, H. (2013). Iridoids, monoterpenoid glucoindole alkaloids and flavonoids from *Vinca major*. *Biochemical Systematics and Ecology, 49*, 69–72. doi:10.1016/j.bse.2013.03.028

306. Solowey, E., Lichtenstein, M., Sallon, S., Paavilainen, H., Solowey, E., & Lorberboum-Galski, H. (2014). Evaluating Medicinal Plants for Anticancer Activity. *The Scientific World Journal, 2014*. doi:10.1155/2014/721402

307. Sreevidya, N., & Mehrotra, S. (2003). Spectrophotometric method for estimation of alkaloids precipitable with Dragendorff's reagent in plant materials. *Ournalof AOAC International, 86*(6), 1124-1127.

308. Stagos, D. (2020). Antioxidant activity of polyphenolic plant extracts. *Antioxidants, 9*(1). doi:10.3390/antiox9010019

309. Stauffer, D., & Aharony, A. (1994). *Introduction to percolation theory* (Revised second eddition ed.): Taylor and Francis e-Lybrary.

310. Stenesh, J. (Ed.) (1989) Dictionary of biochemistry (2 ed.). Canada: John Wiley & Sons.

311. Suciu, M., Ionescu, C. M., Ciorita, A., Tripon, S. C., Nica, D., Al-Salami, H., & Barbu-Tudoran, L. (2020). Applications of superparamagnetic iron oxide nanoparticles in drug and therapeutic delivery, and biotechnological advancements. *Beilstein Journal of Nanotechnology, 11*, 1092–1109.

312. Sukhdev, S., Shamsher, K. S., & Indu, K. (2017). Antilipase activity guided fractionation of *Vinca major*. *Journal of King Saud University – Science*. doi:10.1016/j.jksus.2017.03.005

313. Suman, T. Y., Radhika Rajasree, S. R., Kanchana, A., & Beena Elizabeth, S. (2013). Biosynthesis, characterization and cytotoxic effect of plant mediated silver nanoparticles using *Morinda citrifolia* root extract. *Colloids and Surfaces B: Biointerfaces, 106*, 74– 78. doi:10.1016/j.colsurfb.2013.01.037

314. Suwalak, S., & Voravuthikunchai, S. P. (2009). Morphological and ultrastructural changes in the cell structure of enterohaemorrhagic Escherichia coli O157:H7 following treatment with Quercus infectoria nut galls. *Journal of Electron Microscopy, 58*(5), 315-320. doi:10.1093/jmicro/dfp024

315. T.P.L. The Plant List. Retrieved from http://www.theplantlist.org/1/

http://www.theplantlist.org/browse/A/Apocynaceae/Vinca/;

http://www.theplantlist.org/tpl/record/kew-213148

http://www.theplantlist.org/tpl/record/kew-213152

http://www.theplantlist.org/tpl/record/kew-213157

http://www.theplantlist.org/tpl/record/kew-213165

http://www.theplantlist.org/tpl/record/kew-213172

http://www.theplantlist.org/browse/A/Apocynaceae/Catharanthus/

http://www.theplantlist.org/tpl/record/kew-35719

http://www.theplantlist.org/tpl/record/kew-35718

http://www.theplantlist.org/tpl/record/kew-35712

http://www.theplantlist.org/tpl/record/kew-35715

http://www.theplantlist.org/tpl/record/kew-35714

http://www.theplantlist.org/tpl/record/kew-35723

http://www.theplantlist.org/tpl/record/kew-35724

http://www.theplantlist.org/tpl/record/kew-35713

316. Ticha, I. (1985). Ontogeny of leaf morphology and anatomy. In Z. Šestăk (Ed.), *Photosynthesis during leaf development* (Vol. 11). Prague: Springer, Drodrecht.

317. Tiong, S. H., Looi, C. Y., Hazni, H., Arya, A., Paydar, M., Wong, W. F., Cheah, S.-C., Mustafa, M. R., & Awang, K. (2013). Antidiabetic and antioxidant properties of alkaloids from *Catharanthus roseus* (L.) G. Don. *Molecules, 18*, 9770-9784. doi:10.3390/molecules18089770

318. Țiță, I. (2008). *Botanică farmaceutică* (III ed.): Editura Sitech.

319. Tulyaganov, T. S. N., A M (2000). Alkaloids of *Vinca minor*. *Chemistry of Natural Compounds, 36*(5), 540.

320. Turker, H., Yıldırım, A. B., & Karakaş, F. P. (2009). Sensitivity of bacteria isolated from fish to some medicinal plants. *Turkish Journal of Fisheries and Aquatic Sciences, 9*, 181-186. doi:10.4194/trjfas.2009.0209

321. Vachnadze, V. Y., Dzhakeli, E. Z., Dadeshidze, I. A., & Kintsurashvili, L. G. (2010). Quantitative spectrophotometric determination of alkaloids in roots of *Vinca herbacea*. *Pharmaceutical Chemistry Journal, 44*(4), 199-201.

322. Valgas, C., de Souza, S. M., Smânia, E. F. A., & Smânia Jr., A. (2007). Screening methods to determine antibacterial activity of natural products. *Brazilian Journal of Microbiology, 38*, 369-380.

323. van de Venter, M., Roux, S., Bungu, L. C., Louw, J., Crouch, N. R., Grace, O. M., Maharaj, V., Pillay, P., Sewnarian, P., Bhagwandin, N., & Folb, P. (2008). Antidiabetic screening and scoring of 11 plants traditionally used in South Africa. *Journal of Ethnopharmacology, 119*, 81–86. doi:10.1016/j.jep.2008.05.031

324. Veerasamy, R., Xin, T. Z., Gunasagaran, S., Xiang, T. F. W., Yang, E. F. C., Jeyakumar, N., & Dhanaraj, S. A. (2011). Biosynthesis of silver nanoparticles using mangosteen leaf extract and evaluation of their antimicrobial activities. *Journal of Saudi Chemical Society, 15*, 113–120. doi:10.1016/j.jscs.2010.06.004

325. Venkateshwar, C., Rao, S. G., & Kumar, R. S. (2013). Epidermal study of medicinal plants with special reference to identification, adulteration and authentification of crude leaf drugs. *Annals of Phytomedicine, 2*(1), 115-125.

326. Verma, P., Khan, S. A., Mathur, A. K., Shanker, K., & Lal, R. K. (2014). Regulation of vincamine biosynthesis and associated growth promoting effects through abiotic elicitation, cyclooxygenase inhibition, and precursor feeding of bioreactor grown *Vinca minor* hairy roots. *Applied Biochemistry and Biotechnology, 173*, 663–672. doi:10.1007/s12010-014-0883-5

327. Verma, P., Mathur, A. K., & Shanker, K. (2012). Enhanced vincamine production in selected tryptophan-overproducing shoots of *Vinca minor*. *Plant Cell, Tissue and Organ Culture, 111*, 239–245. doi:10.1007/s11240-012-0185-y

328. Vigneshwaran, N., Ashtaputre, N. M., Varadarajan, P. V., Nachane, R. P., Paralikar, K. M., & Balasubramanya, R. H. (2007). Biological synthesis of silver nanoparticles using the fungus *Aspergillus flavus*. *Matterials Letters, 61*, 1413-1418. doi:10.1016/j.matlet.2006.07.042

329. Vofely, R. V., Gallagher, J., Pisano, G. D., Bartlett, M., & Braybrook, S. A. (2018). Of puzzles and pavements: a quantitative exploration of leaf epidermal cell shape. *New Phytologist, 221*, 540–552. doi:10.1111/nph.15461

330. Wang, J., Lv, X., Xu, J., Liu, X., Du, T., Sun, G., Chen, J., Shen, X., Wang, J., & Hu, L. (2020). Design, synthesis and biological evaluation of vincamine derivatives as potential pancreatic B-cells protective agents for the treatment of type 2 diabetes mellitus. *European Journal of Medicinal Chemistry, 188*. doi:10.1016/j.ejmech.2019.111976

331. Wang, L., He, H.-P., Di, Y.-T., Zhang, Y., & Hao, X.-J. (2012). Catharoseumine, a new monoterpenoid indole alkaloid possessing a peroxy bridge from *Catharanthus roseus*. *Tetrahedron Letters, 53*, 1576–1578. doi:10.1016/j.tetlet.2012.01.060

332. Wang, Z., Yang, Z., Zhang, L., Wang, X., Peng, C., Meng, D., & Yan, D. (2017). Toxic effects of vinca alkaloids from *Catharanthus roseus* (L.) G. Don on *Tetrahymena thermophila* BF 5 growth by microcalorimetry. *Thermochimica Acta, 651*, 53-57. doi:10.1016/j.tca.2017.02.018

333. Wankhede, S. B., Routh, M. M., Rajput, S. B., & Karuppayil, S. M. (2013). Antifungal properties of selected plants of Apocynaceae family against the human fungal pathogen *Candida albicans*. *International Current Pharmaceutical Journal, 2*(7), 122-125.

334. Web of Science. Retrieved from https://webofknowledge.com

335. Wei, X., Khan, A., Song, D., Dai, Z., Liu, Y.-P., Yu, H.-F., Wang, B., Zhu, P.-F., Ding, C.-F., Zhao, X.-D., Wang, Y.-F., & Luo, X.-D. (2017). Three new pyridine alkaloids from *Vinca major* cultivated in Pakistan. *Natural Products and Bioprospecting, 7*, 323–327. doi:10.1007/s13659-017-0137-7

336. Weraduwage, S. M., Chen, J., Anozie, F. C., Morales, A., Weise, S. E., & Sharkey, T. D. (2015). The relationship between leaf area growth and biomass accumulation in *Arabidopsis thaliana*. *Frontiers in Plant Science, 6*, 167. doi:10.3389/fpls.2015.00167

337. Wu, L., Ye, M., & Zhang, J. (2018). Vincamine prevents lipopolysaccharide induced inflammation and oxidative stress via thioredoxin reductase activation in human corneal epithelial cells. *American Journal of Translational Research, 10*(7), 2195-2204.

338. Wu, X., & Guy, R. H. (2009). Applications of nanoparticles in topical drug delivery and in cosmetics. *Journal of Drug Delivery Science and Technology, 19*(6), 371-384. doi:10.1016/S1773-2247(09)50080-9

339. Xue, D., Zhang, X., Lu, X., Chen, G., & Chen, Z. H. (2017a). Molecular and Evolutionary Mechanisms of Cuticular Wax for Plant Drought Tolerance. *Frontiers in Plant Science, 8*, 621. doi:10.3389/fpls.2017.00621

340. Xue, Y., Bigras, G., Hugh, J., & Ray, N. (2019). Training Convolutional Neural Networks and Compressed Sensing End-to-End for Microscopy Cell Detection. *IEEE Transactions on Medical Imaging, 38*(11), 2632-2641. doi:10.1109/TMI.2019.2907093

341. Xue, Y., & Ray, N. (2017b). Cell Detection in microscopy images with deep convolutional neural network and compressed sensing. *arXiv preprint*. doi:arXiv:1708.03307

342. Yildirim, A. B., Karakas, F. P., & Turker, A. U. (2012). *In vitro* antibacterial and antitumor activities of some medicinal plant extracts, growing in Turkey. *Asian Pacific Journal of Tropical Medicine*, 616-624. doi:10.1016/S1995-7645(13)60106-6

343. Yin, H., & Sun, Y.-H. (2011). Vincamine-producing endophytic fungus isolated from *Vinca minor*. *Phytomedicine, 18*, 802–805. doi:10.1016/j.phymed.2011.01.005

344. Yuvarajan, R., Natarajan, D., Ragavendran, C., & Jayavel, R. (2015). Photoscopic characterization of green synthesized silver nanoparticles from *Trichosanthes tricuspidata* and its antibacterial potential. *Journal of Photochemistry and Photobiology B: Biology, 149*, 0–307. doi:10.1016/j.jphotobiol.2015.04.032

345. Zabolotnaya, E. S., Bukreeva, É. V., & Lazurevskii, T. V. (1968). *Vinca herbacea* Waldst et Kit. alkaloids. *Khimiko-Farmatsevticheskii Zhurnal, 2*(1), 32-34.

346. Zavoi, S., Fetea, F., Ranga, F., Pop, R. M., Baciu, A., & Socaciu, C. (2011). Comparative fingerprint and extraction yield of medicinal herb phenolics with hepatoprotective potential, as determined by UV-Vis and FT-MIR spectroscopy. *Notulae Botanicae Horti Agrobotanici, 39*(2), 82-89.

347. Zhang, F., Chen, B., Xiao, S., & Yao, S. (2005). Optimization and comparison of different extraction techniques for sanguinarine and chelerythrine in fruit of *Macleaya cordata* (Wild) R. Br. *Separation and Purification Technology, 42*, 283-290. doi:doi:10.1016/j.seppur.2004.09.002

348. Zhang, Z.-J., Du, R.-N., He, J., Wu, X.-D., Li, Y., Li, R.-T., & Zhao, Q.-S. (2016). Vinmajorines C - E, Monoterpenoid Indole Alkaloids from *Vinca major*. *Helvetica Chimica Acta*, *99*(2), 157-160. doi:10.1002/hlca.201500211

349. Zhang, Z.-J., Du, R.-N., He, J., Wu, X.-D., Li, Y., Li, R.-T., & Zhao, Q. (2015). Three new monoterpenoid indole alkaloids from *Vinca major*. *Journal of Asian Natural Products Research*. doi:10.1080/10286020.2015.1094463

350. Zhou, J., & Giannakakou, P. (2005). Targeting microtubules for cancer chemotherapy. *Current Medicinal Chemistry - Anti-Cancer Agents*, *5*, 65-71.

351. Zhu, J., Yu, Q., Xu, C., Li, J., & Qin, G. (2018). Rapid estimation of stomatal density and stomatal area of plant leaves based on object-oriented classification and its ecological trade-off strategy analysis. *Forests*, *9*. doi:10.3390/f9100616

352. Zhu, W., & Gao, J. (2008). The Use of Botanical Extracts as Topical Skin-Lightening Agents for the Improvement of Skin Pigmentation Disorders. *Journal of Investigative Dermatology Symposium Proceedings*, *13*(1), 20-24. doi:https://doi.org/10.1038/jidsymp.2008.8

353. Ziegler, J., & Facchini, P. J. (2008). Alkaloid biosynthesis: Metabolism and trafficking. *Annual Review of Plant Biology, 59,* 735–769. doi:10.1146/annurev.arplant.59.032607.092730

ISBN: 978-606-37-1705-5